Stellar coronal astronomy

Fabio Favata (fabio.favata@rssd.esa.int)
Astrophysics Division of ESA's Research and Science Support Department – P.O. Box 299, 2200 AG Noordwijk, The Netherlands

Giuseppina Micela (giusi@oapa.astropa.unipa.it)
INAF – Osservatorio Astronomico G. S. Vaiana – Piazza Parlamento 1, 90134 Palermo, Italy

Abstract.

Coronal astronomy is by now a fairly mature discipline, with a quarter century having gone by since the detection of the first stellar X-ray coronal source (Capella), and having benefitted from a series of major orbiting observing facilities. Several observational characteristics of coronal X-ray and EUV emission have been solidly established through extensive observations, and are by now common, almost text-book, knowledge. At the same time the implications of coronal astronomy for broader astrophysical questions (e.g. Galactic structure, stellar formation, stellar structure, etc.) have become appreciated. The interpretation of stellar coronal properties is however still often open to debate, and will need qualitatively new observational data to book further progress. In the present review we try to recapitulate our view on the status of the field at the beginning of a new era, in which the high sensitivity and the high spectral resolution provided by *Chandra* and XMM-*Newton* will address new questions which were not accessible before.

Keywords: Stars; X-ray; EUV; Coronae

Table of Contents

1. Foreword

Given the breadth of the subject and the sheer volume of published literature, reviewing in depth all aspects of coronal astronomy is a daunting task. We have therefore deliberately chosen to concentrate on specific aspects of the field, skipping a number of topics, several of which would by themselves deserve a large review. We have concentrated mostly on the observational aspects, and have skimmed over (apart from mentioning them where relevant) most of the often controversial open-standing theoretical issues. These include for example coronal heating mechanisms and dynamo theory, for which we do not review the large body of theoretical work in any detail, but only discuss them in the context of their relationship with observations.

The observational topics which we have decided to discuss in detail are (in addition to the historical overview of Sect. 2) the general characteristics of X-ray emission across the H-R diagram (Sects. 4.1–4.4), the relationship between X-ray activity and rotation (Sect. 4.5), coronal activity cycles (Sect. 5.2), the spatial structuring of stellar coronae (Sect. 6), flares (Sect. 7), the temporal evolution of X-ray activity along the lifetime of a star, (Sects. 8 and 9), the still controversial field of coronal metal abundances (Sect. 10), the recent evidence obtained from high-resolution spectroscopy on the density and thermal structuring of stellar coronae (Sect. 11) and the use of X-ray observations (unbiased surveys in particular) as a tool to study Galactic structure.

X-ray emission in the pre-main sequence (PMS) phase, which would deserve (and has received in the recent past, Feigelson and Montmerle, 1999) a complete review by itself is only briefly discussed to put the evolution of X-ray activity in the main sequence phase in the proper context. In several places we have considered EUV observations (performed by EUVE) on the same ground as X-ray observations, given that they sample the same range of plasma temperatures as X-ray observations; no distinctions between the X-ray and EUV wavelength range has therefore been implemented. At the same time, the body of work on forbidden coronal lines (such as the Fe XXI 1354 Å line), mostly performed with HST observations, will not be reviewed here for reasons of space, the interested reader being referred to some of the recent papers on the subject, e.g. Johnson et al. (2002), Robinson et al. (2001), Ayres et al. (2001), Pagano et al. (2000) or Linsky et al. (1998).

An effort has been made to collect the relevant information in a systematic way in a number of tables. Table I (page 4) gives (approximate) spectral types and object classes for all individual stars mentioned in the present review, Tables II and III (pages 60 and 61) contain a brief description and reference to the main published detailed analyses of stellar flares, Table IV (page 65) contains reference to the main published analyses of X-ray observations of open clusters (as well as summary information about the clusters), while Ta-

Table I. Indicative spectral types and object class for all stars discussed in the present paper. "nZAMS" = young, near Zero-Age Main Sequence.

Name	Class	Spec. type	Name	Class	Spec. type
α Cen		G0V+K5V	FK Aqr	flare	M1.5V
α CrB	Algol	A0V+G5V	HD 283572	PMS	G2III
χ^1 Ori	nZAMS	G0V	HR 1099	RS CVn	G9V+...
ε Eri		K2V	HR 5110	RS CVn	F2IV+...
λ And	RS CVn	G8III+ ...	HU Vir	RS CVn	K0IV+...
π^1 UMa	nZAMS	G1.5V	II Peg	RS CVn	K0V+...
σ Gem	RS CVn	K1III+ ...	LHS 2065	flare	M9V
σ^2 CrB	RS CVn	G0V+ ...	LkHα 92	PMS	K
ξ Boo A		G8V+K4V	LP 944$-$20	BD	M9V
44 Boo	W UMa	G0V+G0V	LQ Hya	flare	K0V
47 Cas		F0V	MWC 297	HAeBe	Be
AB Dor	nZAMS	K1	P 1724	PMS	G8
AD Leo	flare	M3.5V	Procyon		F5V
Algol	Algol	B8V+K2IV	RS CVn	RS CVn	F4+...
Altair		A7V	Sirius		A1V
AR Lac	RS CVn	G2IV+K0III	UV Cet	flare	M5.5V
AU Mic	flare	M0V	UX Ari	RS CVn	G5V+K0IV
BY Dra	flare	K6V	VB 10	flare	M8V
Capella	RS CVn	G5III+...	VB 50	nZAMS	G1V
Castor		A2V	VB 8	flare	M7V
CF Tuc	RS CVn	G3V+...	VW Cep	W UMa	K0V+K0V
CN Leo	flare	M5.5V	W UMa	W UMa	F8V+F8V
EK Dra	nZAMS	F8V	Wolf 630	flare	M3V
EQ 1839.6	flare	M3.5V	YLW 15	Class I PMS	–
ER Vul	W UMa	G0V+G0V	YLW 16A	Class I PMS	–
EV Lac	flare	M3.5V	YY Gem	flare	M0.5V

ble VI (page 92) contains reference to the main published analyses of coronal abundances based on high-resolution X-ray spectra. An index is also provided to the individual stars.

2. Historical overview

During total solar eclipses the corona is visible as a faint "halo" extending out to a few solar radii from the (occulted) photosphere, so that, in an empirical sense, the existence of the corona around the Sun must have been

known since the earliest times. The understanding of the nature of this extended atmosphere around the Sun had to wait for the birth of astronomical spectroscopy. During the eclipse of Aug. 7 1869 the American astronomer C. Young discovered an isolated weak green line in the visible coronal spectrum (Young, 1869), which he initially (incorrectly) identified with a Fe I line – although he found it surprising that only one Fe line would be present in the spectrum. Later eclipse observations produced evidence for additional lines; a more accurate wavelength determination of the green coronal line (5303.2 Å) in 1898 was inconsistent with any known spectral feature. This led to the hypothesis that the lines in the spectrum were produced by a new, hitherto unknown element, christened "coronium". It was only in 1942 that the emission spectrum of coronium was correctly identified with the lines of highly ionized Fe (in particular Fe XIV, Edlén, 1945). Such high ionization states of Fe require temperatures $T \simeq 1\,\mathrm{MK}$. This result posed a puzzling question: what physical process could heat the solar corona to a temperature more than two orders of magnitude hotter than the solar photosphere ($T = 5770\,\mathrm{K}$)? The high temperature of the solar corona was confirmed by the detection of its thermal X-ray emission, which took place in 1946 with a sounding rocket instrument developed by the U.S. Naval Research Laboratory group directed by H. Friedman.

The fashionable theory for coronal heating was, until the late 1960's, that it was due to acoustic waves, produced by the convective turbulent motions of the solar atmosphere, and dissipated in the corona. Such a mechanism would likely produce a rather spatially homogeneous corona, as the acoustic waves would be produced everywhere in the photosphere. The detailed pictures of the X-ray emitting corona produced by the imaging X-ray telescopes flown on the Skylab space station in 1973–1974 showed instead that the solar corona is highly structured, with most of the X-ray bright plasma confined in arch-, or loop-like structures, whose foot points often coincided with the location of sunspots on the photosphere. The coronal regions outside the loops are X-ray faint, and were dubbed "coronal holes". The evolution of the instrumental capabilities of solar X-ray telescopes is shown in Fig. 1.

Coronal loops were also observed to be dynamic entities, and flaring (sudden brightening of one or more individual loops, followed by a slower decay in its X-ray luminosity) was found to be a common occurrence. A comprehensive review of the early solar X-ray work can be found in Vaiana and Rosner (1978).

The high degree of structuring of the solar corona requires a way of confining the plasma in the individual loops. Magnetic fields (which were already known to be associated with sunspots) offered the obvious explanation. The structured, magnetically confined corona was difficult to reconcile with the acoustic heating theory, although a model in which the plasma would be

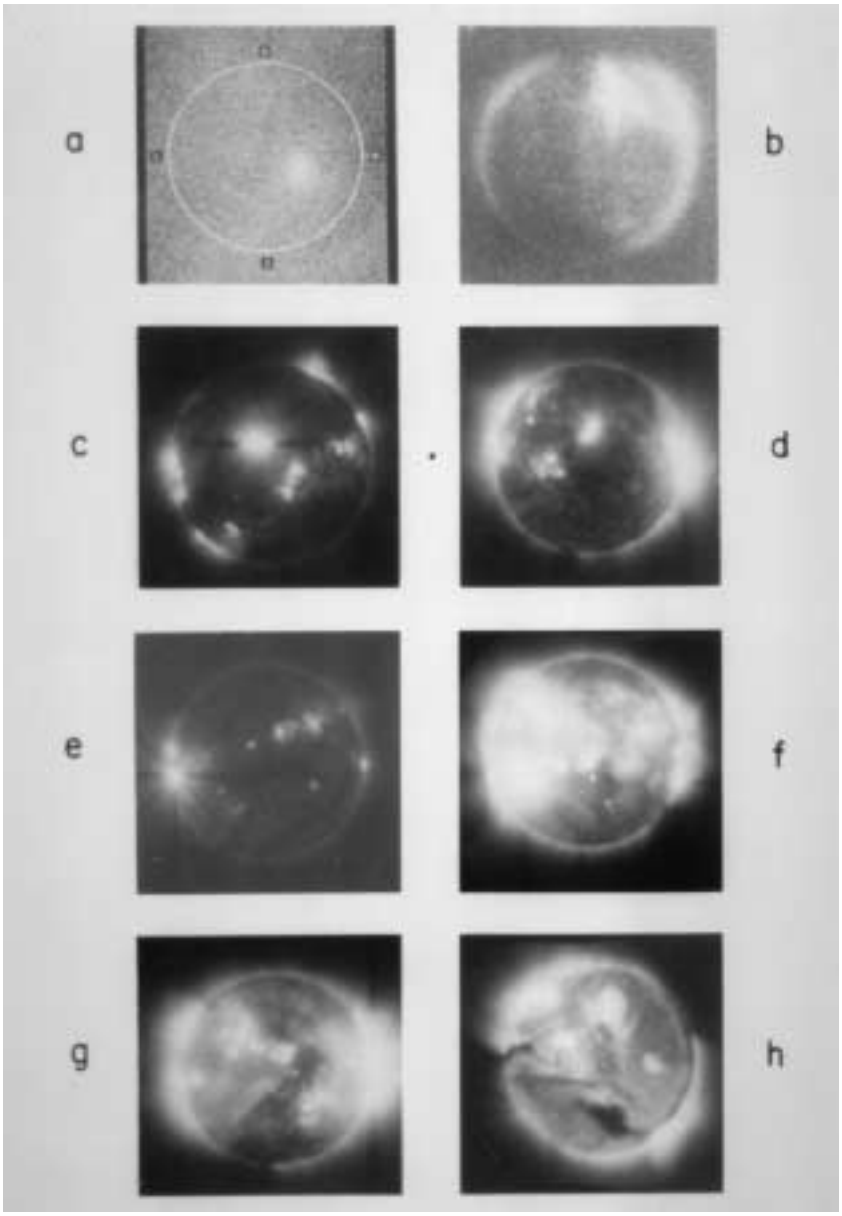

Figure 1. Solar X-ray images at various resolutions obtained through rocket flights, showing the evolution of the spatial resolution of various X-ray telescopes. Image *a* is obtained in 1963 with the first set of X-ray grazing incidence optics, while images *b* to *h* show the evolution of grazing incidence optics from 1965 to 1973, just prior to the Skylab solar X-ray telescope. Taken from Vaiana et al. (1973), where a more detailed description of each image can be found.

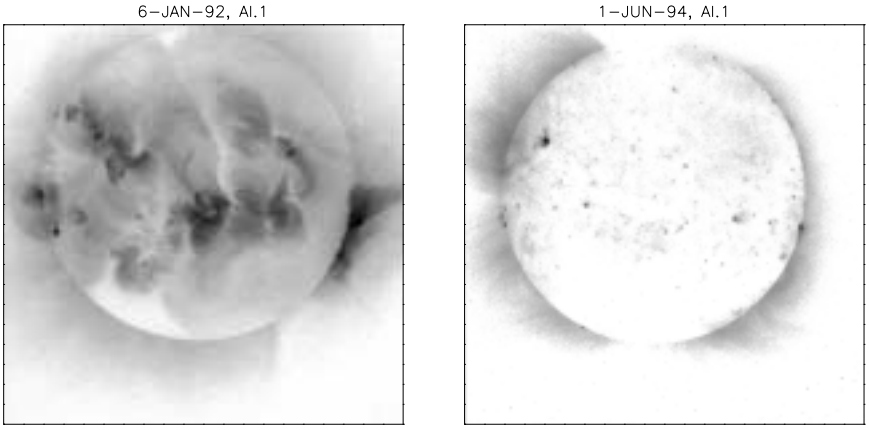

Figure 2. Soft X-ray images from the Yohkoh observatory taken close to solar maximum (left) and solar minimum (right), showing the significant differences in the coronal structures along the solar cycle (adapted from Peres et al., 2000). The X-ray luminosity in the band of the ROSAT PSPC detector (0.1–2.4 keV) changes by a factor of $\simeq 20$ between the two images.

magnetically confined but acoustically heated would still be compatible with several observational facts related to the solar corona.

Any predictive theory of coronal heating must however explain several other characteristics of the corona, including the large variation in X-ray luminosity taking place during the solar cycle (see Sect. 5.2). The significant difference in the solar coronal structure and luminosity between the cycle maximum and the cycle minimum is easily visible in Fig. 2; the change in soft X-ray luminosity, a factor of $\simeq 20$ (in the band of the ROSAT PSPC detector, 0.1–2.4 keV) between the two images[1] is for example incompatible with a corona heated by a predominantly acoustic mechanism.

The detection of coronal X-ray emission from stars other than the Sun had to wait until the identification, by Catura et al. (1975), of the binary system Capella as the optical counterpart to a soft X-ray source detected during a rocket flight in 1974. Interestingly, the rocket experiment had briefly been pointed to Capella only to calibrate the attitude control system. Soon thereafter, Capella and Sirius were again detected as soft X-ray sources by the ANS satellite (Mewe et al., 1975), and a few years later several active (RS CVn-type) binaries were detected in soft X-rays with the HEAO-1 satellite (Walter et al., 1978; Walter et al., 1980).

An understanding of whether coronae are a common occurrence around cool stars (or whether the individual sources detected up to then were some-

[1] The variability on time scales of the solar rotation period has comparable amplitude, see Fig. 10.

how pathological cases, none of them indeed being “normal” main sequence stars) had to wait for the launch in 1978 of the *Einstein* satellite, the first imaging X-ray observatory. The imaging capability of the IPC detector on-board *Einstein* allowed it to detect X-ray emission from hundreds of normal stars, so that Vaiana et al. (1981) could state that X-ray emission was a common occurrence across the whole H-R diagram (Fig. 3), with the apparent exception of late B and early A stars and very cool giants. The widespread occurrence of stellar X-ray emission put the last nail on the coffin of the acoustic heating theory, as only stars in a rather narrow range of spectral types would have enough “acoustic flux” to heat a corona. The inadequacy of the acoustic model to explain the characteristics of the X-ray emission from the RS CVn binaries detected with the HEAO-1 satellite had already been pointed out by Walter et al. (1980). Since then it has been shown that, in stars with convective envelopes (e.g. main sequence stars of spectral type F and later) a mechanism similar to the solar one, with a magnetically confined corona, offers a much better explanations of the observations, although several observational features of coronal emission still defy explanation.

Copious X-ray emission was also observed with *Einstein* from early-type stars and from giant stars, as apparent in Fig. 3. For the early type stars the lack of convective envelopes (and an observed tight correlation with the bolometric luminosity) make it implausible that the X-ray emission is caused by the same mechanism as in low-mass stars, so that wind-driven shocks have been claimed as being the source of the X-ray emission. Neither early type stars nor giants will be covered in detail in the present review. It is however worth mentioning that the current view of X-ray emission from early-type stars is undergoing significant changes based on results from high-resolution spectra from both *Chandra* and XMM-*Newton* (e.g. Schulz et al., 2002).

A few important properties of stellar coronal emission (later confirmed by the ROSAT observations) were already established through the *Einstein* survey. Thermal X-ray emission (which was attributed to the presence of solar-like coronae) was observed to be common across all cool stars, with a wide range (up to a few orders of magnitudes) in intrinsic X-ray luminosity. The thermal nature of the emission was soon confirmed by the spectra from the SSS detector on-board *Einstein* (Swank et al., 1981). It was immediately apparent that there was little correlation between the “classic” stellar parameters (i.e. mass, photospheric temperature and luminosity) and the coronal luminosity. Stars occupying the same location in the H-R diagram easily have coronal luminosities differing by factors of 1000. Also, it was evident that the Sun is a weak coronal source, with an average coronal X-ray luminosity lying at the low end of the broad distribution spanned by solar-type stars. Very soon, Pallavicini et al. (1981) showed that one key parameter influencing the level of coronal emission was stellar rotation, so that many *Einstein* observations of cool stars (from late F to M as well as active binaries) could be well fit through

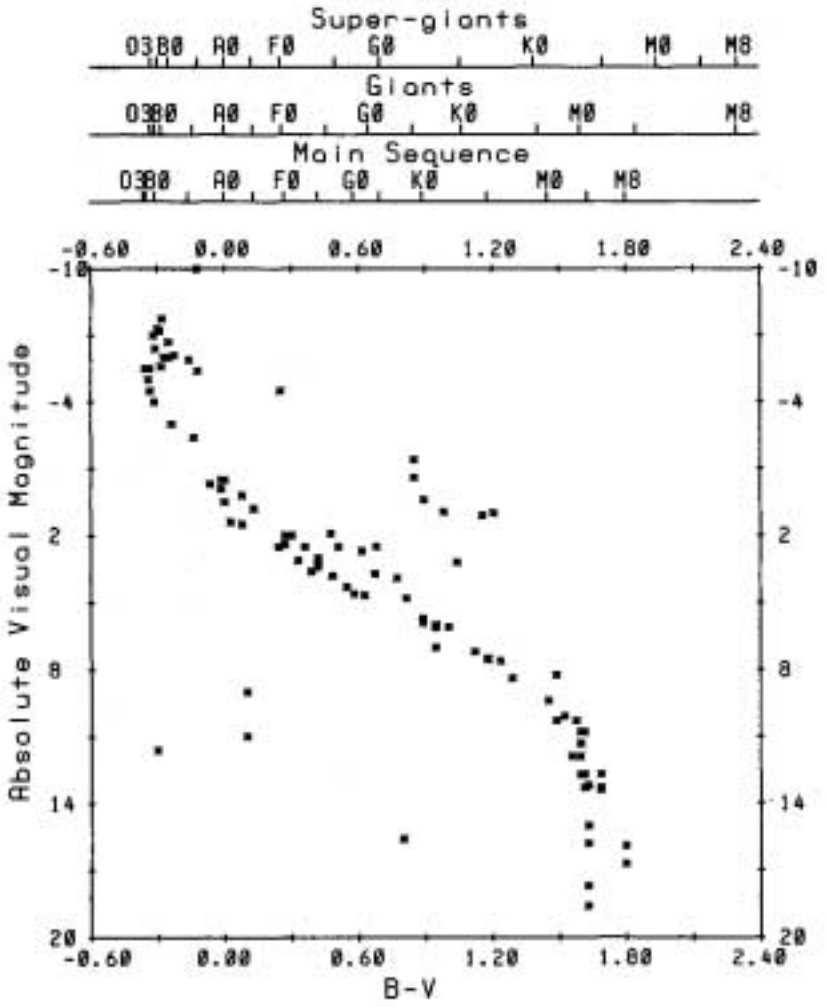

Figure 3. Original plot from Vaiana et al. (1981), showing the position in the H-R diagram of stars detected as X-ray sources in the early *Einstein* survey of stellar X-ray emission.

a simple square law (Fig. 4), $L_{\rm X} \propto (v \sin i)^2$. Another key early result was the correlation between X-ray luminosity and characteristic coronal temperature (Schmitt et al., 1990a).

The still limited sensitivity and sky area coverage of the *Einstein* observations had not allowed to establish whether all cool stars indeed are coronal sources or whether some stars are actually X-ray dark and thus do not have a corona. The launch of the ROSAT satellite in 1990 allowed to address these questions in detail. ROSAT had an improved sensitivity (when used in pointed mode) with respect to *Einstein*, and it also performed, as the first phase of its

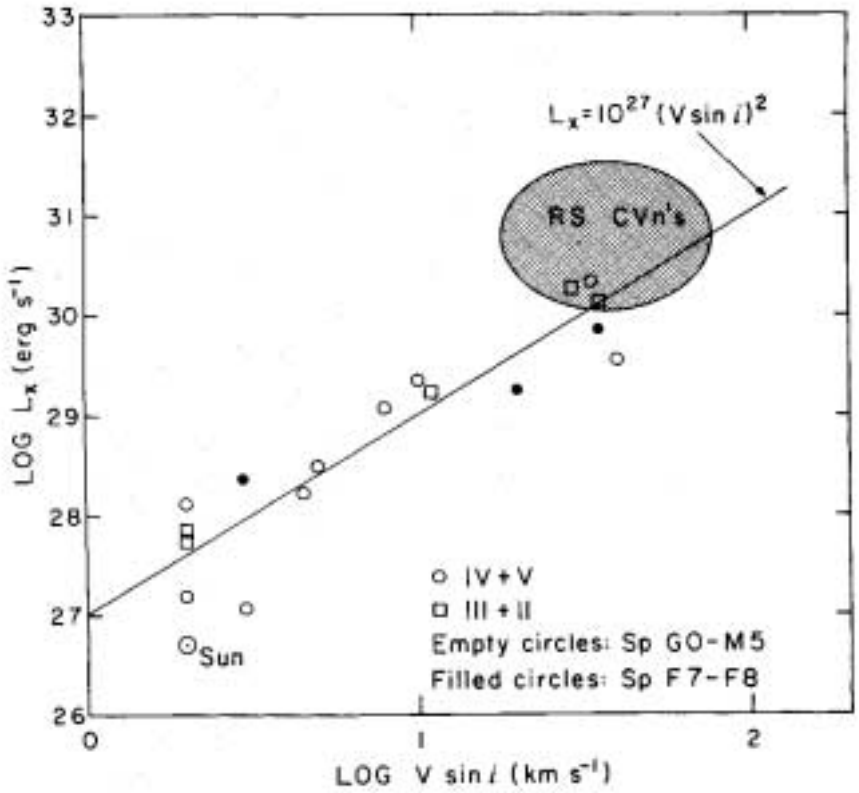

Figure 4. Original plot from Pallavicini et al. (1981), showing X-ray luminosity as a function of projected rotational velocity $v \sin i$. The continuous line is a square law fit.

mission, an all-sky survey (the ROSAT All Sky Survey, RASS), during which some 25 000 coronal sources were detected (see e.g. Motch et al., 1997 and Zickgraf et al., 1997 for a discussion of the relative fraction of coronal sources in the RASS), providing a sample of unprecedented size. This allowed to determine the X-ray emission levels of complete volume limited samples of stars. Schmitt (1997) for example discusses the X-ray emission from all A, F and G-type stars within 13 pc from the Sun, using a mixture of RASS and pointed ROSAT observations, and showing that coronae are truly universal in F and G stars (see Sect. 4.1).

3. Relevance of coronal astronomy

Stellar coronae, which are composed of hot plasma intertwined with magnetic fields, are driven by physical processes which are applicable (and thus of interest) to a broad range of astrophysical phenomena.

In addition, coronae are an essential feature of low-mass stars, and therefore have a significant impact on their structure and evolution, as well as on the structure and evolution of the planetary system which may surround the star. In the case of the Sun the corona is at most a negligible perturbation on the total energy balance, with an average total fractional X-ray coronal luminosity (expressed in the ROSAT 0.1–2.4 keV band) as low as $L_{\rm X}/L_{\rm bol} \simeq 10^{-7}$ at solar minimum (Peres et al., 2000). However, in the most active stars, the quiescent coronal X-ray luminosity can reach $L_{\rm X}/L_{\rm bol} \simeq 10^{-3}$, and during intense flaring events in low-mass stars the total X-ray luminosity at the peak of the flare may become comparable to the total stellar luminosity (see Sect. 7.1.3), so that the corona is clearly not any longer (even though for limited periods of time) a "small perturbation" but rather an important term in the stellar energetics. Also, such energetic events close to the stellar surface are likely to have a non-trivial influence on the outer structure of the star, and even in its quiescent state the presence of the corona (and of the implied magnetic field) in the active stars is likely to affect the structure of the convection zone. The Sun in its youth most likely underwent a phase of high activity, so that proper understanding of coronal evolution is essential to understand the evolution of the early Sun and planetary system.

Coronae are thought to be (largely) magnetically confined, and this is certainly true for the flaring plasma; therefore the ubiquity of coronae in late-type stars is an indication of the pervasiveness of magnetic fields. These magnetic fields are produced in the stars through some form of dynamo processes (which can differ in different types of stars, see Sect. 4.3), and play a key role in the evolution of the star's rotation: the magnetic field channels a hot, ionized stellar wind which carries away angular momentum from the star and is therefore responsible for its rotational braking. At the same time these processes regulate the amount of mass loss from the star. Magnetic fields will also substantially modify the stellar interior structure, as they alter the convective instability conditions (Ventura et al., 1998b), and thus likely affect the structure of the convective envelope (see discussion in Sect. 4.3), although their detailed influence on stellar structure and evolution has yet to be assessed.

In addition, magnetic fields influence the photospheric thermal structure (such as the sunspots visible on Sun's surface, or the large spots inferred by Doppler imaging on active stars), and will therefore have an impact on e.g. the determination of photospheric stellar abundance, including key elements of cosmological relevance such as lithium. Already Giampapa (1984) noted how the measured abundance of Li varies in sunspots, and the debate on the influence of activity on e.g. the observed large dispersion of Li measured in the Pleiades (Soderblom et al., 1993) is still ongoing (Stuik et al., 1997).

Therefore stellar coronae – and the physical processes which produce them, in particular the stellar dynamo and the implications of the relative

magnetic fields on the interior structure, energy transport and mixing processes – are an essential ingredient in the evolution of a cool main sequence star, and proper understanding of the structure and evolution of the corona is necessary for a full understanding of the structure and evolution of stars in general.

Coronae also have a strong influence on the circumstellar environment, and in particular on the environment in which planets form and evolve. This is true in all phases of a planet's life, although the influence in the early stages is bound to be more significant. The copious flux of X-rays produced by the corona in the early (pre-main sequence) stages of the life of a star will ionize the circumstellar disk, and strongly modify the environment in which planets form. The state of the art in modeling the influence of very young stellar coronae on the (proto-) planetary environment has recently been reviewed by Glassgold et al. (2000). More generally, the mass loss from active stars can be an important input to the chemical evolution of the inter-stellar medium (ISM). Although the early suggestion of Mullan et al. (1992) for high quiescent mass loss rates in low-mass stars has been refuted by Lim and White (1996) (see also Wargelin and Drake, 2002 on the subject), episodic mass losses, perhaps in the form of giant coronal mass ejections (for which the evidence is discussed in Sect. 7.3.2) could still be an important input to the chemical evolution of the inter-stellar medium. Given the evidence (Sect. 10.4) for activity-dependent chemical fractionation in the corona, the material returned to the ISM is likely to be selectively enhanced or depleted with respect to the "parent" star, also during the pre-main sequence phase.

One of the important parameters that can significantly affect a (proto-) planetary environment is the number of ionizing photons incident on e.g. the planetary atmosphere. As a result of the evolution of the X-ray properties of a "typical" main sequence star (Sect. 9) this number evolves strongly with time. A preliminary computation (Micela, 2002) shows that the number of harder (and thus more ionizing) X-ray photons decays more steeply in time than the number of softer X-ray photons. For example, the flux of hard (1–10 keV) X-ray photons at the Earth has decreased by more than two orders of magnitude since the Sun was the same age as the Pleiades, from $\simeq 10^{10}$ cm^{-2} s^{-1} then to $\simeq 3 \times 10^{7}$ cm^{-2} s^{-1} today. This only includes the contribution of the corona, and therefore does not include the large number of EUV/UV photons generated by the transition region, and is only based on the evolution of the "quiescent" coronal emission.

Flares are also likely to have a large impact on planetary environment and atmospheres and in the pre-main sequence phase (and in the first phases of the main sequence) stars exhibit very powerful flares (Sect. 7.1.3). These sudden releases of large quantities of very energetic photons from very young stars will play a role on planetary formations, while in the first phases of the main sequence they will affect the environment of already formed planets,

at a level depending on the duty cycles and energy released during these flares. The effect of this on the global evolution of e.g. climate on planets has still not been assessed, but clearly resolution of the so-called "faint young Sun paradox" (Ulrich, 1975) has to properly consider the evolution of the terrestrial atmosphere under the influence of the evolving solar coronal emission. Feigelson et al. (2002b) have shown, using *Chandra* observations of the Orion nebula cluster, that the energetics of flares – and relative proton fluxes in the proto-planetary nebula – in very young solar analogs (age $\leq 1\,\mathrm{Myr}$) is sufficient to explain the observed meteoritic abundance of several short-lived radio isotopes. Unfortunately a systematic knowledge of the evolution of coronal variability (flaring rate, duty cycle, energetics, etc.) in stars is yet lacking.

The influence of the corona on the planetary environment extends well into the star's main sequence life, certainly up to the age of the Sun. The influence of the Sun on the terrestrial climate is a subject of lively research and debate, but the evidence is accumulating that the bulk of the influence on the Earth's climate comes from the phenomena associated with the Sun's activity (e.g. Lean, 1997; Soon et al., 2000), so that understanding the evolution of the solar corona is likely to be essential to understand the evolution of the Earth's climate and even perhaps the origin of life. This evidence for a link between the state of the Sun's corona and terrestrial climate is both empirical and theoretical. Among the empirical evidence perhaps the best known case is the Maunder minimum, i.e. the period in which the solar cycle appeared to stop, so that sunspots effectively disappeared from the Sun from ca. 1645 to ca. 1715. This coincided with an unusually cold period, known as "the little ice age". Several theoretical studies also show that high-energy solar emission (specially the EUV photons) has a strong influence on the photochemistry of the high atmosphere, and thus e.g. on the formation of clouds in the atmosphere.

Finally, magnetically confined plasmas, on different spatial scales, are a general astrophysical phenomenon, for which stellar coronae form an excellent "case study", as their relative proximity allows the physics to be studied with a degree of detail which is not always possible with more energetic but further away objects.

4. Characteristics of stellar coronal X-ray emission

4.1. X-RAY EMISSION FROM SOLAR-TYPE STARS

The first systematic study of the X-ray emission from late-F and early-G stars was performed with the *Einstein* observatory (Maggio et al., 1987), and confirmed the early conclusion of Vaiana et al. (1981) that X-ray activity is common in solar-type stars, with a large spread in activity level.

The general characteristics of X-ray emission from solar-type stars have been studied in detail with the large-scale stellar survey performed with the ROSAT observatory. Schmitt (1997) performed a complete survey of all stars of spectral types A, F and G in the solar neighborhood (within 13 pc), complementing the RASS observations with pointed observations where necessary, ensuring that no "Malmquist"-type bias is present in the survey. Perhaps the most notable conclusion is the true universality of X-ray emission among solar-type stars: all G-type dwarfs in the sample observed with sufficient sensitivity were detected as X-ray sources, so that coronae appear to be an essential component of solar-type stars. Truly X-ray dark cool dwarfs, if they exist at all, must be very rare.

The X-ray luminosity of nearby F and G dwarfs ranges (in the ROSAT 0.1–2.4 keV band) between $\log L_{\rm X} \simeq 26.5\,{\rm erg\,s^{-1}}$ and $\log L_{\rm X} \simeq 29.5\,{\rm erg\,s^{-1}}$, with a median $\log L_{\rm X} \simeq 27.7\,{\rm erg\,s^{-1}}$, and the coronal X-ray luminosity is clearly correlated with the temperature of the emitting plasma, with the more luminous stars also being hotter. This had already been established as a general property of stellar X-ray emission on smaller samples of stars (see Fig. 3 of Schmitt et al., 1990a), but again the statistical completeness of the ROSAT samples allows to verify this as a fully general property.

If surface X-ray flux (rather than total X-ray luminosity) is taken as a parameter, nearby solar-type stars span almost four orders of magnitude (see Fig. 5), with a well-defined minimum level of coronal emission, which is apparently universal across main sequence late-type stars from F- to M-type, and is not the result (as discussed in detail by Schmitt, 1997) of a selection effect. This minimum X-ray surface coronal flux is $F_{\rm X} \simeq 10^4\,{\rm erg\,cm^{-2}\,s^{-1}}$, which is also the typical level observed in solar coronal holes, so that one possible interpretation for the occurrence of stars exhibiting minimum X-ray luminosity is that they are covered with coronal holes (i.e. with open magnetic field lines), with little if any emitting closed magnetic structures (loops).

At the same time, it appears that the intermediate activity level observed in nearby stars can be simply realized by covering the surface of a solar-like star with active regions (Drake et al., 2000). This was argued already quite early in the history of coronal astronomy, e.g. by Vaiana and Rosner (1978), so that the solar analogy appears as a quite likely one for the coronal properties of normal, disk population solar type stars.

Solar-type stars showing the maximum level of the activity ($\log L_{\rm X} \simeq 30\,{\rm erg\,s^{-1}}$) require plasma densities higher than observed in the core of solar active regions (unless very extended coronae are postulated, which are contrary to the evidence available, from either density measurements, Sect. 11.1 or the evidence on the location and size of the emitting regions, Sect. 6), and thus the use of the solar analogy to understand their coronal emission is not immediately straightforward.

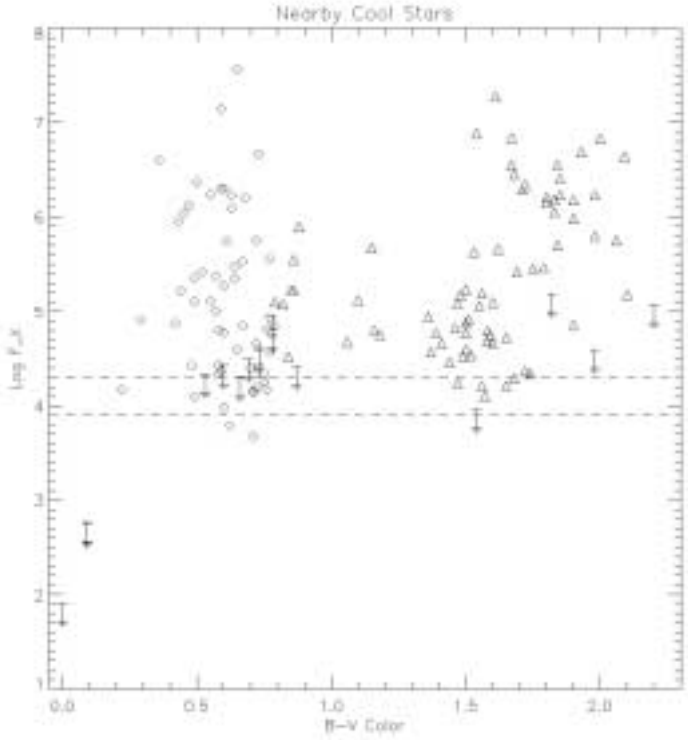

Figure 5. Original figure from Schmitt (1997), showing the X-ray surface flux for a volume-limited, complete sample of nearby cool dwarfs, spanning spectral types F, G, K and M. The wide span (almost four orders of magnitudes) in activity level is evident, as is the existence of a "universal" minimum flux level $F_{\rm X} \simeq 10^4\,{\rm erg\,cm^{-2}\,s^{-1}}$. The dashed lines show the range of flux (in the same band) from solar coronal holes.

The completeness afforded by the ROSAT survey of solar-type stars allows to clearly put the Sun in perspective: with its maximum X-ray luminosity $\log L_{\rm X} \simeq 27.5\,{\rm erg\,s^{-1}}$ the Sun lies near the median of the $L_{\rm X}$ distribution for nearby stars, and thus is a rather inactive star when compared with the general disk population.

4.2. X-RAY EMISSION FROM STARS AT THE CONVECTIVE BOUNDARY

Stellar structure theory predicts that the surface convection zone should disappear, in solar metallicity main sequence stars, at masses larger than $M \simeq 1.8\ M_{\odot}$, that is, for stars of spectral class earlier than late A. Under the assumption that surface convection is a necessary ingredient for a dynamo – and thus for a magnetically confined corona – coronal activity should also disappear. The exact "location" of this coronal boundary in the H-R is difficult to predict theoretically, as it depends sensitively on the detailed physics

of convection – something for which a satisfactory theory is still missing. Thus, sensitive X-ray observations can pin down the exact location of the convection boundary and constrain the physics of convection.

Early IUE observations (see Schmitt et al., 1985 for the early references) already showed that, while chromospheric activity was common in early F stars, it disappeared in A-type stars. Chromospheric studies (which rely on the measurement of line fluxes) are however impaired by the strong UV continuum of A-type stars, as well as by their average high rotation velocity, and X-rays are thus a more sensitive probe of the presence of a corona. The change in coronal properties at the convection boundary was evident in the earliest *Einstein* surveys: Topka et al. (1982) already noted a strong drop in the X-ray detection rate of A-type vs. F-type stars, and Schmitt et al. (1985) showed that single A-type stars are not X-ray emitters, with some apparent detections being due to UV photon contamination in the X-ray detectors (the problem is discussed in detail, for the ROSAT HRI, by Barbera et al., 2000). Many confirmed or suspected binaries with an A-type primary are found to be X-ray emitters, with X-ray luminosities fully compatible with normal coronal emission from a late-type star, so that the observed X-ray emission can be explained as due to the unseen companion.

Altair (of spectral type A7V) was found to be the earliest spectral type intrinsic X-ray emitter, a result later confirmed with ROSAT observations (Schmitt, 1997). Its X-ray spectrum is soft (Panzera et al., 1999), with the dominant component at $T \simeq 1$ MK, and the presence of a chromosphere has been confirmed e.g. by Simon and Landsman (1997). The coronal emission from Altair is rather weak ($L_X = 3 \times 10^{27}$ erg s^{-1}), with a corresponding surface X-ray flux $F_X \simeq 10^4$ erg cm^{-2} s^{-1}, i.e. at the observed minimum level of flux for solar type stars. If the solar analogy is valid for these stars, Altair would thus likely be covered by "coronal holes", i.e. open magnetic structures, with no active regions and relative closed coronal loops.

Some earlier A-type stars are found to be X-ray emitters, often at levels higher than Altair (Panzera et al., 1999), but the lack of detailed information on the star's nature (and in particular on the presence – or lack of – a later type companion) makes it impossible to assess whether they are intrinsic X-ray emitters or simply the brightest component of a (still undetected as such) binary system harboring an optically faint, X-ray active, later type companion. The latter interpretation is reinforced by the very deep X-ray observations of some early A-type stars, in particular Vega, for which the non-detection in a deep PSPC observation has allowed to put a very stringent upper limit to its X-ray luminosity of $L_X < 3 \times 10^{25}$ erg s^{-1} (Schmitt, 1997), supporting the idea that confirmed bona fide single early A-type stars are indeed X-ray dark. A direct demonstration of the existence of X-ray dark A-type stars is also provided by the observation of the eclipsing binary α CrB discussed in Sect. 6.2.1 (see Fig. 13). Thus, spectral type A7V appears to be the location

in the H-R diagram where (at least for near-solar metallicity stars) dynamo action appears.

More massive (O and early B) stars are copious X-ray emitters, but their X-ray emission is thought to be due to "non-coronal" mechanisms (i.e. to shocks in the stellar wind), with an X-ray luminosity well correlated with the bolometric luminosity, with $L_X/L_{bol} \simeq 10^{-7}$. X-ray emission from early-type stars will not be discussed further in the present review.

One challenge to the interpretation of coronal activity in early type stars comes from the frequent detection of strong X-ray activity in the pre-main sequence progenitors of A stars, i.e. the Herbig Ae and Be stars (HAeBe). These are often claimed to be structurally similar to their main-sequence counterparts (with no convective envelopes), although they are still surrounded by significant amounts of circumstellar material, as evidenced by their IR excesses. X-ray emission is a common occurrence among HAeBe stars. An early *Einstein* survey (Damiani et al., 1994) of known HAeBe stars detected $\simeq 50\%$ of them as X-ray sources, a result confirmed by the ROSAT survey of Zinnecker and Preibisch (1994). These works showed that HAeBe stars have relatively high X-ray luminosities ($L_X/L_{bol} \simeq 10^{-6}$–$10^{-5}$ – significantly higher than typical for the wind-driven X-ray luminosity of main-sequence O and B stars, $L_X/L_{bol} \simeq 10^{-7}$). Zinnecker and Preibisch (1994) found no correlation between the X-ray luminosity and the rotational velocity (as would be expected for "normal" coronal emission), but a correlation between X-ray luminosity and mass loss rate, pointing to a wind-related origin (and making it difficult to explain such correlations with the presence of unseen companions).

Later observations with ASCA (Hamaguchi et al., 2002) show that the X-ray spectra of HAeBe stars are well fit with thermal models, with rather high plasma temperatures ranging between 1 and 5 keV, again significantly higher than the typical X-ray temperatures of O and B stars. One challenge to the wind-related explanation comes from the observation of a significant flaring event on the highly reddened HBe star MWC 297, which shows all the characteristics of a normal intense coronal flare, with an increase in X-ray luminosity of a factor of 5 over the quiescent value, and an increase in temperature from 30 MK during quiescence to 80 MK during the flare. The X-ray spectrum of MWC 297 during the flare is shown in Fig. 6. The *e*-folding time of the flare decay is 60 ks, again typical of intense stellar flares. Such an event would point to the X-ray emission from MWC 297 being of coronal origin, or – at least – magnetically confined, given that long-duration flaring events must be confined, (Reale et al., 2002), and could therefore not occur in an expanding wind.

One element which has not yet been considered in explaining the origin of the X-ray emission from HAeBe stars is whether they indeed have no convective envelope. The case of Altair shows that even an extremely thin

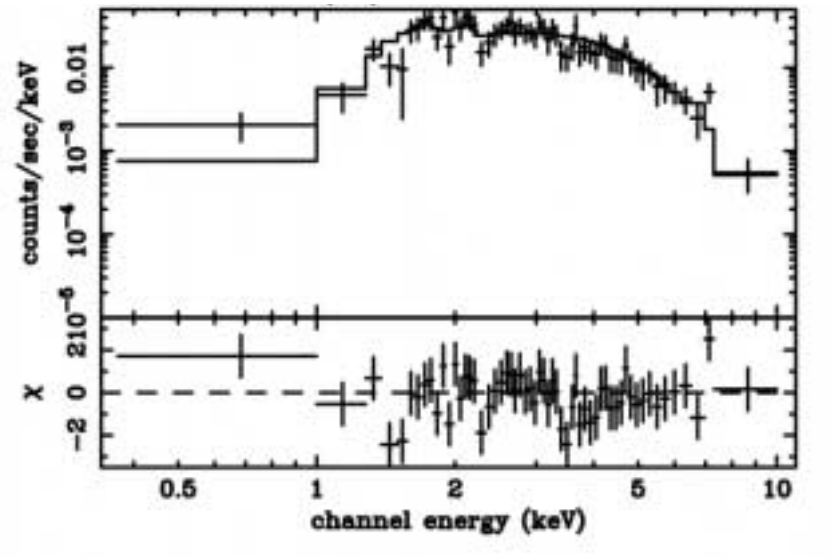

Figure 6. The ASCA SIS spectrum of the X-ray emission from the Herbig Be star MWC 297 during the flare reported by Hamaguchi et al. (2000), plotted together with the best-fitting thermal model. Note the hardness of the spectrum, indicative of the high flaring temperature.

convective envelope is sufficient to sustain significant magnetic activity. The recent models of Siess et al. (2000) indicate that a star like Altair has a very thin convection zone, extending to a depth of only $2 \times 10^{-3}\ R_*$. While these models show that main sequence early A and B stars indeed have a fully radiative structure, the same models predict the presence of thin (but non-negligible, up to a depth of 0.01 R_*) convective envelopes in pre-main sequence early A and B stars. Whether these envelopes are indeed sufficient to sustain the dynamo action required to explain the observed vigorous X-ray activity in HAeBe stars (with much higher plasma temperatures and X-ray surface fluxes than observed e.g. in Altair) remains to be assessed.

4.3. X-RAY EMISSION AT THE LOW MASS END

The early surveys of the X-ray characteristics of low-mass dwarfs using *Einstein* observations (Rosner et al., 1981; Golub, 1983; Bookbinder, 1985; Johnson, 1986) showed that coronal X-ray emission is very common also in these stars, with some evidence present in these early data for a decay in the X-ray activity level at the lower masses.

However, a systematic analysis of all the *Einstein* data on low-mass stars had to await the work of Barbera et al. (1993), who showed that K-type dwarfs are common X-ray emitters with X-ray luminosity ranging between $\log L_{\rm X} \simeq 27.0$ erg s^{-1} and $\log L_{\rm X} \simeq 29.5$ erg s^{-1}, with a median $\log L_{\rm X} \simeq 27.7$ erg s^{-1}, i.e. very similar to the behavior of G dwarfs. M dwarfs were also found to be

common emitters, although at a level somewhat lower than the earlier spectral types, with a range of luminosity between $\log L_X \simeq 26$ erg s^{-1} and $\log L_X \simeq 29$ erg s^{-1}, and a median $\log L_X \simeq 27.2$ erg s^{-1}.

One issue which was raised from the *Einstein* data is whether there is a change in the coronal emission level around spectral type M5. The theoretical basis for the question is the change in stellar structure taking place at this spectral type: earlier type stars have a solar-type structure, with a radiative core and a convective envelope, which gets deeper in the later spectral types, until it disappears completely at around spectral type M5, where stars become fully convective (as first pointed out by Copeland et al., 1970). According to theory this leads – as discussed in Sect. 5.1 – to a change in the type of dynamo expected to be at work in the stellar interior, and thus to possible differences in the level of coronal emission.

X-ray emission from very late-type stars was soon detected with *Einstein*, with Johnson (1981) reporting an X-ray detection of the very low mass star VB 8 (whose spectral type, dM7e, only became available later Dahn et al., 1986, so that it was not clear initially that the star was fully convective). Using the whole *Einstein* database of observations Barbera et al. (1993) showed that the *Einstein* data were indeed compatible with a drop in the X-ray emission level of M dwarfs at spectral type M5 (or absolute magnitude $M_V = 13.4$), at the $\simeq 99\%$ confidence level. The drop was present both in the X-ray luminosity and in the X-ray surface flux. They also found a correlation between X-ray activity level and kinematics (a statistical age indicator) for these stars, which they interpreted as evidence for an age-activity correlation, with activity decreasing in the older stars as expected (see Sect. 9.2 for a discussion of the age evolution of X-ray activity in dM stars).

Later Schmitt et al. (1995) addressed the X-ray emission of K and M dwarfs using a complete volume limited sample observed with ROSAT (analogously to what done for F and G dwarfs, see Sect. 4.1). Once more, it was shown that X-ray emission (and thus the presence of a corona) is a universal feature, also for cooler dwarfs, which have a minimum surface X-ray flux level similar to the one observed in F and G dwarfs (Fig. 5). Again, X-ray dark K and M disk population dwarfs, if they exist at all, are extremely rare. The higher sensitivity of the PSPC allowed to detect M dwarfs with X-ray luminosity as low as $\log L_X = 25.7$ erg s^{-1}. Similar to what was found for F and G dwarfs, more X-ray luminous stars have hotter (harder) spectra.

Fleming et al. (1995) explored the properties of the ROSAT K and M dwarf sample, concluding that no change in the X-ray properties of M dwarfs was visible down to absolute magnitude $M_V = 15$. In particular no decrease in the X-ray activity at spectral type M5 was visible, so that the earlier *Einstein* results would seem to have been affected by selection effects. Also, no correlation is present in the Fleming et al. (1995) ROSAT sample between the X-ray emission level and the kinematic properties, while a correlation

was found between X-ray emission level and photospheric metallicity, with metal-poor stars showing a lower X-ray emission level. Such decay with the metallicity is consistent with the results obtained for dM stars in open clusters (Sect. 9.2), which allow younger and more metal-rich M dwarfs to be sampled than available in the nearby field population.

The decay of X-ray emission with metallicity observed in the volume-limited sample of Fleming et al. (1995) could either be an indirect reflection of the age-activity correlation (which would thus question the validity of kinematics as an age indicator for nearby stars) or be due to a difference in the coronal structure induced by the varying metal abundance on e.g. the radiative losses of the coronal plasma. Although it is still unclear which one of the two interpretations applies (see Sect. 9.5), given the very weak correlation observed between age and metallicity in field dwarfs (e.g. Edvardsson et al., 1993) and the presence of an age-activity correlation for dM stars (Sect. 9.2) the latter would appear to be a more plausible hypothesis.

Giampapa et al. (1996) analyzed the PSPC spectra of a number of M dwarfs sufficiently bright for a spectral analysis of the X-ray emission, arguing that (under the assumption of a two component isothermal model fit to the PSPC spectrum – commonly referred to as a "2-T fit") the temporal variability of X-ray emission is concentrated in the hot component (with typical temperatures $T \simeq 10$ MK), while the emission measure of the cooler component (with $T \simeq 2$–4 MK) is constant in time. This led them to hypothesize that two physical components are actually present in the coronae of dMe stars. By modeling the two components with hydrostatic loop models, they further showed that the cool component must be composed of small ($L \ll R_*$) high-pressure ($p_0 > p_{0\odot}$) loops, while two solutions are possible for the hotter component, i.e. large loops ($L \gtrsim R_*$) with a filling factor $f \simeq 0.1$ or small loops ($L \lesssim R_*$) with a very small filling factor $f \ll 1$. Later Favata et al. (2000a), analyzing several flares on the dMe star AD Leo showed that the flaring loops (when modeled with the hydrodynamic models of Reale et al., 1997, as discussed in Sect. 7) are in all cases small (with typical sizes $L \simeq 0.3 R_*$), ruling out the first of the two possibilities, so that coronae on dMe stars appear to be confined to compact loops, with no evidence for large loops extending to large distances from the star. Micela et al. (1997b) analyzed the temporal variability of the emission measure produced through 2-T fits for a set of older (and thus less active) M dwarfs, showing that, although the hot component indeed exhibits more intense variations than the cool one, the variations are strongly correlated, pointing to the corona being composed of a single set of structures (rather than the two distinct sets of structures hypothesized by Giampapa et al., 1996). In principle there could be a difference in the coronal structures of young and old M dwarfs (the stars of Micela et al., 1997b being one order of magnitude fainter in X-rays than the ones of Giampapa et al., 1996), so that a similar correlation analysis on the more

active stars would be useful to understand whether the observed temporal variations of the components are indeed independent.

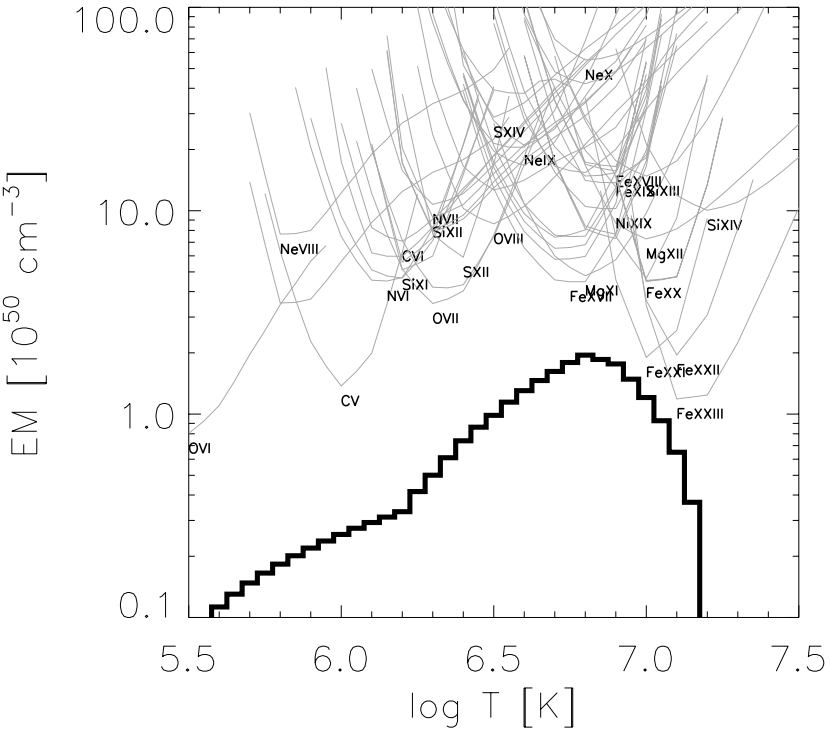

Figure 7. The differential emission measure for the corona of AD Leo, derived from the *Chandra* LEGTS spectrum, from Maggio et al. (2002).

Maggio et al. (2002) have studied the high resolution *Chandra* spectrum of AD Leo, showing that a continuous differential emission measure (DEM), with no evidence of bimodality, as shown in Fig. 7, is necessary to explain the rich X-ray spectrum (as earlier discussed by Cully et al., 1997 in their analysis of the EUVE spectrum of a flare on AD Leo). The two discrete temperatures found by Giampapa et al. (1996) in the fit to the PSPC spectrum are in good agreement with the peak of the DEM (for the hot temperature) and with the "barycenter" of its low-temperature tail (for the cool temperature). Thus, perhaps a more likely interpretation is one in which only one set of coronal structures is present (with a single typical size and filling factor), filled with low temperature plasma in quiescence, and in which the hot plasma appears during the frequent flaring episodes visible in the light curve of the harder photons.

While no drop in coronal activity is visible at the fully convective boundary, a significant change in coronal properties is apparent for the still cooler dwarfs, with a drop in the coronal heating efficiency evident for stars fainter

than $M_V \simeq 17.5$ (see Fig. 8). Only very few stars with $M_V > 17.5$ are known in the solar neighborhood (and are thus accessible to X-ray observations) so that the data are quite sparse and any conclusion perforce preliminary.

The coolest stellar objects for which X-ray activity has been conclusively established are the M8V star VB 10 (Gl 752B) and the M9V star LHS 2065. Fleming et al. (2000) detected a flaring event in a ROSAT HRI observation of VB 10, with a peak X-ray luminosity of order $L_X \simeq 3 \times 10^{27}\,\mathrm{erg\,s^{-1}}$. No quiescent X-ray emission was visible in the ROSAT observation. Recently, Giampapa and Fleming (2002) obtained a deep *Chandra* observation of VB 10, detecting its quiescent X-ray emission at a level of only $L_X \simeq 3 \times 10^{25}\,\mathrm{erg\,s^{-1}}$ ($L_X/L_{bol} \simeq 10^{-5}$), significantly lower than the quiescent X-ray luminosity of M dwarfs with $M_V \lesssim 16.5$. Schmitt and Liefke (2002) detected (also using a ROSAT HRI observation) a flaring event on LHS 2065, with comparable peak X-ray luminosity (at $L_X \simeq 4 \times 10^{27}\,\mathrm{erg\,s^{-1}}$) as the VB 10 flare. Also, evidence for quiescent X-ray emission (at rather high luminosity, $L_X \simeq 2 \times 10^{26}\,\mathrm{erg\,s^{-1}}$) is found in the second of the two HRI observations analyzed (the two observations are separated by 6 months). Whether this is a true "quiescent" emission level or whether it is due to unresolved flaring activity (which would explain why the same quiescent emission level is not seen in the first of the two observations) will have to await for deeper observations of this object.

Whether X-ray activity is indeed as common (albeit at lower level) in these very late M dwarfs as it is in the earlier M dwarfs is still largely an open question (for lack of observational data). On the basis of observations of the Hα line Giampapa and Fleming (2002) argue that there is evidence for a general rather precipitous drop in the activity of very cool dwarfs. The data in Fig. 8 have been interpreted as suggestive of a dichotomy in the behavior of very late-type dwarfs, with the quiescent emission level decreasing rapidly with spectral type, while the level of the flaring coronal emission (at least for the more intense flares) remains essentially constant.

4.3.1. *Brown dwarfs*

Brown dwarfs are stellar objects with masses below 0.075–0.08 $M_\odot$. Below this mass (whose accurate value depends on e.g. the metallicity) the central temperature of the star never rises to the hydrogen burning limit (as first pointed out by Copeland et al., 1970), so that they will continue their gravitational contraction (with the exception of a brief deuterium burning episode for objects with $M \gtrsim 0.01\,M_\odot$) until eventually electron degeneracy sets in. In a sense brown dwarfs thus never reach the main sequence but continue contracting down the H-R diagram along the analog of pre-main sequence tracks for low-mass stars. Their optical luminosity is a strict function of age (being driven by gravitational contraction). If at their brightest these stars

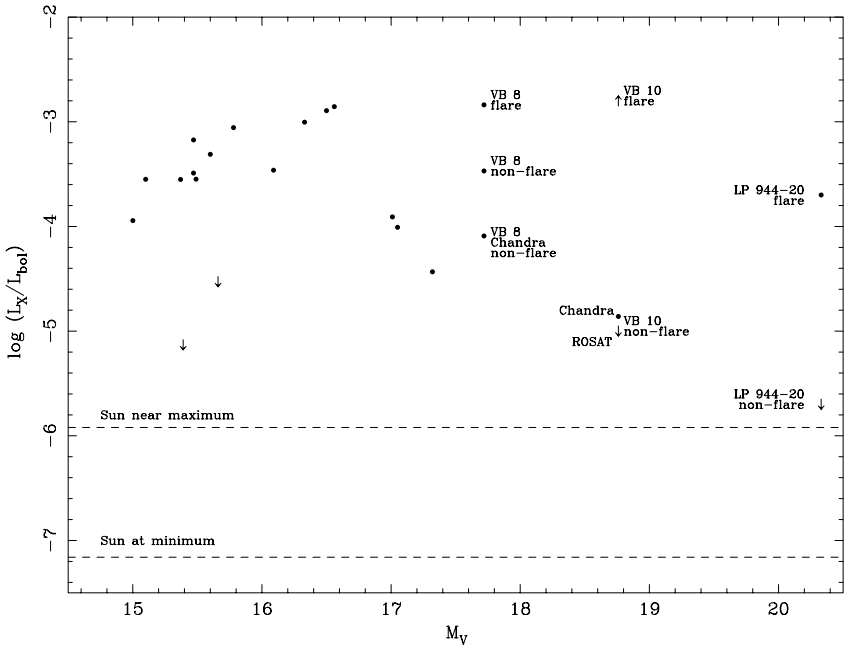

Figure 8. The X-ray emission level of late-type dwarfs (from Giampapa and Fleming, 2002). For the coolest objects both the quiescent and flaring X-ray luminosity levels are indicated. Note the apparent dichotomy between the flaring emission level (which stays roughly constant) and the quiescent level, which decreases significantly in the cooler stars.

emit at a saturated level (i.e. $L_{\rm X}/L_{\rm bol} \simeq 10^{-3}$, see Sect. 4.5) one would then expect the X-ray luminosity of brown dwarfs to be a strong function of age.

A similar question as the one regarding the transition to fully convective stars at around M5 applies to brown dwarfs, i.e. whether the transition to nuclear burning in the (fully convective) core affects the X-ray properties of a star. Their internal structure is fully convective, not unlikely the low-mass end of the dM stars, so that the same issues related to the working of the dynamo (see Sect. 4.3) arise here. Whether brown dwarfs are (significant) X-ray emitters at all has been answered positively only recently. The first systematic investigation of the X-ray properties of brown dwarfs was performed by Neuhäuser et al. (1999), who searched the ROSAT All Sky Survey (as well as a number of pointed ROSAT observations) for X-ray emission from known young ($t \lesssim 10\,$Myr) brown dwarfs, finding 2 X-ray sources among the 27 brown dwarfs surveyed. Further studies of individual young stellar associations have shown that X-ray emission is common among young brown dwarfs. For example Preibisch and Zinnecker (2001) have surveyed with

Chandra ACIS the very young cluster IC 348 ($t \simeq 1.3$ Myr), detecting as X-ray sources 4 out of 13 known brown dwarfs in the cluster. The detected X-ray luminosities range between 8×10^{27} erg s^{-1} and 4×10^{28} erg s^{-1}. The fractional X-ray luminosity for these objects is $L_X/L_{bol} = 10^{-4}$–10^{-3}, with coronal temperatures $T = 1$–2 keV (Preibisch and Zinnecker, 2002) similar to low-mass stars, with the X-ray brightest emitting at the saturation level, and the rest at lower levels. This would be compatible with a basic similarity in the X-ray emission mechanism between brown dwarfs and low-mass stars, i.e. the same type of corona is possibly at work in both stellar types. Evidence for flaring emission is also reported by Preibisch and Zinnecker (2002). Therefore, the crossing of the sub-stellar boundary seems to have little influence on the existence and structure of the corona, with a substantial continuity in coronal properties between stars and brown dwarfs.

The *Chandra* observations of the Orion nebula cluster (Feigelson et al., 2002a; Flaccomio et al., 2003a) also suggest that the behavior of X-ray emission from young brown dwarfs can be understood as a simple extension of the behavior of low-mass stellar objects, i.e. that they indeed generally emit, at this young age, at a level close to the saturation, with $L_X/L_{bol} \simeq 10^{-3}$.

Contrary to the very young brown dwarfs discussed above, older brown dwarfs appear to have low levels of quiescent X-ray emission. Recently, flaring X-ray emission has been detected in a *Chandra* observation from a much older ($t \simeq 500$ Myr) rapidly rotating brown dwarf, LP 944−20 (Rutledge et al., 2000). The flare lasted 1–2 hr, with an estimated peak X-ray luminosity $L_X \simeq 1.2 \times 10^{26}$ erg s^{-1}, corresponding to $L_X/L_{bol} \simeq 2 \times 10^{-4}$, and an estimated peak temperature $T \simeq 0.3$ keV. No X-ray photons were detected from the preflare, quiescent phase, with an upper limit to the quiescent X-ray luminosity $L_X < 10^{24}$ erg s^{-1} ($L_X/L_{bol} < 2 \times 10^{-6}$). Recently Martín and Bouy (2002) used a deep XMM-*Newton* observation to revise the upper limit to the quiescent X-ray luminosity downward to $L_X < 3 \times 10^{23}$ erg s^{-1}. Therefore, these older objects, while still displaying activity (as testified by the flare) have a very low level of quiescent X-ray emission. Whether they have a quiescent corona at all is a subject of debate. Martín and Bouy (2002) also estimate, using all the available X-ray observations of LP 944−20, that strong flares are rare, taking place less than $\simeq 1\%$ of the time.

4.4. X-RAY EMISSION FROM ACTIVE BINARIES

The high chromospheric activity level of some short-period binary systems, of which RS CVn is the prototype, was known already well before the beginning of coronal X-ray astronomy. Their high soft X-ray luminosity was apparent in the data from the HEAO-1 satellite (Walter et al., 1978; Walter et al., 1980), but, as with the other stellar types, the determination of their activity level as a class came with the data from the *Einstein* observatory

(Pallavicini et al., 1981). Majer et al. (1986) presented the results from an *Einstein* survey of active binaries, which established their high X-ray luminosity level (the objects in their sample were spanning a range $29.0 \leq \log L_{\rm X} \leq 31.5$ erg s^{-1}), and high coronal temperatures. Fits to the IPC spectra invariably required two temperatures, the lower at $T \simeq 3$ MK, the hotter at $T \gtrsim 10$ MK, indicative (given the low spectral resolution of proportional counters) of an underlying continuous emission measure distribution spanning a broad temperature range. They also found no correlation between the rotational velocity of the stars and their X-ray luminosity (as expected for stars emitting X-rays at their "saturation" level, see Sect. 4.5).

The need for multiple emission components, or temperatures, in the X-ray spectrum of active binaries had already been established, on a smaller sample of objects, by Swank et al. (1981), who had analyzed the X-ray spectra from eight well known active binaries, obtained with *Einstein*'s Solid State Spectrometer, which had a spectral resolution comparable to the CCD detectors of ASCA. Swank et al. (1981) also used the scaling laws of Rosner et al. (1978) to show that one possible scenario compatible with their spectral data was that X-ray emission was being produced, in these objects, in large, low-pressure loop structures. This was soon taken as justification for scenarios involving large, interconnecting loops in binary systems (e.g. Uchida and Sakurai, 1983) as discussed in Sect. 6.2.1. The study of flares on these objects shows however that the active corona is confined in structures smaller than the stars, so that these extended active coronal structures are unlikely to exist (Sect. 7.2).

A more complete survey of the X-ray emission of active binaries was performed with the ROSAT All-Sky Survey. A large sample of 112 systems was studied by Dempsey et al. (1993a), who confirmed the large X-ray luminosity observed with *Einstein*, and the lack of strong correlation with rotation or with other stellar parameters. The emission was found to peak at $L_{\rm X}/L_{\rm bol} \simeq 10^{-3}$, again indicative of emission near the saturation level. A study of the coronal temperatures derived from the PSPC spectra, for the 44 systems with sufficient statistics (Dempsey et al., 1993b), confirmed the presence of a bimodal distribution in the best-fit temperatures, with values typically centered at $T \simeq 2$ MK, and $T \simeq 16$ MK, fully in line with the earlier *Einstein* results. Dempsey et al. (1997) studied, in a similar fashion, the characteristics of the X-ray emission of a sample of 35 BY Dra systems (see below) finding similar X-ray spectral characteristics as for the RS CVn-type systems.

The high activity level of these stars is generally interpreted as due to their fast rotation, itself a consequence of (partial) tidal locking of the stellar rotation period with the orbital period of the binary. Apart from this, active binaries are a rather heterogeneous group, with all short-period binary systems with a late-type component included in the class, irrespective of the evolutionary status and of other characteristics. Different authors have

employed different definitions, and most studies have based themselves on the catalog of chromospherically active binaries of Strassmeier et al. (1993), itself a compilation of data from the literature. While the original definitions of the various subclasses of active binaries included e.g. the presence of photospheric spots, currently systems with one or both evolved components are classified as RS CVn-type, while systems where both components are late-type low-mass K or M dwarfs are classified as BY Dra-type. Active binary system in which both components are F or G dwarfs are classified as W UMa-type if in a contact binary, and lack a specific class for detached systems, although they are often included in the RS CVn group. This lack of homogeneity is probably one of the reasons for which attempts to ascertain properties of the coronal emission from active binaries as a class, e.g. by correlating with other stellar parameters, have not been successful.

Algol-type binaries, in which one of the two components is an X-ray dark early type star, are also bright X-ray sources. Also for them the tidal locking of the stellar rotation of the late-type component to the orbital period of the system is likely to be the driver of the high X-ray luminosity. A survey of their X-ray emission (compared to RS CVn-type objects) has been performed by Singh et al. (1995) and Singh et al. (1996a).

4.5. Correlation between X-ray activity and rotation

The magnetic fields visible on the solar surface and responsible for the solar activity phenomena are thought to be produced in the stellar interior through some dynamo mechanism. While a complete, self-consistent dynamo theory is still missing, the driving mechanism appears to be the complex interaction between rotation and convection, with faster rotation resulting in enhanced dynamo action. On the basis of a general stellar-solar analogy a similar mechanism is thought to be operating in the other "solar-like" stars, for which an activity-rotation connection is thus expected.

A correlation between stellar rotation and activity level was already noticed in the early *Einstein* observations, by Walter and Bowyer (1981) on a sample of RS CVn systems, and by Pallavicini et al. (1981) on a larger sample of stars of different types. These observations found a quadratic relationship between the X-ray luminosity and the rotational velocity projected along the line of sight ($v \sin i$), as shown in Fig. 4. Following these pioneering studies, a large number of papers were devoted to the exploration of this relationship, enlarging the samples and the parameter ranges (see e.g. Schmitt et al., 1985; Maggio et al., 1987; Hempelmann et al., 1995 to mention a few), essentially confirming that a quadratic dependence links rotation and X-ray activity level through the range of parameters explored. Note that while rotational period $P_{\rm rot}$ is a better quantity against which to study the dependence of activity level, projected rotational velocities are much easier to observe, and thus formed the

basis of the early work. Later, when photometrically determined periods have become available for large samples of stars, they have been used, resulting in a tightening of the correlations observed earlier against $v \sin i$.

At the same time it became evident that fast rotators do not follow the quadratic relationship found by the early work. Rather, the X-ray luminosity of stars with rotational velocity above a given value remains approximately constant around a maximum allowed value of L_X corresponding to a fixed fraction ($\simeq 10^{-3}$) of the star's bolometric luminosity, something which became known as "saturation" (Sect. 4.5), as first discussed in the X-ray context by Vilhu (1984). The typical case is that of the fast rotators among Pleiades dK stars, whose *Einstein* observations provided early evidence of the phenomenon (Caillault and Helfand, 1985; Micela et al., 1985).

Saturation, which from an observational point of view is defined by the flattening of the relationship of activity with rotation, had been observed earlier for chromospheric and transition region emission: Vilhu and Rucinski (1983) found that the chromospheric and transition region emission of solar-type stars saturates at rotational period of $\simeq 3$ days, and Saar (1991) found a saturation of the filling parameter[2] f. The phenomenon can be interpreted in a framework in which the increase of activity level is mostly driven by an increase in coverage of the stellar surface by active regions; saturation would then correspond to the maximum coverage possible of the stellar surface by active regions. At the same time this implies a saturation of the maximum quantity of energy that the heating mechanism is able to deposit in corona; the existence of saturation would thus indicate that the dynamo mechanism has a maximum efficiency governed by the the bolometric luminosity.

The existence of a "universal" saturation level $L_X/L_{bol} \simeq 10^{-3}$ naturally implies that different stellar types will show a different level of maximum, saturated X-ray luminosity, with fainter, lower-mass stars saturating at lower L_X and therefore at lower rotational velocity (larger P_{rot}). In the X-ray regime Pizzolato et al. (2003), using a relatively large sample of stars, have recently shown that the saturation period goes from 1 day for early dG stars to $\simeq 4$ days for early dM stars.

A useful parameterization of this dependence of the saturated X-ray luminosity and rotational period on the stellar type has been obtained in the form of a relationship between L_X/L_{bol} and the so-called "Rossby number", defined as the ratio between the rotational period and the convective turnover time (which is a function of the bolometric luminosity). Originally the relationship between activity and Rossby number had been determined empirically by Noyes et al. (1984), based on Ca II H&K observations, and has been later applied to the the X-ray regime in various samples (Micela et al., 1984;

[2] representing the total fraction of the stellar surface which is covered by the coronal loops under certain model assumptions.

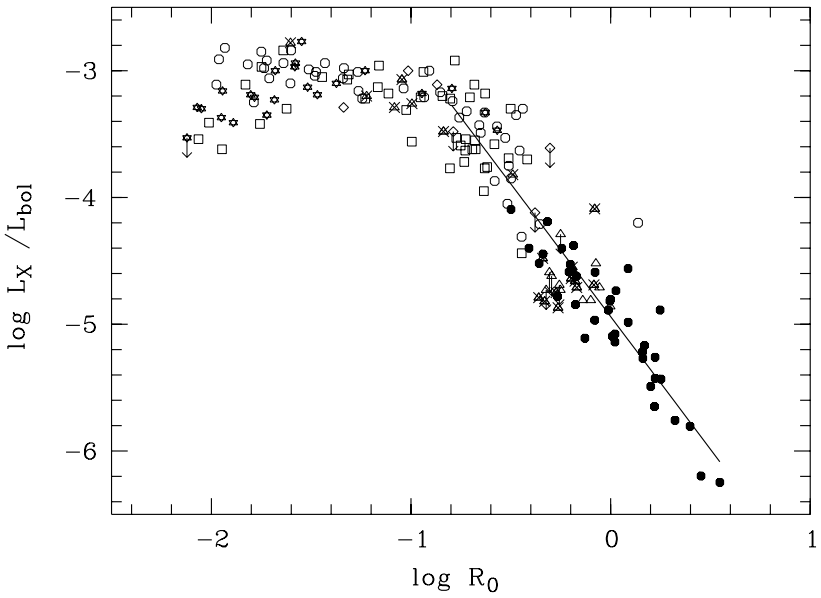

Figure 9. Fractional X-ray luminosity vs. Rossby number for open cluster (open symbols) and field stars (filled symbols). Different symbols refer to different clusters. Both the tight correlation between X-ray luminosity and Rossby number for $\log R_0 \gtrsim -1$ and the saturated regime for $\log R_0 \lesssim -1$ are visible. From Randich (2000).

Schmitt et al., 1985; Maggio et al., 1987; Hempelmann et al., 1995; Patten and Simon, 1996; Randich, 2000).

In the non-saturated regime the L_X/L_{bol} vs. Rossby number relationship is equivalent to the L_X vs. P_{rot} relationship, since the convective turnover time is proportional to $\sqrt{L_{bol}}$, while in the saturated regime it unifies the L_X vs. P_{rot} relationships for all spectral types. In practice two characteristic times, the rotational period P_{rot} and the convective time τ_{conv} (computed at some position in the convection zone), appear to compete. When $P_{rot}/\tau_{conv} > R_0^{crit}$, the $L_x - $rotation relationship holds, while when $P_{rot}/\tau_{conv} < R_0^{crit}$ saturation occurs. The change between the two regimes occurs when $P_{rot}/\tau_{conv} \simeq R_0^{crit}$ (as apparent from Fig. 9, $R_0^{crit} \simeq 0.1$), and in fact, although with a large spread, the rotational period at which the saturation occurs is linearly related to the convective turnover time (Pizzolato et al., 2003).

In addition to the well observed phenomenon of the saturation, a super-saturation, i.e. a decrease of X-ray luminosity for the very fast rotators, has in some cases been observed, in particular in late-type stars in young clusters

(Randich, 1998). A hint of decrease in X-ray luminosity, attributed to super-saturation, is visible at the lowest values for the Rossby number in Fig. 9.

The origin of saturation and of super-saturation is unclear and several hypotheses have been put forward to understand the origin of these phenomena. The mechanisms which have been invoked include dynamo saturation (see e.g. Charbonneau and MacGregor, 1992), the suggestion that in fast rotators more open-field regions are created, or that fast rotation induces a concentration of magnetic flux to the poles (Solanki et al., 1997), or that the centrifugal force produces an increase of density in the outer parts of the magnetic loops, stressing, distorting and opening the closed magnetic field (Jardine and Unruh, 1999).

5. Open problems in coronal physics

Many key issues in coronal astronomy are still far from resolved, and many widely accepted paradigms do not rest on physical modeling but rather on analogies with the Sun and qualitative reasoning. For example the mechanism (or mechanisms) responsible for the heating of the corona is still not clear, and no satisfactory theory of coronal heating exists even for the Sun. Here we will briefly discuss two of the open problems with direct observational implications, namely the dynamo mechanisms and the presence of activity cycles.

5.1. Dynamo mechanisms

Coronal activity dissipates magnetic fields, which in the Sun are observed to emerge continuously from the interior, so that magnetic fields must be continuously generated within the solar – and stellar – interior through some hydromagnetic dynamo process. Dynamo action is the result of a highly non-linear interaction between several components, which include the bulk gas motions in the stellar interior (in particular in the convective envelope), the stellar rotation, and the pre-existing magnetic fields. Questions such as the exact location of the dynamo, or which are the relevant fluid motions, are still largely subject to debate (although recent helioseismic results – see e.g. Christensen-Dalsgaard, 2002 for a recent review – have led to significant advances). However, a self-consistent dynamo theory with predictive power is still missing. A review of dynamo theory is outside of the scope of the present work, and we refer the reader to the excellent introduction of DeLuca and Gilman (1991), who discuss the key characteristics of the solar-type dynamo. The dynamo at work in solar-type stars is thought to depend on the interaction between the twisting effect on the field induced by the convective eddies (the "α" effect) and the shearing of the field's toroidal component by

the star's differential rotation (the "ω" effect), and is therefore called an α–ω dynamo. Such dynamo cannot operate in the bulk of the convective envelope (see p. 288 of DeLuca and Gilman, 1991 for a discussion of the "dynamo paradox"), and both theoretical indications and recent helioseismic results show that the solar dynamo is most likely located at the base of the convection zone at the interface with the radiative core.

The α–ω dynamo is thus not expected to operate in fully convective stars (as for example low-mass pre-main sequence and main sequence stars of spectral type later than about M5, Sect. 4.3). Another type of dynamo depends solely on the action of the convective eddies (Durney et al., 1993) – thus called an α^2 dynamo – and can therefore be at work also in fully convective stars. Less magnetic flux should be generated by a turbulent dynamo (as compared to the case of the solar-type "shell" dynamo) because there is no stable overshoot layer where the fields can be stored and amplified, and only small-scale magnetic regions should emerge uniformly distributed on the surface (in contrast with the larger scale magnetic fields generated by the α–ω solar-like dynamo[3]), because the crucial ingredient is small-scale turbulent flow field, rather than large-scale rotational shear.

However, convection has the tendency to pump magnetic fields downward ("turbulent pumping", Brandenburg et al., 1992; Tobias et al., 1998), so that – in a fully-convective star – fields may accumulate near the center. Sufficiently strong magnetic fields can lead to the formation of a radiative core (Cox et al., 1981), which could be the seed for a resurrection of a "shell" dynamo mechanism, so that the strong activity observed in some late dwarfs (Sect. 4.3) could still be due, through this feedback process, to the same dynamo mechanism as in earlier type stars.

Coronal observations, regarding elements such as the presence or lack of coronal cycles (Sect. 5.2), the location of coronal structures on active stars as well as their characteristic sizes, constrain the sites of emergence and the scales of the magnetic fields in stars other than the Sun. Also, whether the transition to full convection indeed leads to different coronal characteristics (Sect. 4.3) is another observational constraint to dynamo theory.

5.2. ACTIVITY CYCLES

One of the earliest established properties of sunspots was the cyclical variation of their number. The existence of such cycle was first postulated by Schwabe (1843), and later the period of about 11 years was extablished. The variation in number of sunspots is connected with the cyclic variation

[3] Although the presence of large-scale asymmetries in the convection patterns in the star, e.g. in the form of a "handedness" between the northern and southern emispheres of the star could induce the generation of large-scale magnetic fields, even for a pure α^2 dynamo (D. Hughes, priv. communication).

observed for a large number of solar coronal physical parameters, including the intensity of the X-ray and EUV emission, as well as the chromospheric emission level and others. As shown in Fig. 10 the average X-ray luminosity of the Sun in the 0.73–2.5 keV band (as observed by Yohkoh) along the cycle varies by some two orders of magnitude, although e.g. rotational modulation creates a large spread in the X-ray luminosity.

There is significant evidence that the activity cycle of the Sun is not always operating, and that in particular there are extended periods of time during which the cycle appears to "switch off". The best known (and studied) one is perhaps the "Maunder minimum", a period of time between 1645 and 1715 in which the Sun showed no evidence for spots (and thus likely a very low X-ray and chromospheric activity).

The existence of activity cycles in other solar-type stars has been conclusively established by the ongoing long-term monitoring program of chromospheric emission in a large sample of solar-type stars (using the emission in the Ca II H&K lines as a diagnostic), which began already in 1966 thanks to the foresight of O. Wilson. A sufficiently long observational baseline is now avalaible, allowing to assess whether cycles with periods of several years are present in the target stars. The Mt. Wilson data have been discussed by Baliunas et al. (1995), the main result being that solar-like cycles are present in a number of stars, but they are not an universal feature. In addition to cyclic stars, a number of stars in the Mt. Wilson sample show a constant Ca II index, with a featureless light curve in time, and another significant group show a evidence for irregular, non-cyclical variations. Whether the "flat" stars are stars with no activity cycles at all, or whether they are cyclic stars which have been observed during a temporary "Maunder-like" minimum activity state is still an open question, although some stars appear to show evidence for a transition from a cyclic state to a flat state. One general trend apparent from the Mt. Wilson sample is that stars with high (chromospheric) activity levels have a higher tendency to show irregular variations, while intermediate activity level stars are more likely found in a cyclic state, and low-activity ones tend to have flat lightcurves. The scatter of this relationship is however very large (see Fig. 2 of Baliunas et al., 1995), so that the activity level alone is not a good predictor of a star's cyclic behavior.

The original Mt. Wilson sample has not been selected in a statistically "clean" way (it is not e.g. volume limited), so that it is not unfortunately possible to make meaningful statements about for instance the relative fraction of stars with cycles.

In the solar case the amplitude of the cycle modulation of the Ca II chromospheric flux is small, less than 50%, while in the X-rays the amplitude is much larger, some two orders of magnitude. Notwithstanding the level of modulation which would thus be expected, whether stars other than the Sun exhibit a cyclic behavior in their X-ray emission is still an open question.

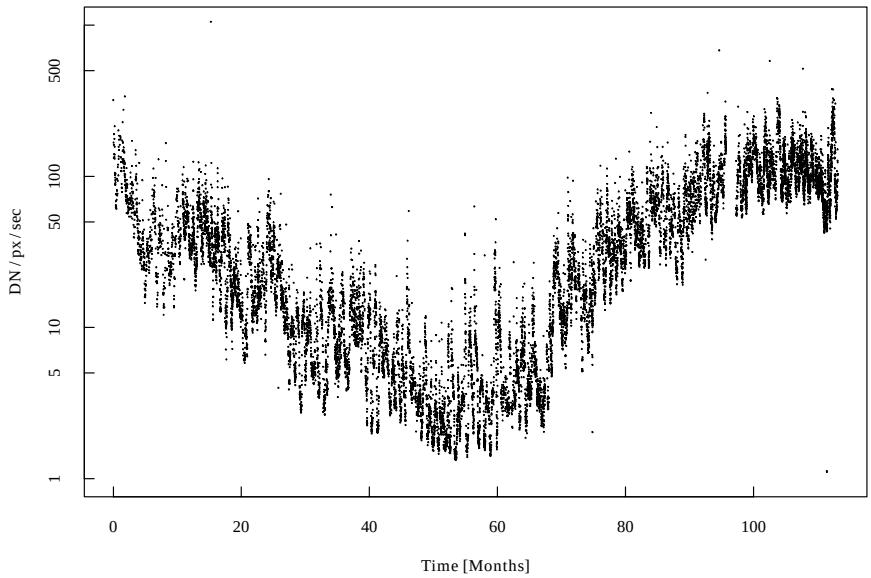

Figure 10. Solar coronal X-ray luminosity along an entire solar cycle (starting in mid 1991) in the 0.73–2.5 keV band (AlMg filter) from Yohkoh synoptic observations. In addition to the long-term variability due to the effects of the 11 year cycle the cyclic variability due to the solar rotational modulation is evident. The units are instrumental.

The reason for this is at least in part observational: no comparable long-term stellar observational data base is available in the X-rays as it is in the chromospheric lines, given that satellite observing time is a much scarcer resource than the observing time at the moderate ground-based telescopes used for the Ca II monitoring program.

The (lack of) evidence for stellar X-ray cycles had been reviewed by Stern (1998). High-activity stars (e.g. RS CVn-type binaries) show evidence for their X-ray flux being reasonably constant (i.e. within a factor of $\simeq 2$) on time scales of several years. Kashyap and Drake (1999) studied the long-term variability of RS CVn-type binaries using *Einstein* and ROSAT data, finding marginal evidence for larger variations being present on a 10 yr time scale than on 1–2 yr scale. This constrains the possible amplitudes of cyclic variations (in the ROSAT bandpass) to a factor of ≤ 4 (much smaller than the amplitude of the solar cycle).

Stars in young open clusters (thus, high-activity objects) are good targets for these studies, having been observed with many X-ray observatories: for the Pleiades, there is evidence that a large fraction (up to $\simeq 40\%$, Gagné et al., 1995b) of solar-type stars indeed show significant (larger than a factor of 2)

long-term variations in their X-ray luminosity, and that the level of variability on long (10 yr, the interval between the *Einstein* and ROSAT observations) time scales is marginally higher than the level of variability apparent on short time scales (few months to 1 yr, the span of the PSPC data set). In principle this additional variability level could be due to cyclic variability, but the evidence is marginal at best. The addition of a ROSAT HRI observation (Micela et al., 1998) has allowed for a 15 yr baseline to be covered, but has not changed the earlier conclusions.

For stars in the Hyades, the evidence for significant long-term variability is even weaker. Stern et al. (1995b) compared the RASS observations of stars in Hyades with the *Einstein* observations of the same stars, showing that for more than 90% of the stars the variability over the 10 yr baseline was at most a factor of 2. Interestingly, among the few objects showing evidence for significant long-term variability are three of the four giants in Hyades. Thus, observational results are compatible with a lack of (strong) cyclic behavior for high activity main-sequence stars. Additional information will be available from the recent observations of young open clusters performed by *Chandra* and XMM-*Newton*; the detailed comparison with the earlier observations has however not yet been performed. The general lack of observed cyclic variability in very active stars has been interpreted (Drake et al., 1996b; Kashyap and Drake, 1999) as due to their being dominated (also for stars which are not fully convective) by an α^2 dynamo, rather than by a solar-type α–ω dynamo so that indeed the coronae of highly active stars, with saturated activity levels, would be driven by a different underlying mechanism than stars with a solar activity level.

Indirect evidence for the presence of X-ray cycles in low-activity, normal disk population solar-type stars is accumulating. Hempelmann et al. (1996) have performed a study of the RASS observations of the solar-type stars which show cyclic behavior in the Mt. Wilson sample, showing that (once the dependence on rotational velocity is removed) the X-ray flux of these stars shows evidence for a modulation (of about a factor of 10) in phase with the Ca II cycles. The data sample is quite sparse, and the observed modulation is also compatible with a null result at the $\lesssim 6\%$ level, so that it constitutes at most suggestive evidence for the presence of cycles in these stars.

Similar evidence has been obtained by Marino et al. (2002) analyzing the variability of a group (ca. 10) of field solar-type stars which have been observed with the ROSAT PSPC with an observational baseline spanning up to 4 years. In most cases these stars, while not variable on short time scales, show significant variability on the time scale of a few years, with a typical range in long-term X-ray luminosity of a factor of $\simeq 3$. This exclusively long-term variability is compatible with being due to cycle-like variations.

For later-type low-activity M dwarfs Marino et al. (2000) show that no such dichotomy in long vs. short term variability is present: the X-ray vari-

ability level of M dwarfs is in general higher than for G dwarfs, but with no evidence for additional variability on longer time scales with respect to the short time scales. Also, the distribution of variability amplitudes for M dwarfs is compatible with the distribution of amplitudes for solar flares, so that the observed variability is compatible with being due (mostly) to flare activity. Drake et al. (1996b) studied the behavior of the very late type dMe star VB 8, which does not show significant X-ray variability over 10 yr, a result which they interpret in terms of a corona dominated by an α^2 dynamo.

Tentative direct evidence for X-ray cyclic modulation has been claimed for the young solar analog EK Dra, for which Güdel et al. (2002b) show a long-term (10 yr baseline) X-ray light curve, in which some modulation is evident, in phase with the amplitude of the photometric modulation (and thus purportedly with starspot coverage). This modulation is however small (a factor of $\simeq 2$), much smaller than for the solar cycle, and X-ray fluxes have been determined with a variety of X-ray detectors, so that the lack of homogeneity may result in some bias in the data.

Proper study of the X-ray cyclic behavior in stars other than the Sun requires a program of dedicated periodic monitoring of solar-type stars on long time scales. The long foreseen life of *Chandra* and XMM-*Newton* makes such monitoring programs possible, and indeed two such programs have been approved for the XMM-*Newton* AO-1 and AO-2 observing cycles. Therefore, the knowledge on X-ray cyclic behavior on normal stars – other than the Sun – should improve significantly in the upcoming years.

6. The structure of stellar coronae

6.1. Structuring of the solar corona

The earliest imaging X-ray observations of the solar corona (see Fig. 1) show that the X-ray corona is highly structured; later Skylab observations showed that most of the X-ray emitting plasma is contained in magnetically confined loops. Coronal loops are well visible in the Yohkoh observations shown in Fig. 2, and the high degree of structuring revealed by the more recent high spatial resolution observations of the TRACE observatory is shown in Fig. 11. The theoretical characteristics of such structures were discussed by several authors in the late 1970's (Rosner et al., 1978; Craig et al., 1978; Jordan, 1980), who established some fundamental scaling laws relating the length of coronal loops to the peak plasma temperature and pressure. The Rosner et al. (1978) formulation of these scaling laws (the one which has been most often used and referred to in the literature) is

$$T_{\max} \propto (pL)^{1/3} \tag{1}$$

which applies to quasi-static loops smaller than the pressure scale height of the plasma, with uniform cross section and heating rate per unit volume along the loop. In quasi-static, steady-state loops the heating rate is balanced by radiative and conductive losses at each location along the loop, with the plasma being in hydrostatic equilibrium. Later works extended this relationship to loops higher than the pressure scale height (Serio et al., 1981) and to expanding loops (Vesecky et al., 1979; Ciaravella et al., 1996; van den Oord et al., 1997). The above scaling law relates local parameters ($T_{\rm max}$ and p) to the global loop parameter L, suggesting that the physical conditions of steady-state coronal loops depend only on the local heating deposition along the loop.

In the stellar context, the simple quasi-static coronal loop has often been used as a building block to model different characteristics of the observed integrated emission. This includes the modeling of stellar flares (Sect. 7) as well as attempts at modeling the observed, disk-integrated emission measure distribution (e.g. Sect. 11.2.1). Thus, understanding whether indeed real solar coronal structures behave as quasi-static, steady-state loops directly affects the understanding of stellar coronal observations.

The applicability of these simple scaling laws to actual solar coronal loops was tested on data from Skylab observations by e.g. Rosner et al. (1978), and subsequently on loops observed by Yohkoh by e.g. Porter and Klimchuck (1995) and Kano and Tsuneta (1995). Porter and Klimchuck (1995) found that the observed lifetime of the Yohkoh loops is much longer than the computed cooling times, so that the loops indeed appear to be in a state of quasi-static equilibrium.

The more recent observations of the solar corona performed with TRACE are showing (thanks to their high spatial and temporal resolution) a more complex and still somehow controversial picture. Some analyses (e.g. Aschwanden et al., 2000) of loops seen in the TRACE images result in much flatter temperature profiles and higher densities than predicted by the simple scaling laws of Eq. 1. Aschwanden et al. (2000) interpret their findings as implying that coronal loops are in general not uniformly heated, or even heated from the top, but appear to be heated in their lower parts, so that significant mass upflows are required (see also Aschwanden, 2001).

Other analyses of loops seen in TRACE images on the other hand find loop structures which are well described by quasi-static loop models (Testa et al., 2002). Whether different populations of loops exist in the solar corona (perhaps with a difference between “cool” loops, seen by TRACE and “hotter” loops, seen by Yohkoh, as proposed by e.g. Aschwanden et al., 2000), or whether the issue lies in the different analysis methods used by different authors is still unclear. One issue affecting most studies of solar loops is that the structures being studied are individually chosen, so that the applicability

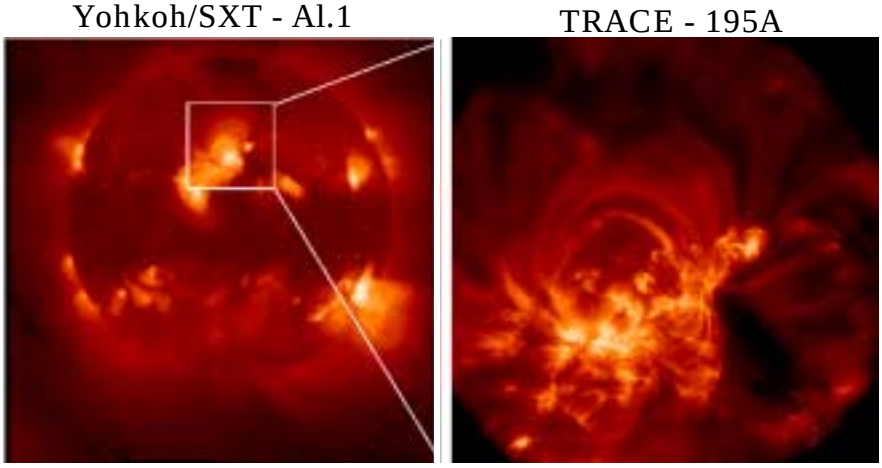

Figure 11. The left panel shows the solar corona as seen by Yohkoh on 13 Aug. 1998, while the right panel is a zoom of one of the active region, as seen by the TRACE observatory; the high level of structuring of the coronal loops is clearly visible. From Testa et al. (2002).

of the results obtained in terms of the population statistics of solar coronal loops (and thus their applicability to the stellar case) is unclear.

The interpretation of the TRACE data is still being debated. Whether the physics of loops is indeed much more complex and dynamic than embodied in quasi-static models, and whether the simplistic modeling approaches at times carried out on stellar X-ray spectra, or the use of scaling laws to derive e.g. spatial scales when the a density and temperature are known, are likely to lead to correct results remains to be seen.

In the Sun, even assuming that the individual loops can be reasonably well described by the simple quasi-static models discussed above, in practice the corona is constituted by a broad population of loops, spanning a range of characteristics and parameters, which cannot be easily determined by the inspection of the disk-integrated X-ray emission alone (i.e. by studying "the Sun as a star", as discussed in Sect. 11.2). Even if solar-like loops are the basic building block of stellar coronae, it is likely that as broad a population of loops exists there as in the solar corona, and that the integrated X-ray spectrum alone will not necessarily unveil the complexity of the emitting region population (see e.g. Judge, 2002).

For stars, no direct evidence for the presence of coronal loops exists (due to the obvious lack of imaging resolution), although it's most often assumed that stellar coronae have similar types of structures as the solar one. As discussed below indirect evidence for the presence of magnetically confined structures in stellar coronae is supplied both by density measurements of the quiescent corona (Sect. 11.1), which are too high for a purely gravity-confined, hydrostatically supported plasma, and thus require a mechanism for

confinement, and by the observation of flares, which again can only take place (with the observed characteristics, Reale et al., 2002) in confined structures (Sect. 7).

Finally, scaling laws empirically determined in actual coronal structures, both solar and stellar, can constrain the underlying heating mechanisms (as reviewed by both Mandrini et al., 2000 and Klimchuck, 2002). Although the theoretical heating models must be more fully developed and the observational uncertainties must be reduced before any definitive statements about specific heating mechanisms can be made, the technique could in the future supply significant constraints to more refined theories.

6.2. TOOLS FOR STUDYING THE CORONAL STRUCTURES

Given that stars are, in X-rays, unresolved point sources, all studies of their coronal structure have to rely – unlike the solar case – on indirect tools. Often – for lack of better information – it is assumed that the coronae of active stars are simply scaled up versions of the solar corona. As discussed above, the solar corona can be schematically represented by an ensemble of loop-like structures with characteristic sizes smaller than the solar radius itself[4], located at intermediate latitudes, with the polar region devoid of significant coronal activity (being the seat of the so-called coronal holes). While for stars with X-ray luminosity a few times the solar one the scaling from the solar picture is perhaps straightforward, whether and how this scaling can be extended to objects with X-ray luminosity up to 10^4 times (and with temperatures up to 10 times higher) the solar value is still an open question (e.g. Drake et al., 2000), also given that (as discussed in Sect. 4.1) loops with solar-like plasma pressures, even if they were to fill the whole available volume, cannot explain the observed X-ray luminosity.

Several relevant questions about the structuring of the stellar coronal emission are thus still the subject of debate, but perhaps the most fundamental ones are the size of the coronal structures (with the attendant implications on e.g. the plasma density, the strength of the confining magnetic field and the characteristics of the underlying dynamo) and their location on the star. Even more fundamentally, whether indeed the coronae of stars much more active than the Sun are composed of solar-like loop structures – as it is assumed by analogy with the Sun – and whether these loops are well described by quasi-static models, is still to be proven unambiguously.

In the following we will describe the main tools which are available (and have been used) to address the study of the stellar coronal structure, reviewing the main results obtained in each area.

[4] loops have typical sizes $L \lesssim 0.3 R_\odot$, as evident from the inspection of X-ray images, e.g. Fig. 2.

6.2.1. *Eclipse mapping*

The study of the optical light curves of eclipsing binary systems is a classical tool to determine their radii (as well as other physical characteristics), and in principle the same should be applicable to the study of their X-ray light curves. However (as reviewed e.g. by Schmitt, 1998) the process suffers from several drawbacks. One of them is that the reconstruction of a 3-dimensional optically-thin structure from its 1-dimensional projection (the light curve) is a mathematically ill-posed problem, which is extremely sensitive to noise. The solutions to this type of deconvolution problems are far from unique, and additional constraints have to be imposed to the solution to guarantee convergence. These constraints (which often embody an a priori "prejudice" about the nature of the coronal structures) significantly affect the nature of the solution. As shown by Schmitt (1998) it is easy to conceive very different coronal structures which would produce light curves essentially impossible to distinguish observationally. Also, eclipse mapping techniques rely on the assumption that all variations observed in the light curve are due to the spatial modulation of an otherwise constant source distribution. In practice, all coronal sources (including the Sun) are observed to be highly variable on a variety of temporal scales (see Sect. 7.1.2), so that the deconvolution process will interpret these intrinsic intensity variations as spatial modulation, producing spurious structures. In general, X-ray light curves of eclipsing binary systems will not be as unambiguous as their optical light curves, as shown e.g. for the *Chandra* observation of 44 Boo in Fig. 12.

Notwithstanding the above difficulties, several attempts at deconvolving the observed X-ray light curve in terms of the underlying source spatial structure have been made, mainly in eclipsing active binary systems. AR Lac has perhaps been the target most often observed for this type of study, starting with the *Einstein* observation of Walter et al. (1983), who monitored the emission level throughout two primary and one secondary eclipses. The temporal coverage of the IPC data was spotty, but some evidence for a primary eclipse in the X-ray is visible, while no secondary eclipse appears. Walter et al. (1983) concluded that both stars had small scale height coronae ($H \simeq 0.02\ R_*$), and that the primary star in addition also had an extended ($H \simeq 1\ R_*$) coronal component. Later, White et al. (1990) repeated the experiment with a longer EXOSAT observation (which, unlikely the *Einstein* observation, had continuum time coverage), spanning almost a complete orbital cycle. The light curve is complex: in the low-energy band (0.05–2.0 keV) an X-ray primary eclipse is present, with a hint of secondary eclipse. In the high-energy band (1.0–6.0 keV) no eclipses are visible, and a flare is present at primary ingress (the flare is also visible in the soft light curve). The data are interpreted as evidence for a corona with two distinct components, a compact cooler corona and a diffuse hotter corona.

The same experiment was performed by Siarkowski et al. (1996) using a complete (1 orbital phase) AR Lac light curve obtained by ASCA. Both SIS and GIS data were used with an iterative deconvolution method (described by Siarkowski, 1992). In this case, the hard (2.0–7.0 keV) and soft (0.4–1.5 keV) light curves track each other closely, with a deeper primary eclipse and a shallower secondary eclipse clearly visible, very unlike the EXOSAT hard X-ray light curve. As expected, the deconvolution method interprets each variation in the X-ray light curve as due to spatial modulation, and the solutions found for the ASCA light curves are strongly dependent on the a priori constraints imposed (in this case from the assumed initial emission distribution). No unambiguous solution is thus found (even in a case in which the modulation is clearly visible in the light curve), although the authors show a preference for a solution which concentrates much of the emitting material in the interbinary region (something which the *Chandra* HETGS observations of active binaries, Sect. 6.2.4, are showing not to be the case). While the change in the hard X-ray light curve between the EXOSAT and ASCA observations could in principle be interpreted as a change in the actual coronal structure (with the hot extended corona "disappearing"), it once more points out the difficulty in discriminating temporal variations from actual spatial modulation.

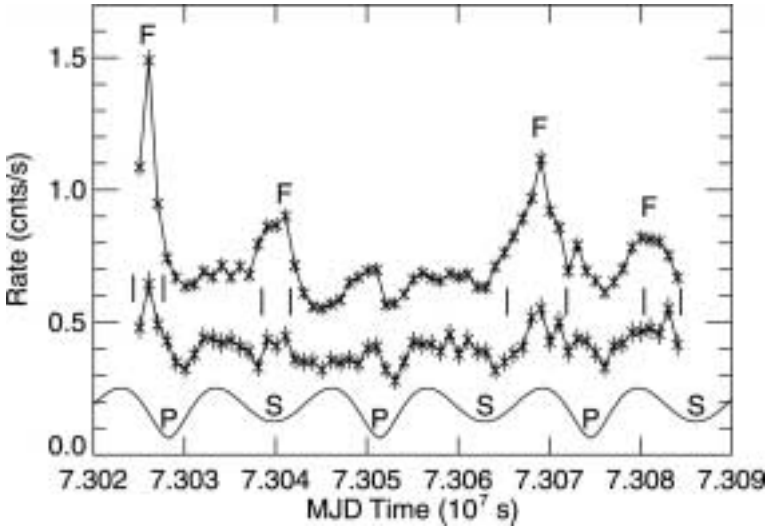

Figure 12. Top panel: X-ray and optical light curves for the eclipsing contact binary 44 Boo. The uppermost curve is the total *Chandra* X-ray light curve, while the middle curve represents the low-temperature component of the X-ray emission (0.66–0.89 keV). The lowest curve is the scaled optical light curve, with the primary (P) and secondary (S) minima marked. Four flares (F) are identified, with vertical bars denoting their duration. From Brickhouse et al. (2001).

This is clearly demonstrated by the recent *Chandra* observation of AR Lac (Huenemoerder et al., 2002). The observation lasted 100 ks, and both primary

and secondary eclipses were observed twice, as were the quadratures. The X-ray flux at primary eclipse (see Fig. 1 in Huenemoerder et al., 2002) changed by a factor of 2 between the two observations, and a clear flare-like event is visible at one of the secondary eclipses. In quadrature, the X-ray flux changes by several tens of percent, showing that the light curves do not repeat themselves reliably, and therefore that temporal variability dominates over spatial modulation. Each individual *Chandra* observation (if the lack of repeatability was not known) could be interpreted through a deconvolution algorithm, but what would be the physical meaning of the result is an open question. Finally, the most comprehensive data set of AR Lac light curves is the one of Pease et al. (2002), who combine *Chandra*, EUVE and RXTE data. By modeling the observed (multiple) eclipses in the light curves as spherically symmetric atmospheres with intensity decaying exponentially with height above the photosphere, they find that the coronae are extended to $\sim R_\star$. At the same time they show that the significant stochastic flare-like variability present in the light curves will, in general, invalidate 3-D reconstructions of coronal structure based on sparse or single-orbit coverage.

A successful example of "eclipse experiment" is on the other hand supplied by the eclipsing system α CrB. This is an ideal target, as it is composed (like Algol) of an X-ray active and an X-ray quiet star, removing much of the ambiguity on the location of the X-ray emitting plasma. The X-ray emission from the active star, a G5V star with an intermediate (Hyades-like) activity level, is eclipsed by the X-ray dark B-type companion. Observation of a number of eclipses were carried out with the PSPC (Schmitt and Kurster, 1993; Schmitt, 1998), showing that the X-ray eclipse is total, and that the ingress and egress are quite sharp, with an X-ray eclipse duration very similar to the optical eclipse. These features require a corona confined to a small height above the stellar photosphere, with no evidence for extended structures. More recently, the X-ray eclipse of α CrB has been studied with XMM-*Newton* (Güdel et al., 2002b; Güdel et al., 2003b). Also in the XMM-*Newton* data the eclipse is total, as shown in Fig. 13, and the sharpness of the egress shows that the coronal structures on the G star must be confined to a thin shell with $H \lesssim 0.05\,R_*$. While Güdel et al. (2002b) try to interpret the lack of smoothness in the egress light curve as due to discrete structures present in the corona, the usual caveat about the impossibility of distinguishing intrinsic temporal variations from spatial modulations applies also here.

In some cases well-defined X-ray eclipses are present. Examples include the EUVE light curve of the RS CVn-type binary CF Tuc (Schmitt et al., 1996b) and the XMM-*Newton* EPIC X-ray light curve of the double dM system YY Gem (Güdel et al., 2001b; Stelzer et al., 2002). For CF Tuc Schmitt et al. (1996b) show that a deep ($\simeq 50\%$) modulation is present in the EUVE light curve, with a high stability across four orbital periods (indicating the presence of stable, long-lived structures); they do not attempt to deconvolve

the coronal structure from the light curve; however at a qualitative level such strongly modulated light curve is indicative of the presence of rather spatially concentrated coronal emission. The same EUVE CF Tuc data set has been analyzed by Gunn et al. (1997) who (on qualitative grounds) find a suggestion, in the data, for the presence of an "intra-binary region of enhanced emission". This is not however based on a full inversion of the light curve but rather on the somewhat higher level of EUV emission around phase 0.5, which could be explained in other ways (e.g. by the presence of "preferred longitudes" on the stars).

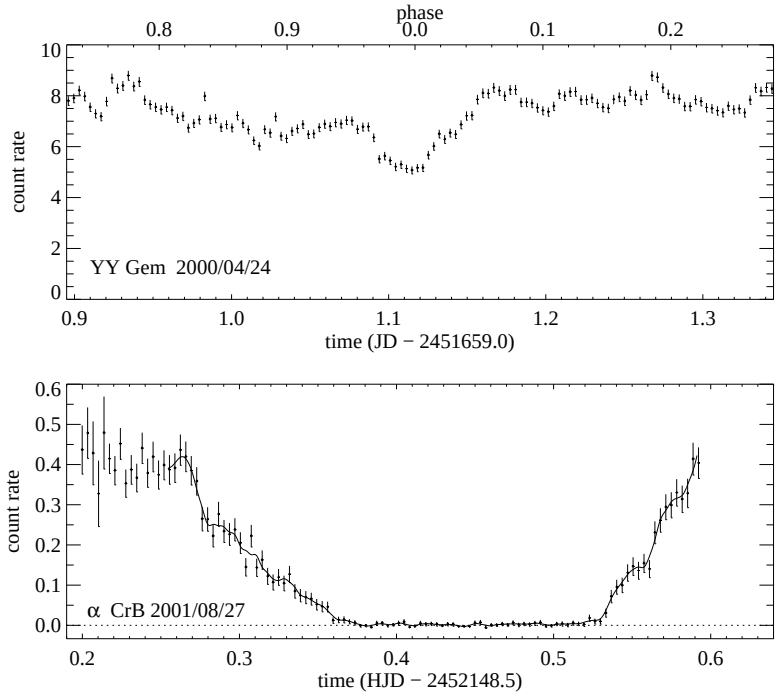

Figure 13. The top panel shows a segment of the XMM-*Newton* EPIC light curve of YY Gem around primary eclipse, adapted from Güdel et al. (2001b); note the well-defined, albeit rather shallow, eclipse, and the significant intrinsic variability. The bottom panel shows the XMM-*Newton* EPIC light curve of α CrB, again around primary eclipse, adapted from Güdel et al. (2003b). Note the deep, total eclipse and the sharp ingress and egress, indicative of a confined corona.

For YY Gem the eclipses are (Fig. 13) better defined (also thanks to the high S/N afforded by the large XMM-*Newton* effective area), with $\simeq 30\%$ of the flux being eclipsed, leading Güdel et al. (2001b) to apply the Siarkowski (1992) method to attempt to reconstruct the plasma spatial distribution. Obvious flares were removed from the light curve, and the corona was constrained to lie within $1\,R_*$ from the photospheres. The eclipses are asymmetric, and the deconvolution process (to which the same caveat as discussed above for

AR Lac applies) indicates a rather compact corona, with much of the emission coming from a few bright spots located at high latitudes.

In many eclipsing active binaries (with the exceptions discussed above) however one feature evident in their X-ray light curves is just the lack of deep eclipses, contrary to what is seen in the optical light curve. In several cases no eclipse at all is visible. This is e.g. generally the case for the narrow, contact W UMa-type binaries, composed of two solar type stars (see Fig. 12). For systems with high inclination ($i \simeq 90^\circ$) the optical eclipses are obviously very deep (i.e. typically a factor of $\simeq 2$), yet their X-ray (and EUV) light curves typically show little – if any – modulation. Examples include VW Cep, which shows no evidence of modulation in its PSPC light curve (see McGale et al., 1996, who also show a number of PSPC observations of other W UMa-type systems) and 44 Boo (Brickhouse et al., 2001).

EUVE light curves are ideal for studying the presence of rotational and eclipse modulation, as very long integration times were needed to obtain the high-resolution spectra, and light curves were obtained simultaneously "for free". The contact system 44 Boo has been observed with EUVE for two consecutive orbital cycles by Brickhouse and Dupree (1998). No deep modulation is present in their light curve, although they show evidence for a shallow modulation (at the 10–15% level) in the EUVE count rate, at a period which is slightly different from the optical one, something which they interpret as due to the emission from a near-polar region, the difference in period being due to differential rotation on the star. The more recent *Chandra* observations (Brickhouse et al., 2001) also support these conclusions. Phased EUVE light curves for three short-period binaries (44 Boo, VW Cep and ER Vul) are also presented by Rucinski (1998); again, no strong orbital modulation is present in the data.

Osten and Brown (1999) have published a systematic study of the EUV light curves of several active binaries (a comprehensive study of the EUV light curves of active stars in general has been done by Sanz Forcada, 2001). For many eclipsing systems, such as HR 1099 and II Peg, as well as ER Vul, they show that no eclipses are present in the (phased) light curves.

The general lack of eclipses in binary systems has often been interpreted as evidence for the presence of a rather diffuse corona, composed of large structures, with characteristic sizes larger than the component stars of the systems. Together with initial evidence (later refuted, see Sect. 7) for the large size of flaring loops this was taken to imply that the coronal structures in active binaries were large, and would typically span both stars. This led to the so called "standard model" (supported also by early inferences based on X-ray spectral data about large, low-pressure loops, see Sect. 4.4), in which magnetic structures would extend across the inter-binary region and flaring would be the consequence of the magnetic stress induced by the orbital rotation of the two stars (see e.g. Uchida and Sakurai, 1983, and Fig. 14).

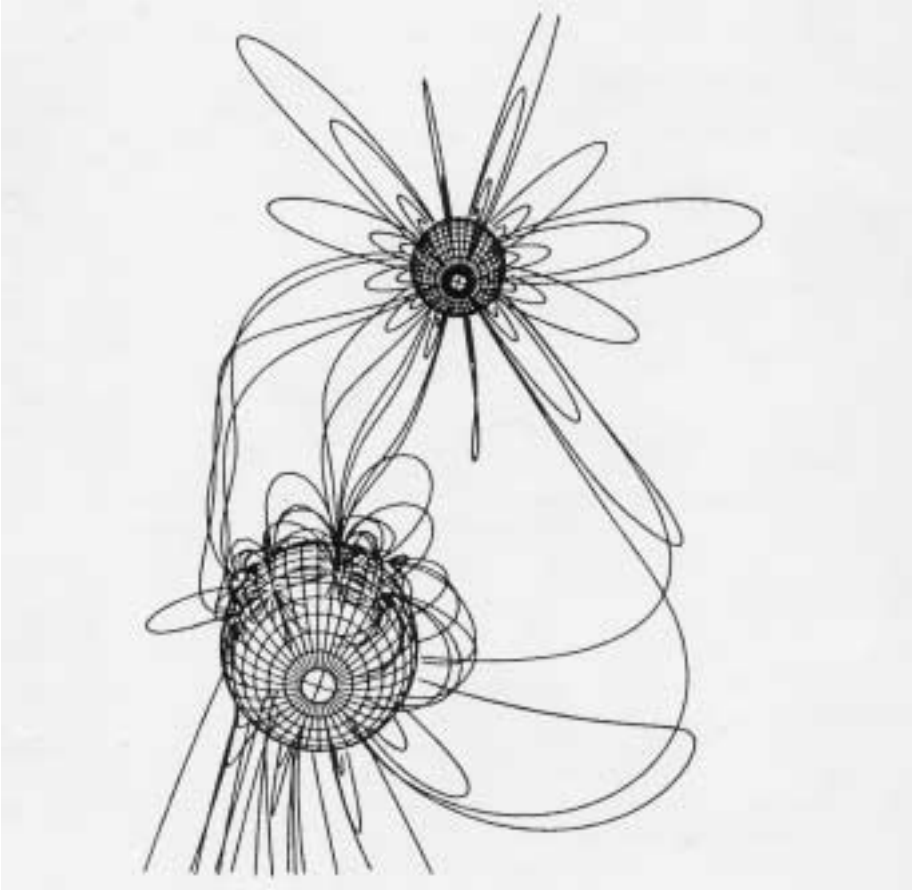

Figure 14. A representation of what it was considered to be the "standard model" of coronal structures in binary stars, with magnetic structures spanning the inter-binary regions (from Uchida and Sakurai, 1983). Later observations have shown that coronal structures are likely to be more compact and thus located on the individual stars.

However as shown e.g. by Brickhouse et al. (2001) for 44 Boo the lack of eclipses is compatible with a compact corona with localized (in this case polarly located) X-ray emission; together with the evidence, coming from flare analysis, for compact loops, it appears more and more likely that the corona of even the most active stars is quite compact and does not extend to large (larger than the stellar radius) distances from the star itself.

Self-eclipsing of coronal structures (i.e. rotational modulation) should in principle also constrain the structure of the corona. However, clear evidence for rotation modulation of the coronal emission in single stars has not been observed to date, even though some long data sets, spanning several rotational periods have been analyzed for this purpose. One example is the analysis of the EUVE light curves of AB Dor by White et al. (1996), in which no signifi-

cant rotational modulation is detected. The lack of modulation is however not a strong constraint on the structure of the quiescent corona, as it can be due to a very uniform, spherically symmetric corona, or to the presence of very large structures, or to a compact, polarly located set of emitting structures. The latter possibility is indeed likely the case for the flaring corona of AB Dor, see Sect. 7.3.1.

6.2.2. *Eclipsed flares*

The first clear observation of an eclipsed flare is presented by Choi and Dotani (1998), who report the observation of a moderate flare on the contact active binary system VW Cep (which otherwise shows little modulation on its quiescent X-ray flux, see Sect. 6.2.1). The eclipse of the flaring region appears to be total (with the X-ray emission reverting to its pre-flare value), and the occurrence of the eclipse at phase 0.46 allows to unambiguously locate the flare on one of the two stars (the primary in the system). The occurrence very near phase 0.5, as well the the totality, allowed Choi and Dotani (1998) to conclude that the flaring region is located on the pole of the primary star. The low S/N of the event did not allow a detailed analysis of the eclipse light curve. Nevertheless the totality of the eclipse implies that the flaring structure must lie close to the stellar photosphere, with a height $H \lesssim 0.5\ R_*$.

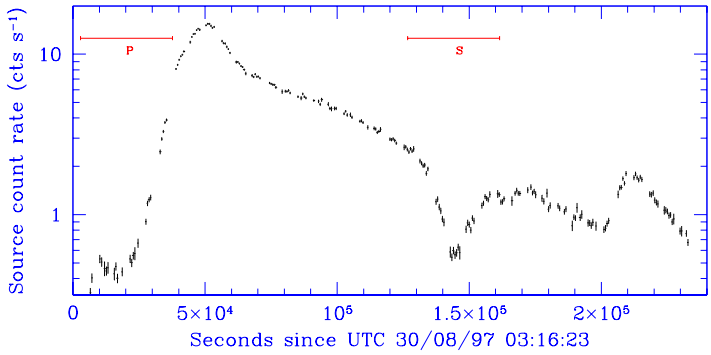

Figure 15. Light curve of the SAX Algol flare as seen in the MECS detector (from Favata and Schmitt, 1999). The total eclipse of the flare at secondary eclipse is well visible. The coronal structure implied by the observed eclipse is shown in Fig. 16

A much higher S/N eclipse was detected on a long-lasting flare observed by SAX on Algol. Algol (like α CrB, page 40) is an ideal system for this kind of investigation, as the activity is concentrated on the K-type secondary, with the X-ray dark B-type primary acting as an eclipsing body only. This removes

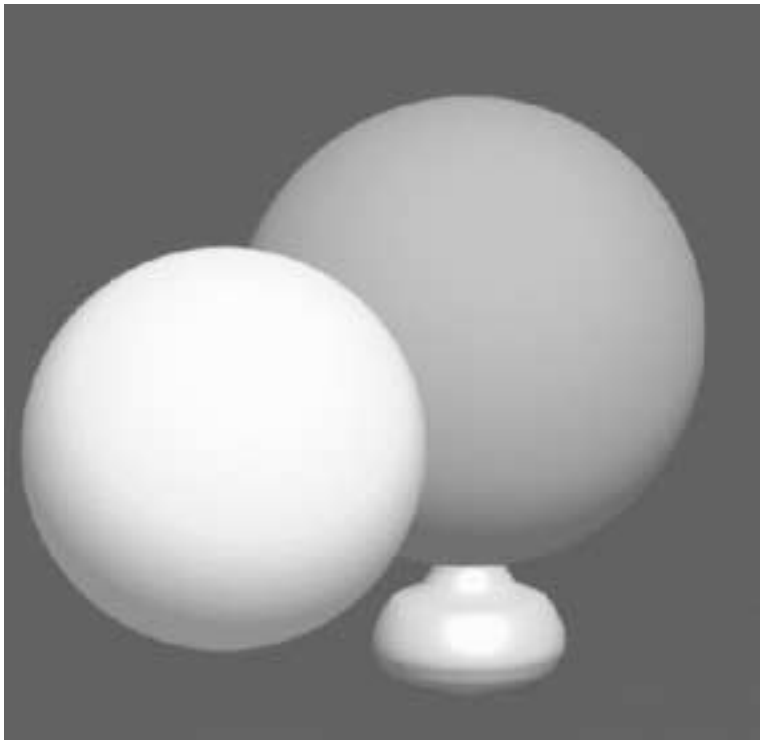

Figure 16. The location and size of the volume to which the plasma producing the large flare observed by SAX on Algol (light curve shown in Fig. 15) must be confined is shown (mushroom shaped structure on the south pole of the secondary).

a large part of the ambiguity associated with the interpretation of eclipse light curves. Schmitt and Favata (1999) show that the Algol SAX flare is located on the polar region of the K-type star, and that it must be confined within a rather compact region with a maximum height above the stellar surface $H < 0.6\,R_*$ (see Fig. 16). The results are very similar, both in terms of location and size of the flaring region, to the results obtained by Choi and Dotani (1998) for the moderate VW Cep eclipsed flare – even though the two stellar systems are quite different.

As discussed in Sect. 7 the determination of the size and location of the SAX Algol flaring region has for the first time allowed to compare the results from the analysis of light curves of the flare decay with a geometrical determination of the size of the same region, showing that methods which do not take into account the presence of sustained heating during the flare decay will overestimate the size of the flaring region by large factors.

It is worth noting that the polar location of the flaring regions on both Algol and VW Cep is in contrast with a direct extrapolation of the solar case to more active stars. In the Sun the polar regions are devoid of significant

coronal emission, and in particular no active regions are observed to emerge at the poles. This is thus direct evidence for the corona of active stars being significantly different, in its spatial structuring and location, from the solar corona, implying that the solar analogy must, at best, be used with caution for the understanding of these coronae.

The general lack of self-eclipses of the flaring emission in single stars, even when the flares have a duration comparable to the stellar rotational period (e.g. the two long-duration flares seen by SAX on AB Dor, Maggio et al., 2000) is also indicative of the active component of the corona being generally placed near the stellar poles (where it cannot be self-eclipsed). Stelzer et al. (1999) discuss four flaring events in which they claim that the lack of a sharp impulsive rise phase (rather, a slower rise is visible in the light curves) should be interpreted as evidence for self-eclipse of the flaring structure. However, the Algol SAX flare discussed above also shows a gradual rise phase, as do several of the events discussed by e.g. Pallavicini et al. (1990) and Osten and Brown (1999), see Sect. 7.1.1. For Algol, the presence of a clear eclipse during the decay allows the hypothesis of a self-eclipse during the rise phase to be conclusively ruled out. Thus, slow rise phases are possible in large flares without a need for self-eclipses, and the conclusions of Stelzer et al. (1999) are not the only possible interpretation of the data. Also, Doppler spot maps of active stars consistently show large polar spots (e.g. Rice and Strassmeier, 2001 and previous papers in the same series), again consistent with the corona of active stars being mainly concentrated near the polar region.

6.2.3. *Density diagnostics*

Under the assumption of optical thin emission, the observed intensity of the X-ray emission, together with an estimate of the X-ray temperature, can be used to derive the "emission measure", defined as $EM = \int n_e n_{\rm H} dV \simeq \langle n_e^2 \rangle V$. As discussed in Sect. 11.1 a direct determination of the density of the emitting plasma is available through high-resolution spectroscopy, e.g. through the ratio of the forbidden to intercombination line in the He-like triplets of several species. These can be used to derive an estimate of the characteristic size of the emitting region, $l \simeq (EM/n_e^2)^{1/3}$. These measurements are however time- and space-averages over a dynamic and highly structured corona, so that it's unclear to what level of detail can they be used to constrain the coronal structure (see Judge, 2002). Some examples of the use of spectroscopically derived densities to constrain the size of the stellar corona are discussed in Sect. 11.1, e.g. for Capella (page 97) and for Procyon (page 99).

6.2.4. *Velocity diagnostics*

A new diagnostic which is being made available through high-resolution X-ray spectra is the radial velocity of the emitting plasma: in active binaries the difference in radial velocity at quadrature can in principle be used to discrim-

inate what fraction of emission is associated with each component. Given sufficiently narrow binaries (and thus high orbital velocities), the *Chandra* HETGS has sufficient spectral resolution to discriminate the two components. Huenemoerder et al. (2002) show that indeed for AR Lac (for which the radial velocity amplitude is 230 km s^{-1}) the lines observed at the higher resolution are broader at quadrature than at conjunction, showing that both components are significantly X-ray bright, while Brickhouse et al. (2001) show (Fig. 17), for the *Chandra* HETGS observation of 44 Boo, that the changes in the lines profile with phase imply that the emission is located at high latitudes.

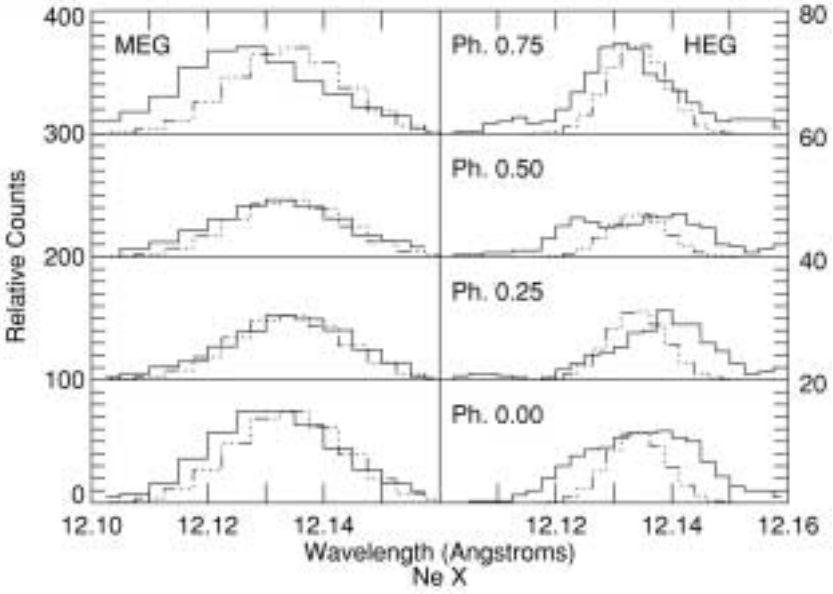

Figure 17. The Ne X *Chandra* HETGS line profiles of 44 Boo, from Brickhouse et al. (2001), for four different phases. The dash-dotted histogram shows the instrumental profile; the lines at phases 0.00 and 0.50 are significantly broadened with respect to the instrumental profile, showing that both components of the binary system are significant X-ray emitters.

The *Chandra* HETGS spectra of HR 1099 have been analyzed by Ayres et al. (2001), who find clear orbital modulation of the wavelength of the Ne X line at 12.1 Å, binned at 1 hr resolution. The observed modulation implies that the X-ray emitting plasma is largely concentrated on the K1 IV primary of the HR 1099 system, with negligible contribution from the inter-binary region.

7. Flares

The coronal X-ray emission from both the Sun and stars is highly variable in time. In the short term (minutes to several hours) this variability is dominated

by flares, i.e. sudden brightening of individual coronal structures (loops) or of groups of structures (arcades of loops) followed by a decay. During significant flares the X-ray emission from the flaring structure will dominate the emission from the rest of the corona. The decay time of solar flares typically ranges from minutes to hours, and large stellar flares have been observed with decay times of up to several days.

Through their providing dynamical information (as opposed to the static information provided e.g. by time integrated spectra) flares allow for the physical characteristics, and in particular the size, of the flaring region, to be determined, as well as the magnetic field strength, the plasma density, etc. At the same time, they provide constraints on e.g. the heating mechanism, and in general represent the most extreme manifestation of coronal activity.

7.1. TYPICAL STELLAR EVENTS

The sample of studied stellar flares is strongly affected by selection effects, in that to be recognized as such a flaring event must stand sufficiently above the photon noise. In addition, to be studied to some detail, sufficient statistics and appropriate temporal coverage must be available. Therefore, the sample of stellar flares available in the literature is naturally biased toward strong and long-lasting events (unlikely the solar case in which also smaller events can be recognized and studied with relative ease).

Studies on the characteristics of unbiased samples of flaring events on stars other than the Sun are few. One such study was performed on a significant sample of EXOSAT observations of dMe stars by Pallavicini et al. (1990). Studying a sample of 36 observations of 22 individual stars (spanning about 1 Ms of observing time) they found that flares come in a wide variety of durations, ranging from few minutes to several hours. A similar study was performed by Osten and Brown (1999), who analyzed the EUVE light curves of 16 RS CVn-type binary systems, spanning a total of 12 Ms of observations. The systems were found to flare for about one third of the time (i.e. 4 Ms of the observing time are affected by flares).

The frequency distribution of stellar flares as a function of the total energy release was found in both cases to follow a power law of the form $N(>E) \propto E^{\gamma}$. For the EXOSAT dMe sample the power law (with index $\gamma = -0.7$) applies for total energies $E \geq 10^{32}$ erg, flattening at lower energies due to selection effects (weaker flares being more difficult to detect). For the RS CVn EUVE sample the index is very similar, $\gamma = -0.6$, for flare energies $E \geq 10^{33}$ erg. Again, the flattening at lower energies is likely to be a selection effect. Flare energy and flare duration are also positively correlated (as expected), but not linearly, with $E_{\rm flare} \propto \Delta t^{1.4}$. Finally, in both the EXOSAT dMe sample and the EUVE RS CVn sample, a positive correlation is found between the flare energy and the system's quiescent X-ray luminosity.

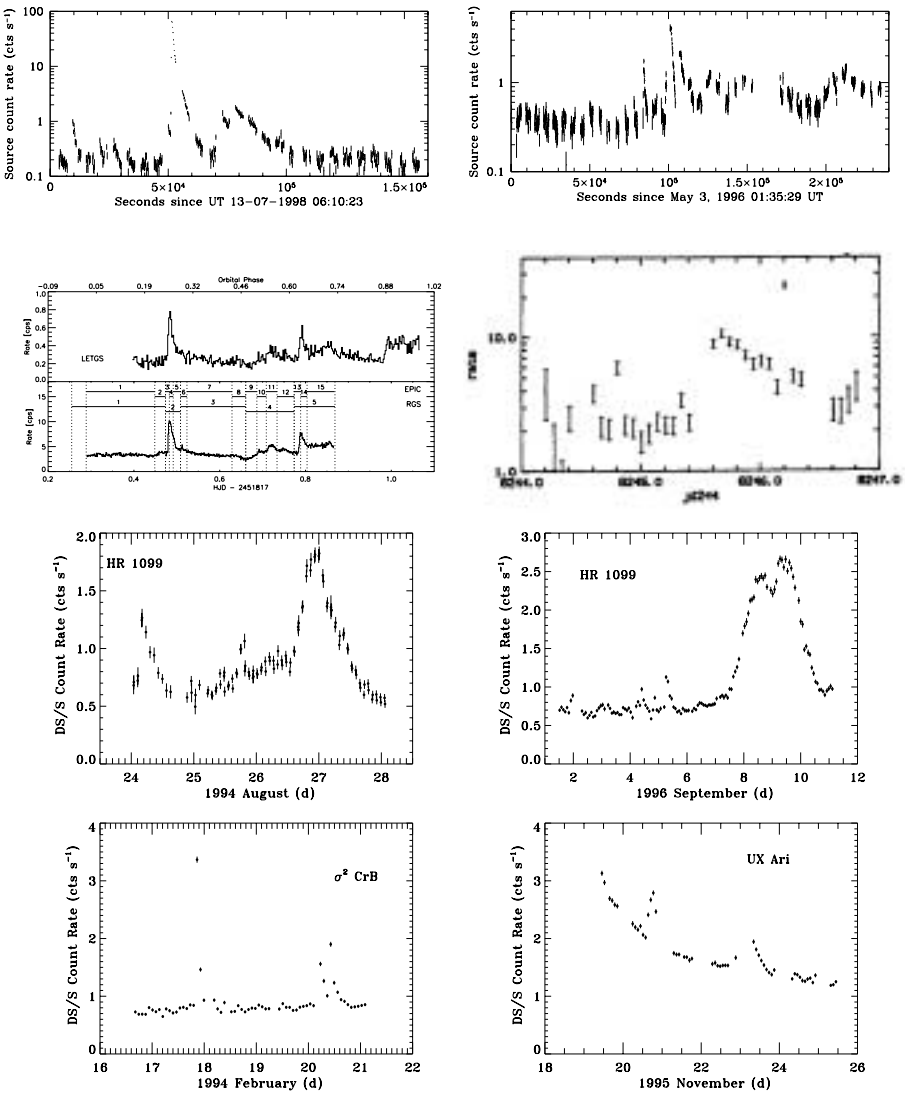

Figure 18. Several examples of stellar flares from the literature. We have selected a number of long observations, showing the large variety of behavior observed in flares, including some very long decay times (e.g. UX Ari with EUVE and EV Lac with ROSAT) as well as some very slow rise times. From top left to bottom right: the ASCA SIS light curve of EV Lac, showing a very intense, although relatively short-lasting flare, as well as several minor events, from Favata et al. (2000c); the ASCA SIS light curve of AD Leo, from Favata et al. (2000a); the YY Gem light curve from Stelzer et al. (2002), showing simultaneous *Chandra* and XMM-*Newton* observations; the long-duration flare observed on EV Lac in the ROSAT All Sky Survey, from Schmitt (1994); the EUVE light curves of HR 1099, σ^2 CrB and UX Ari, adapted from Osten and Brown (1999); note the very symmetrical shape of one of the HR 1099 events.

The flares detected in the RASS are discussed by Schmitt (1994), who analyzes some very remarkable events, such as a very long duration EV Lac flare (shown in Fig. 18).

7.1.1. *Shape of flaring light curves*

Stellar flares show, as well visible in Fig. 18, a variety of shapes and characteristics in their light curves. In the Pallavicini et al. (1990) sample there is a mix of events with very rapid rise times and events with very long rise times, comparable with the decay time. Some events (e.g. on YY Gem) are largely symmetric, with a slow rise followed by an identically slow decay. Whether they are flares in the sense of sudden brightening of individual (groups of) coronal structures is not clear. A similar variety of event types is visible in the Osten and Brown (1999) sample, again with (in addition to several "classic" events) apparently symmetric events (e.g. on HR 1099, which "hovers" around the maximum for some time before decaying), and some evidence for very long-duration events (e.g. the apparent decay of a flare on UX Ari, lasting for a week, for which the rise phase was not observed). Osten and Brown (1999) find a correlation between rise and decay time, i.e. long-duration events tend to also show long rise times.

One interesting element emerging from a number of stellar flares is the presence, in many cases, of a double exponential decay in the light curve, with the initial decay always faster than the later phase. Osten and Brown (1999) find evidence for such double decay in 8 out of 30 EUVE events analyzed, and a similar shape is evident in several well studied X-ray flares (e.g. the large events on Algol, Favata and Schmitt, 1999 and on EV Lac, Favata et al., 2000c), so that this clearly is a rather general feature of (large) stellar flares. Osten and Brown (1999) also find that the time scales of the fast and slow decays are correlated. In the case of Algol (as visible in the light curve of Fig. 33) the change in slope in the decay phase is clearly associated with a strong re-heating event, with the temperature increasing just in correspondence with the "knee" in the light curve.

The physical meaning of the knee is not clear, although it is tempting to interpret is as a physical change in the flaring region (e.g. as a change in geometry). Such double exponential decay is also often observed in large solar events: one good example is the Nov. 2–3 1992 event, a well-known large flare classified as X9 by GOES 7. This flare has been studied in detail by several authors, but in the present context its study with "stellar techniques" by Reale et al. (2001) is of particular relevance. A detailed study of the morphological changes of the flaring region at the knee in the light curve has not yet been performed, but the initial evidence (F. Reale, private communication) is that indeed some changes take place, with the initial (steep decay) part of the flare being due to a single loop, and the knee marking the extension of the

event to nearby (but still well confined) loops. This will need to be studied in more detail to understand the underlying physics.

7.1.2. *Microflare heating*

A recurring idea which has surfaced in the literature is that the quiescent emission from stellar coronae (and perhaps also the solar corona) is in fact the result of a super-position of a stochastic sequence of very small (micro- and nano-) flaring events. This was originally proposed by Parker (1988) in the solar context (where the individual events were called "nanoflares"), who also suggested that the individual events would be heated by the dissipation at the many tangential discontinuities arising spontaneously in the bipolar fields of the active regions of the Sun as a consequence of random continuous motion of the footpoints of the field in the photospheric convection. In its applications to the stellar case, however microflare heating is not necessarily (unlikely the solar case) an ab initio explanation of coronal heating (as it is not obvious that the mechanism which triggers and heats the solar nanoflares would be capable of driving the small, but likely much larger than the solar ones, flaring events inferred for the coronae of active stars). The high coronal temperatures observed in very active stars would in this framework be explained as due to continuous, unresolved flaring. Such ideas have prompted investigations of the statistical distribution of flaring events in stars.

In the Sun the distribution of small flaring events has been shown to follow a power-law distribution of the form $dN/dE = kE^{-\alpha}$. To fully account for the total coronal luminosity, the power-law index must be $\alpha > 2$. Initial determination of the power-law index appeared to show that $\alpha < 2$ (Hudson, 1991; Crosby et al., 1993), so that the microflare heating hypothesis would not hold. However, the value of the power-law index α is strongly dependent on the assumptions about e.g. the form of the line-of-sight depth, and more recent work (Parnell and Jupp, 2000; Winebarger et al., 2002) shows that $\alpha > 2$ down to energies as small as 10^{23} erg, which implies that the events with the lowest energy dominate the energy output of the corona, i.e. the quiescent coronal emission is indeed dominated by (unresolved) micro-flaring events.

In stars, the limited statistics of the light curves make it difficult to study the distribution of small flares; however, several studies have been performed on a statistical basis to assess whether the observed light curves are compatible with being due to the superposition of continuous, low-level flaring. Early results where somewhat contradictory. The systematic analysis of Pallavicini et al. (1990) discussed in Sect. 7.1 showed no evidence, in M stars, for a corona heated by microflares, in agreement with the earlier work of Ambruster et al. (1987) based on *Einstein* data (in which the data gaps however made such analysis more difficult).

Kashyap et al. (2002) have analyzed the EUVE light curves of the active dMe stars AD Leo, Wolf 630 and FK Aqr, as well as a *Chandra* observa-

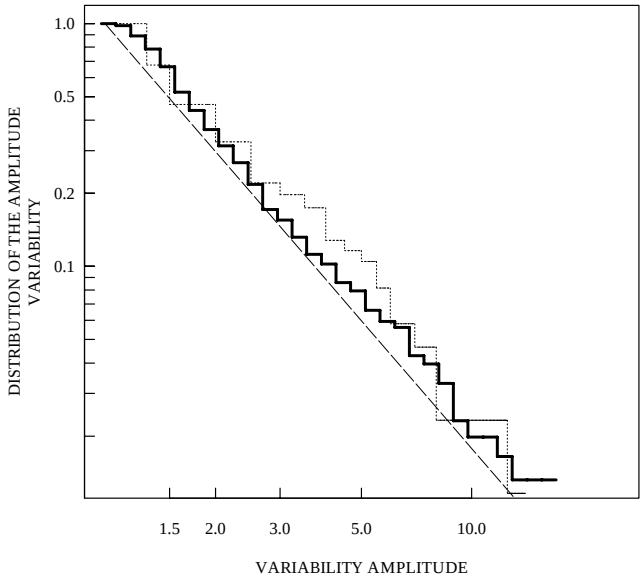

Figure 19. Normalized cumulative distribution of the amplitude variability of a sample of nearby dM stars (solid line), together with the distribution for pre-main sequence stars in ρ Oph (dotted line) and the distribution for solar flares (dashed line). The vertical axis gives the fraction of stars which show a variability level greater than a given amplitude, the horizontal axis gives the variability amplitude, expressed as the ratio between the X-ray flux measured in a given observation and the minimum X-ray flux measured for the same star in all the available observations. The similarity of the three distributions is evident. From Marino et al. (2000).

tion of Algol, investigating whether the observed emission can be modeled as a superposition of numerous weak flares with a power-law distribution, concluding that in all four cases flares can account for the majority of the observed emission (from 70 to 95%) and that the power law index is $\alpha > 2$, so that in these stars the emission appears dominated by impulsive energy release (with individual events having energy $\gtrsim 3 \times 10^{29}$ erg). For AD Leo Güdel et al. (2003a) also find, using long EUVE and SAX observations, that $\alpha \simeq 2$–2.5, again compatible with most of the observed emission being due to a superposition of flares. Güdel et al. (2003a) also provide a rather extensive bibliography of previous determination of α in different contexts. Similar results on the value of α had been obtained earlier by Audard et al. (1999) analyzing the EUVE light curves of the young solar analogs 47 Cas and EK Dra, although there the observed power law index ($\alpha \simeq 2.2$) is determined for flare energies between 3×10^{33} and 6×10^{34} erg, so that to explain the total observed coronal luminosity the observed power-law index has to extend

to much lower energies, something which the EUVE data do not allow to establish.

Recent work by Marino et al. (2000) suggests that the X-ray variability observed in low-activity dM stars is due to flaring activity similar to that observed in the Sun (see Fig. 19).

7.1.3. *Giant flares*

Flares can reach, in active stars, intensities which are orders of magnitude larger than observed in the Sun. The peak observed plasma temperature in large flares commonly reaches values well in excess of 100 MK (e.g. in V773 Tau, Tsuboi et al., 1998, or in Algol, Favata and Schmitt, 1999, as well as in the dMe star EQ 1839.6+8002, Pan et al., 1997). With such high plasma temperatures thermal hard X-ray emission should be present and observable. The wide band coverage of the SAX instrumental complement (in particular the PDS detector) has indeed shown this to be the case, and high-energy X-rays during large flares have been observed from both Algol (Schmitt and Favata, 1999) and UX Ari (Franciosini et al., 2001). The spectrum of the hard X-ray emission can in both cases be traced up to $E \simeq 100$ keV. No statistically significant evidence of non-thermal emission is present in the SAX PDS data of these events.

Non-thermal emission is widely observed in solar flares, where its observation is made easier by the lower temperature reached by the plasma during the flare, and is interpreted as the signature of the non-thermal particle beams which lead to the chromospheric evaporation and subsequent heating of the plasma. Its observation in the stellar context would be a strong diagnostic of the flare heating process; however direct scaling from the solar case shows that the intensity of non-thermal hard X-ray (and γ ray) emission from stellar flares is likely to be at a level below the detection threshold of the current generation of instruments. The INTEGRAL instrumental complement (launched in October 2002) should in principle offer sufficient performance to potentially detect non-thermal emission from large flares in nearby stars although it is unlikely that a significant fraction of its observing program will be dedicated to active stars. Therefore, with the demise of the SAX observatory it is likely that the observation of high-energy emission from stellar flares will not take place for some time to come.

While the total energy involved in coronal processes in stars like the Sun is a negligible fraction of the total energy budget, for very active (and very young) stars the energetics of large flares can be very significant in comparison with their bolometric luminosity. In the case of very young, PMS stars, this is of particular interest as the large flares are likely to significantly influence the circumstellar (and thus proto-planetary) environment. In particular, during large flares, large quantities of higher-energy photons will be

produced, which will penetrate deep in the circumstellar material and affect the conditions of the accretion disk (see Glassgold et al., 2000).

Recently, 6.4 keV fluorescent emission from "cold", neutral Fe has been observed during a large flare from a pre-main sequence, Class I star in ρ Oph, YLW 16A (Imanishi et al., 2001). The 6.4 keV line is present jointly with the more usual 6.7 keV Fe K line (Fig. 20). Imanishi et al. (2001) attribute the 6.4 keV line to fluorescent emission from neutral circumstellar gas, or from the circumstellar accretion disk, in both cases illuminated by the flaring region. From the near-simultaneity of the line emission they infer that the neutral material must be located at a distance less than 20 AU from the flaring region, consistent with the expected size of the circumstellar disk. They however do not discuss whether the emission could be due to fluorescence from the stellar chromosphere and photosphere.

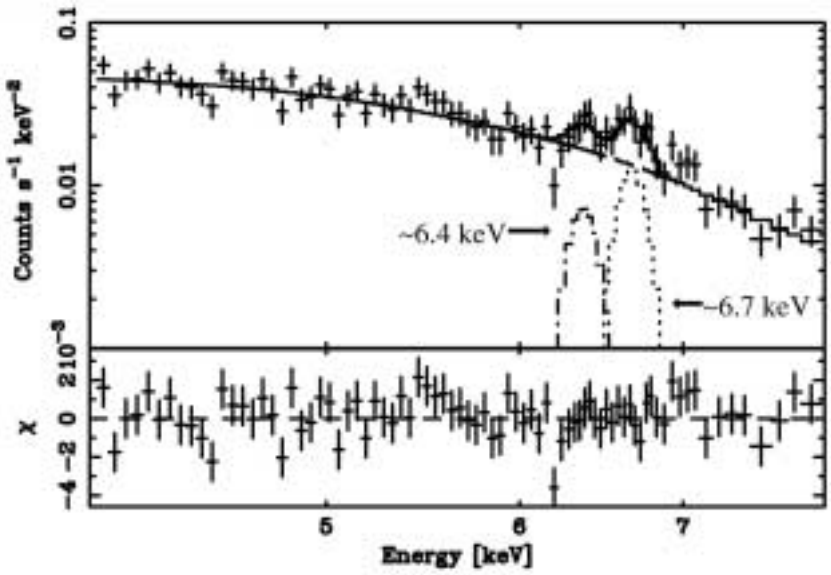

Figure 20. The flaring *Chandra* spectrum of the Class I PMS star YLW 16A, showing neutral Fe line emission at 6.4 keV jointly with Fe K 6.7 keV emission. From Imanishi et al. (2001).

Evidence for the large absolute energies involved in X-ray flaring from active binaries, and their long decay times, was already present in the early Ariel V data (Pye and McHardy, 1983), and the evidence was amply confirmed by all later observatories. Even if impressive in absolute terms, large flares on active binaries (both Algol-type and RS CVn-type) still involve small energies in comparison to the total stellar luminosity. For intrinsically fainter stars however the peak flare luminosity can rise up to values comparable to the photospheric luminosity: for the GINGA EQ 1839.6+8002 event the peak flare X-ray luminosity was $L_{\rm Xpk}/L_{\rm bol} \simeq 30\%$ (Pan et al., 1997), as it was for the ASCA EV Lac event (Favata et al., 2000c). Radiative losses (which are

measured by the X-ray luminosity) are only a fraction (estimated at $\simeq 20\%$) of the total energetics involved in the event (the rest being e.g. thermal conduction to the chromosphere and kinetic energy), so that the total energy dissipation at the peak of these flares is comparable to (if not larger than) the photospheric luminosity. Also for somewhat more massive stars such as AB Dor the peak X-ray flare luminosity can reach a non-negligible value of the bolometric luminosity, with the SAX flare showing $L_{\rm Xpk}/L_{\rm bol} \simeq 10\%$ (Maggio et al., 2000). Given the small size of the flaring regions ($\leq 0.5R_*$ for the EV Lac ASCA flare) these are likely to be quite near the stellar photosphere. The effect of such events taking place close to the photosphere has not to date been modeled, but given the large peak energies involved their influence on the structure (and thus evolution) of the star could be significant. Stellar flares can last for several days, with the longest event on record being the one observed on CF Tuc (Kürster and Schmitt, 1996), for which the decay phase is clearly visible in the data for 9 days. Remarkably, even for such a long-lasting event, the hydrodynamic modeling described in Sect. 7.2 also indicates that the flaring emission is confined into relatively compact structures, with $R \leq R_*$ (Favata, 2001).

Peak absolute X-ray luminosities during large flares can be as high as 10^{31} erg s^{-1} in dMe stars (EV Lac ASCA, EQ 1839.6+8002), reaching few 10^{32} erg s^{-1} in Algol, and up to 10^{33} erg s^{-1} in some pre-main sequence systems (e.g. V773 Tau). The total energy radiated in X-rays during large flares is of order 10^{34} erg for dMe stars (again EV Lac ASCA, EQ 1839.6+8002), reaching few 10^{36} erg for pre-main sequence stars (V773 Tau, YLW 15). In active binaries total energy releases of up to 10^{37} erg have been determined for e.g. the Algol SAX and the CF Tuc PSPC events (see Table II and III for the references to the original works).

7.2. MODELING APPROACHES

Given that flares are highly transient events, their evolution and characteristic time scales supply dynamic information that can be used to infer the size of the structures where the events occur. In fact, models of flare decay have been extensively applied to stellar observations to infer the size of stellar flaring regions. As basic starting point for modeling stellar flares, it is often assumed that they share many features with solar flares, which can then be taken as templates. Solar flares are well known to occur in localized regions in the corona, often in single magnetic loop structures, and the flaring structures often do not change significantly during the evolution of the flare (e.g. Pallavicini et al., 1977).

Most flaring events – as visible e.g. in the flare light curve of Fig. 15 – have three clearly defined phases, i.e. a relatively fast rising phase, a peak phase and a (slower) decay phase. Several different approaches have been devel-

oped and used in the literature to model flares, most of them concentrating on the analysis of the decay phase. A comprehensive review and comparison of the different flare analysis approaches has recently been presented by Reale (2002), and here we will only recall the essential concepts. If one assumes that the flaring loop is heated – by some process – during the rise phase, and that heating ceases to be important during the decay phase, the cooling of the loop will be characterized by two decay times, the radiative decay time and the conductive decay time:

$$\tau_{\rm cond} = \frac{3nkT}{\kappa T^{7/2}/L^2} \qquad \tau_{\rm rad} = \frac{3nkT}{n^2 P(T)} \tag{2}$$

where n is the plasma density, κ is the plasma thermal conductivity, k is the Boltzmann constant and $P(T)$ is the plasma emissivity per unit emission measure. While $\tau_{\rm cond}$ depends explicitly on the loop length, the dependence is also implicitly present in $\tau_{\rm rad}$, through the density, which is constrained, assuming quasi-static conditions, by the scaling law – Eq. (1) – and by the equation of state.

In practice the effective cooling time will be a combination of the two (shorter than either) with relative weights depending e.g. on loop geometry, plasma temperature, etc. As shown by Serio et al. (1991) the effective cooling time of a freely decaying loop (with a size below the pressure scale height) depends linearly on the loop length, through

$$\tau_{\rm th} = \frac{120 L_9}{\sqrt{T_7}} \tag{3}$$

where L_9 and T_7 are in units of 10^9 cm and 10^7 K and τ is in seconds. The obvious inference is thus that a fast decay implies a short loop, a slow decay, a large loop. Many of the methods used by several authors in the literature are – as discussed by Reale (2002) – largely equivalent to this simple assumption. This includes the "quasi-static method" (QS, van den Oord and Mewe, 1989) and the method used by Pallavicini et al. (1990) ("pure radiative cooling"). The quasi-static method assumes a fixed ratio between the radiative and conductive cooling time, while the Pallavicini et al. (1990) approach assumes that radiative cooling dominates. The method of Hawley et al. (1995) extends the approach to include the rise time in the assessment of the loop size, but it is otherwise similar in the underlying physical assumptions.

All these approaches assume that after initial heating the loop decays freely, and thus that long-lasting events unavoidably take place in large flaring structures. According to the original formulation the quasi-static approach includes the possibility of heating during the decay phase, but as shown by Reale (2002), the treatment of heating in the method is inconsistent, so that in practice the application of the method always results in the modeling of freely decaying loops.

Many large X-ray flaring events observed by e.g. *Einstein*, EXOSAT, ROSAT and ASCA have been modeled with the quasi-static approach. Given that some of these events decay on very long time scales – up to days, see Sect. 7.1.3 – the inferred loop lengths are very large, up to several times the size of the parent stars. These (in general incorrect, as discussed below) results – together with the observed lack of (self-)eclipses, see Sect. 6.2.1 – have contributed to create a scenario in which the corona of very active stars is very extended.

Evidently, if heating is present during the decay phase, this will result in a slower decay, and thus – if the event is modeled under the assumption of free decay – in an over-estimate of the size of the flaring loop. Lately, models have been developed which are able to detect whether sustained heating is present during the decay phase (and its time scale) and to determine the intrinsic decay time and thus the correct size of the flaring loop. Reale et al. (1997) have developed such an approach (based on detailed hydrodynamic modeling of the flaring loops), which uses the path of the flare decay in the $\log n_e$–$\log T$ plane, the slope of which is a diagnostic for the presence of sustained heating (as determined on solar flares by Sylwester et al., 1993). This method, whose predictive power has been tested on solar flares (Reale et al., 1997), has recently been applied to a wide variety of stellar flares observed with a variety of detectors. Perhaps the most notable result from the application of this approach is that sustained heating during the decay phase is an almost universal feature of (large) stellar flares, with none of the events studied to date showing evidence for truly "undisturbed" decay. Therefore, the size of the flaring structure is in general significantly smaller that apparent from e.g. the application of the quasi-static approach.

The good predictive power of the hydrodynamic modeling approach has been clearly shown in the case of the Algol SAX flare, where the presence of a total eclipse of the flaring region has allowed to determine the size of the region itself from purely geometrical consideration (Schmitt and Favata, 1999). Comparison of the loop sizes inferred through different approaches shows that the hydrodynamic modeling results in a size for the flaring region significantly smaller than the size resulting from quasi-static modeling. The latter would predict a loop several stellar radii in size (while in practice the eclipse constrains the flaring region to a height $H \leq 0.6\ R_*$); the hydrodynamic approach results in a significantly smaller flaring loop, which is however still larger than the eclipse-determined size. Therefore, even the "best" modeling approaches appear to give an upper limit to the size of the flaring region, rather than an accurate estimate. This is in particular true when sustained heating is dominant, so that the shape of the light curve reflects the shape of the (decaying) heating term, and not the physics of the loop itself. This condition appears to be present in many stellar flares.

A large body of work exists on the modeling of solar flares, which will not be discussed here, except for the one developed for solar two-ribbon flares by Kopp and Poletto (1984), which we mention because it has been applied to the analysis of some stellar flares. The approach assumes that the light curve is dominated by the heating process and that the decay is entirely driven by energy released from reconnection of higher and higher loops. In practice, its application in the solar case assumes that the geometry is known, and the lack of this constraint in the stellar case results in significantly degenerate solutions, so that a priori assumptions are necessary to derive a size for the flaring loop.

7.3. NOTABLE RESULTS FROM FLARE ANALYSES

Several flaring events, observed with a number of X-ray detectors, have been studied in detail. A synoptic view of the most relevant studies is presented in Tables II and III. The events which have been studied are perhaps not representative of the "general population" of stellar flares, as of course detailed studies have concentrated on the largest events, for which such analysis was possible (i.e. sufficient statistics were available). Most of the early studies made use of the quasi-static method (or, more simply, used the pure radiative decay approach); this invariably resulted in quite large derived sizes for the flaring regions. Later, many of these events have been re-analyzed with the hydrodynamic modeling approach, showing that sustained heating is generally present during the flare decay, so that the flaring regions are significantly smaller than implied by the quasi-static analyses.

Flaring loops are thus in general rather compact, and do not extend to great distances from the star's photosphere. In dMe stars the typical loops in which significant flaring events take place (e.g. on AD Leo, Favata et al., 2000a) have characteristic sizes $L \leq 0.5\ R_*$, and even the largest flaring events (e.g. the giant events on EV Lac, Favata et al., 2000c and on EQ 1839.6+8002, Pan et al., 1997) are confined to loops of the same size. As discussed above, these estimates are to be taken as upper limits. Such loops are perhaps not very small, but they are not exceptionally large even by the modest standards of the Sun. Thus, in dMe stars the flaring corona is relatively compact.

In the other stellar types studied in detail until now (active binaries, young and PMS stars), while again the flaring loops implied by the quasi-static analyses extended to great distances from the parent stars, the hydrodynamic modeling of the same events once more shows them to be much smaller, with sizes $L \leq R_*$.

7.3.1. *Location of the flaring structures*
The first direct evidence for the location of the flaring plasma on stars other than the Sun has been obtained by detection of eclipsed flares in binary systems (VW Cep and Algol, Sect. 6.2.2). In both cases, differently from what it could have been expected on the basis of analogy with the solar corona, the flaring regions are located on a pole of the stars. This is also in agreement with the polar location of the flaring radio corona on Algol determined by Mutel et al. (1998).

Unfortunately, for all other flaring events to date this type of direct, geometrical location information is not available. At the same time a polar location is the only one plausible for many long-lasting events: their small relative sizes (as obtained by hydrodynamic analysis), associated with decay times comparable to – or longer than – the stellar rotational period leave the stellar polar region as the only possible location in which the plasma would not be self-eclipsed by stellar rotation. Examples include the AB Dor SAX flare (Maggio et al., 2000) and the EV Lac RASS event (Schmitt, 1994).

Thus, at least for what concerns the flaring component, many active stars appear to have a corona which is very different from the solar one, in which active regions are always located at mid-latitudes (although they migrate through the solar cycle). This also indicates a different structure for the magnetic field and thus a dynamo which, even if driven by an α–ω mechanism, is spatially distributed in a rather different way than the solar one. At the same time, a polarly located (flaring) corona is in agreement with the large polar spots which are consistently resulting from Doppler imaging of active stars (see e.g. Weber and Strassmeier, 2001 and preceding papers). While in principle the quiescent corona could have a quite different spatial distribution than the flaring component, in the Sun the two are co-located, so that in very active stars also the quiescent corona is likely to be concentrated near the stellar poles.

7.3.2. *Evidence for coronal mass ejections*
Coronal mass ejections (CMEs) are common events in the Sun, and are typically associated with flares (although the association is not one-to-one, with many intense flares not showing an associated CME, see discussion in Harra, 2002 and references therein). One would therefore naturally expect that CME events would be associated with large stellar flares. The rapidly cooling ejected material which is easily seen in solar imaging observations cannot be directly detected in the stellar case. This cool material – if present – should however cause absorption of the soft X-ray emission, i.e. it should "shadow" the flaring material. The SAX Algol flare provides the best evidence to date that such events do exist (that Algol would be a good target to observe a flare-related CME event was first suggested by Stern et al., 1992b in the context of the Algol GINGA flare): as shown in the top right panel of Fig. 33 the

Table II. Analyses of stellar flares in active binaries and in young (ZAMS) stars, using the various methods available in the literature. The number in parenthesis after the star's name indicates the number of flaring events analyzed in the paper. KP = two-ribbon flare model, PR = Pure Radiative Cooling, RD = Rise+Decay, QS = Quasi-Static, Hy = Hydrodynamic model (see Sect. 7.2).

Reference	**Star**	**Instr.**	**KP**	**PR**	**QS**	**RD**	**Hy**
RS CVn/Algol							
van den Oord et al. (1988)	σ^2 CrB	EXOSAT	[a]	X	-	-	-
Osten et al. (2000)	σ^2 CrB	ASCA	-	-	X	-	-
Graffagnino et al. (1995)	HR 5110	ROSAT	-	-	X	-	-
Kürster and Schmitt (1996)	CF Tuc	ROSAT	-	-	X	-	-
Endl et al. (1997)	HU Vir	ROSAT	X	-	X	-	-
Mewe et al. (1997)	II Peg	ASCA[b]	-	-	X	-	-
Güdel et al. (1999)	UX Ari	ASCA[b]	X	-	-	-	-
Franciosini et al. (2001)	UX Ari	SAX	X	-	-	-	-
Stern et al. (1992b)	Algol	GINGA	-	-	X	-	-
Favata et al. (2000b)	Algol	GINGA	-	-	-	-	X
van den Oord et al. (1989)	Algol	EXOSAT	-	-	X	-	-
Favata et al. (2000b)	Algol	EXOSAT	-	-	-	-	X
Ottmann and Schmitt (1996)	Algol	ROSAT	-	-	X	-	-
Favata et al. (2000b)	Algol	ROSAT	-	-	-	-	X
Favata and Schmitt (1999)	Algol	SAX	-	-	X	-	X
Active ZAMS							
Maggio et al. (2000)	AB Dor (2)	SAX	-	-	-	-	X
Güdel et al. (2001a)	AB Dor	XMM	-	-	-	-	X
Covino et al. (2001)	LQ Hya	ROSAT	-	X	-	-	X

[a] – The method was applied but failed to reproduce the light curve.

[b] – (near-)simultaneous EUVE observation.

absorbing column density at the peak of the flare is $N_{\rm H} \simeq 3 \times 10^{21}$ cm^{-2}, an order of magnitude higher than during quiescence, and it decays in an irregular way during the flare decay. The observed behavior is compatible with the picture of a cloud of material being ejected from the flaring region at the beginning of the event, and subsequently thinning out as it expands – and cools – into space.

Some evidence along similar lines had also been provided earlier by the V773 Tau ASCA flare, where the absorbing column density rose by a factor

Table III. Analyses of stellar flares in pre-main sequence stars and in flare (dMe) stars, using the various methods available in the literature. The number in parenthesis after the star's name indicates the number of flaring events analyzed in the paper. KP = two-ribbon flare model, PR = Pure Radiative Cooling, RD = Rise+Decay, QS = Quasi-Static, Hy = Hydrodynamic model (see Sect. 7.2).

Reference	**Star**	**Instr.**	**KP**	**PR**	**QS**	**RD**	**Hy**
PMS/YSO							
Preibisch et al. (1995)	P 1724	ROSAT	-	X	-	-	-
Hamaguchi et al. (2000)	MWC 297	ASCA	-	X	-	-	-
Favata et al. (2001)	HD 283572	ROSAT	-	-	-	-	X
Tsuboi et al. (2000)	YLW 15	ASCA	-	-	X	-	-
Favata et al. (2001)	YLW 15	ASCA	-	-	-	-	X
Preibisch et al. (1993)	LkHα 92	ROSAT	-	-	X	-	-
Favata et al. (2001)	LkHα 92	ROSAT	-	-	-	-	X
Tsuboi et al. (1998)	V773 Tau	ASCA	-	-	X	-	-
Favata et al. (2001)	V773 Tau	ASCA	-	-	-	-	X
dM							
Schmitt (1994)	EV Lac	ROSAT	X	-	X	-	-
Favata et al. (2000c)	EV Lac	ASCA	-	-	X	-	X
Hawley et al. (1995)	AD Leo (2)	EUVE	-	-	-	X	-
Cully et al. (1997)	AD Leo (2)	EUVE	-	-	-	X	-
Favata et al. (2000a)	AD Leo (3)	ASCA	-	-	-	-	X
Favata et al. (2000a)	AD Leo (2)	ROSAT	-	-	-	-	X
Favata et al. (2000a)	AD Leo	*Einstein*	-	-	-	-	X
Reale and Micela (1998)	AD Leo	ROSAT	-	-	X	-	X
Reale and Micela (1998)	CN Leo	ROSAT	-	-	X	-	X
Cully et al. (1993)	AU Mic	EUVE	-	X	-	-	-
Cully et al. (1993)	AU Mic	EUVE	-	X	-	-	-
Stelzer et al. (2002)	YY Gem	XMM	-	-	-	-	X
Pan et al. (1997)	EQ 1839.6	GINGA	-	-	X	-	X
Pallavicini et al. (1990)	14dM (32)	EXOSAT	-	X	-	-	-

of 4 at the peak of the flare, to a much higher value than in the Algol case ($N_{\rm H} \simeq 4 \times 10^{22}$ cm^{-2}). The lower statistics of this event do not allow to study its time evolution in detail; nevertheless, the approximate time in which the absorbing column density returns to its quiescent value is comparable in both cases ($t \simeq 40$ ks).

7.4. THE NEUPERT EFFECT

Solar flares show evidence for the so-called "Neupert effect" (Neupert, 1968), i.e. a strong correlation between the soft X-ray (thermal) emission and the time-integral of the (non-thermal) hard X-ray and radio emission. This is expected in a framework in which a flare begins with the rapid acceleration of a burst of non-thermal electrons down the magnetic field lines defining the flaring loop. The electrons spiral along the field lines and radiate gyrosynchrotron emission in the radio, and collide with ambient ions emitting hard X-rays via non-thermal bremsstrahlung. When they hit the chromosphere and photosphere they heat and "evaporate" it, filling the flaring coronal loop with hot, radiating plasma.

In the stellar context, the (non-thermal) hard X-ray emission has not yet been observed (see Sect. 7.1.3), but other proxies have been used to trace the non-thermal particles, in particular radio emission and white light emission during the flare. White light emission during solar flares has been shown (Hudson et al., 1992) to track well the hard X-rays, and it has also been used in the stellar context as a proxy to the non-thermal emission.

Hawley et al. (1995) discuss a strong EUVE flare on AD Leo, which was also observed simultaneously in optical light with ground-based telescopes, both photometrically and spectroscopically. They find that the EUVE flaring emission is roughly proportional to the integral of the U-band light-curve, and that this is also the case in a number of flares from archival data for which both X-ray and white light data are available. This suggests that the white light continuum enhancement observed in stellar flares is indeed an observational signature of impulsive phase non-thermal electron heating, and that even the large stellar flares are based on a scaled-up version of the mechanism driving solar flares.

More recently, Güdel et al. (2002a) have studied a long-duration flare on the active binary σ Gem, observed simultaneously with both XMM-*Newton* (in X-rays) and the Very Large Array (in radio), finding that the derivative of the X-ray light curve is rather similar to the radio light-curve, as expected if the Neupert effect is present (although the radio data do not cover the rise phase of the X-ray flare). Similar evidence had been found by Güdel et al. (1996) using ROSAT and ASCA observations (again supported by simultaneous Very Large Array radio data) of the dMe binary system UV Cet.

8. Activity in the pre-main sequence phase

This review is devoted mainly to coronal emission of main sequence stars and in this section we briefly review some characteristics of X-ray emission of pre-main sequence stars, mainly in connection with physical properties of main sequence stars. For a more comprehensive discussion on activity of pre-main sequence stars see e.g. Feigelson and Montmerle (1999).

Star-forming regions appeared very rich in X-ray sources associated with stellar objects already in the early *Einstein* observations. T Tauri stars have X-ray luminosity level typically from 10 to 10^4 times the solar one, with spectra harder than normal main sequence stars, and with a fairly high frequency of large flares. Furthermore X-ray emission allowed the detection of a new class of T Tauri stars, originally called Naked T Tauri stars (NTTS, Walter et al., 1988) and now called Weak T Tauri stars, (WTTS) with age of the same range of that of the Classical T Tauri (CTTS, which have prominent disks), but less extreme behavior and with their optical characteristics not dominated by the effects of the disk.

A large fraction of PMS stars are observed to emit X-rays at the saturated level ($L_{\rm X}/L_{\rm bol} \simeq -3$); it is unclear whether PMS stars follow a relationship between X-ray luminosity and rotation, relationship that would indicate that mechanisms at work in these stars are similar to those working on (unsaturated) main sequence stars. In particular in the Taurus-Auriga region various authors (e.g. Bouvier, 1990; Deliyannis and Malaney, 1995; Stelzer and Neuhäuser, 2001) find the classic quadratic relationship between $L_{\rm X}$ and rotational period, while in other regions a similar behavior has not been observed. This apparent discrepancy has been tentatively explained as due to a saturation (Walter and Boyd, 1991; Gagné et al., 1995a; Alcalá et al., 1997), or as indicative of an underlying mechanism in which stellar mass is the basic parameter determining the X-ray luminosity level (Feigelson et al., 1993; Lawson et al., 1996).

Whether accretion has a role in determining the X-ray luminosity (either enhancing or inhibiting it) in PMS stars is still a debated question. Some studies (e.g. Feigelson et al., 2002a) find no difference in X-ray properties of CTTSs (in which strong accretion can be ongoing) and WTTSs (in which accretion is negligible), while other authors report significant differences between the two, with CTTSs being under-luminous in X-rays with respect to WTTSs (Flaccomio et al., 2003b). Also, claims have been made that a significant fraction of the X-ray luminosity of some CTTSs is indeed due to accretion (Kastner et al., 2002), and that the X-ray emission of CTTSs appears to be more time-variable with respect to WTTSs (Flaccomio et al., 2000).

Another characteristic of pre-main sequence X-ray emission is the high frequency of flares compared with that observed on the Sun. Already the first

Einstein observation of ρ Oph showed (Montmerle et al., 1983) that short term X-ray variability is a common property of PMS stars, so that this star-forming region was dubbed an "X-ray Christmas tree".

9. Evolution of activity in the main-sequence phase

Already with the early *Einstein* observations it had become evident that stellar X-ray emission evolves during the stellar lifetime. It became soon apparent that coronal emission is influenced by stellar properties other than the "classic" ones (i.e. mass or effective temperature), and that rotation in particular plays a crucial role. Given that rotation evolves with age, this implies that coronal evolution has to be present during the stellar lifetime. When the *Einstein* observations became available it was already well known that chromospheric emission decays along a star's main sequence life following the famous Skumanich law (Skumanich, 1972) with a time dependence $\propto t^{-1/2}$. The evolution of X-ray emission is now known to follow a more complicated law, with a plateau at young age, and a decrease similar to the Skumanich law for older ages, but with a large spread (up to an order of magnitude) around this relation.

Most of our knowledge on evolution of coronal emission derives from observations of open clusters, which supply large, chemically homogeneous and well dated stellar samples. *Einstein* was able to observe only the Hyades, the Pleiades, and the Ursa Major clusters. These few observations, although severely limited by the poor sensitivity of the instrumentation, set the foundations of the knowledge on the evolution of coronae for solar type stars. The first observations of the Hyades (Stern et al., 1981; Micela et al., 1988) detected a large fraction of solar type stars with $L_X \geq 10^{28.5}$ erg s^{-1}, allowing to determine that coronal evolution is dominated by rotational evolution and that the characteristic evolutionary time scales of L_X are a function of stellar mass. The observations of the Pleiades (Caillault and Helfand, 1985; Micela et al., 1985; Micela et al., 1990) confirmed the initial picture of evolution of the X-ray emission, and showed that the evolution is very slow at the beginning (during the first billion years) and much faster afterward. Furthermore the observations of the dK fast rotators of the Pleiades showed that the relation between L_X and rotation flattens at high rotational velocity, with a plateau that is interpreted through a saturation phenomenon of the X-ray emission (Sect. 4.5). The observations of the UMa cluster stars (Schmitt et al., 1990b) gave results apparently contradicting the picture that the other two clusters were delineating: while the UMa cluster has an age intermediate between Pleiades and Hyades, its X-ray luminosity level is lower that of the Hyades. This fact was explained with the difficulty in selecting a significant sample of bona-fide cluster stars (because of the closeness of the UMa cluster).

Table IV. X-ray studies of open clusters within 500 pc from the Sun. Ages and distances are from the WEBDA database (http://obswww.unige.ch/webda). Clusters are listed in order of distance. Logarithmic ages are in yr.

Reference	**Cluster**	**Instr.**	**d[pc]**	**log(age)**
Stern et al. (1981)	Hyades	IPC/*Einstein*	48	8.80
Micela et al. (1988)		IPC/*Einstein*		
Stern et al. (1992a)		RASS/ROSAT		
Pye et al. (1994)		PSPC/ROSAT		
Stern et al. (1994)		PSPC/ROSAT		
Reid et al. (1995)		PSPC/ROSAT		
Stern et al. (1995b)		RASS/ROSAT		
Randich et al. (1996a)	Coma	PSPC/ROSAT	83	8.69
Caillault and Helfand (1985)	Pleiades	IPC/*Einstein*	120	7.92
Micela et al. (1985)		IPC/*Einstein*		
Micela et al. (1990)		IPC/*Einstein*		
Schmitt et al. (1993)		PSPC/ROSAT		
Stauffer et al. (1994)		PSPC/ROSAT		
Hodgkin et al. (1995)		PSPC/ROSAT		
Gagnè et al. (1995b)		PSPC/ROSAT		
Micela et al. (1996)		PSPC/ROSAT		
Micela et al. (1999b)		HRI/ROSAT		
Krishnamurthi et al. (2001)		ACIS/*Chandra*		
Patten and Simon (1993)	IC 2391	PSPC/ROSAT	164	7.64
Patten and Simon (1996)		PSPC/ROSAT		
Simon and Patten (1998)		PSPC/ROSAT		
Randich et al. (1995)	IC 2602	PSPC/ROSAT	164	7.36
Randich et al. (1996b)	α Per	PSPC/ROSAT	170	7.90
Prosser et al. (1996)		PSPC/ROSAT		
Randich and Schmitt (1995)	Praesepe	PSPC/ROSAT	179	8.84
James and Jeffries (1997)	NGC 6475	PSPC/ROSAT	239	8.11
Micela et al. (1999a)	Blanco 1	HRI/ROSAT	240	7.85
Sciortino et al. (2000)	Stock 2	HRI/ROSAT	303	8.23
Giampapa et al. (1998)	IC 4665	HRI/ROSAT	344	7.58
Belloni and Verbunt (1996)	NGC 752	PSPC/ROSAT	364	9.43

Table IV. (Cont.) X-ray studies of open clusters within 500 pc from the Sun. Ages and distances are from the WEBDA database (http://obswww.unige.ch/webda). Clusters are listed in order of distance. Logarithmic ages are in yr.

Reference	**Cluster**	**Instr.**	**d[pc]**	**log(age)**
Dachs and Hummel (1996)	NGC 2516	PSPC/ROSAT	373	7.79
Jeffries et al. (1997)		PSPC/ROSAT		
Micela et al. (2000)		HRI/ROSAT		
Harnden et al. (2001)		ACIS/*Chandra*		
Sciortino et al. (2001)		EPIC/XMM		
Briggs et al. (2000)	NGC 6633	HRI/ROSAT	383	8.66
Harmer et al. (2001)		HRI/ROSAT		
Jeffries and Tolley (1998)	NGC 2547	HRI/ROSAT	428	7.47
Franciosini et al. (2000)	NGC 3532	HRI/ROSAT	443	8.40
Randich et al. (1998)	IC 4756	HRI/ROSAT	480	8.78
Briggs et al. (2000)		HRI/ROSAT		
Barbera et al. (2002)	NGC 2422	ROSAT	497	8.85

With the advent of ROSAT many more clusters have been observed and the range of explored ages is now very large, yielding a picture more complete but at the same time more complex. Table IV reports a list of clusters observed in X-rays, with the relative references. One of the problems in interpreting the data is the limited amount of information available on fundamental cluster properties. Accurate (and X-ray independent) membership, chemical abundance, rotation distribution, and binary frequency are known only for few clusters. The lack of information on these properties can introduce severe biases on the conclusions about coronal evolution. For these reasons in Sects. 9.1–9.3 we will consider only well studied clusters, and separately discuss results relative to other clusters in Sect. 9.4, stressing possible aspects of their properties that apparently do not match with the general picture delineated by the "reference" clusters, and discussing the possible observational limitations. The X-ray emission from open clusters has recently been reviewed e.g. by Micela (2001).

9.1. RESULTS FROM OPEN CLUSTER STUDIES: SOLAR MASS STARS

We will concentrate on the X-ray properties of nearby open clusters, which have well known properties, in particular in terms of reliable membership based on criteria independent from activity. X-ray emission has been often used to identify bona-fide members of young clusters, giving a significant contribution to the study of the low-mass tail of their initial mass function, but in these cases the derived X-ray luminosity distributions are biased towards X-ray-luminous stars.

The best known clusters with good X-ray observations are α Per, the Pleiades, Hyades, Coma, and Praesepe. All these clusters have been targets of relatively deep X-ray observations as discussed in the following. The Coma cluster is a relatively poor one, and its emission has been found to be similar to that of the Hyades (Randich et al., 1996a), so that it will not be discussed further in the following. Observations of Praesepe give anomalous results with respect to the other clusters and will be discussed separately.

The median X-ray luminosity of dG stars in star-forming regions, open clusters and field stars is plotted in Fig. 21 as a function of stellar age. Vertical segments indicate the 1σ spread of the X-ray luminosity distributions. Unfortunately there are no old clusters sufficiently nearby as to allow the determination of the X-ray luminosity distribution of normal dG stars (and the situation is even worst for lower mass stars, which are intrinsically less luminous X-ray sources). The dashed lines in Fig. 21 show the level of $L_{\rm X}$ corresponding to the saturation level of $\log L_{\rm X}/L_{\rm bol} = -3$, computed using the evolutionary tracks of D'Antona and Mazzitelli (1997). The two lines correspond to $1 M_{\odot}$ and $0.8 M_{\odot}$, covering approximately the mass range of Pop. I dG stars. A significant fraction of dG stars in clusters younger than Pleiades emit at the saturation level, while in older clusters all the stars become non-saturated and the mean X-ray luminosity starts to decrease. The coronal emission level, expressed in terms of X-ray luminosity, remains almost constant until an age of 10^8 yr, and then decreases steeply until the solar age, with a drop of one order of magnitude in X-ray emission level in less than a decade in age.

The data show that X-ray emission decreases with age, but that there is no deterministic relationship between $L_{\rm X}$ and age, so that $L_{\rm X}$ can be used as a statistical age indicator, but not as a deterministic one, similarly to kinematic age indicators. One can say that a sample of bright X-ray emitters is *on average* younger than a sample of X-ray quiet stars, but one cannot date single stars on the basis of their X-ray activity level. Indeed chromospheric activity, as measured by the flux emitted in the Ca II H&K lines (parameterized e.g. through the $R'_{\rm HK}$ index), has been widely used to date stars, but also this indicator should be considered as a statistical one. If one were for example to date individual Hyades stars through the relationship derived

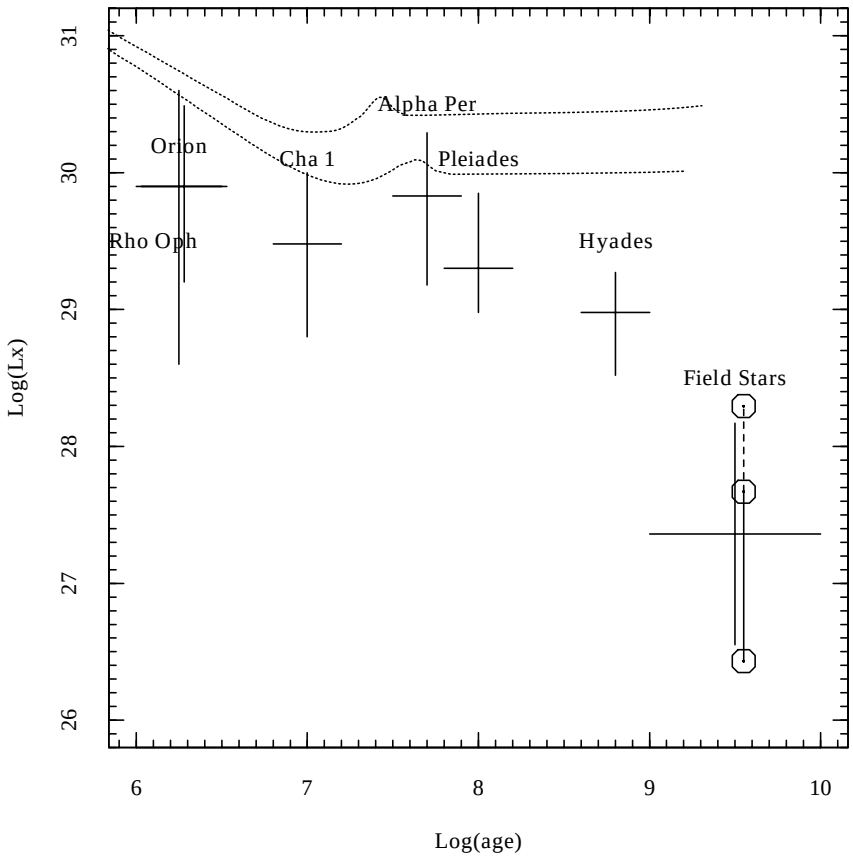

Figure 21. Medians of distributions of the X-ray luminosity for dG stars for a number of star-forming regions, open clusters and nearby stars, plotted as a function of age. Vertical segments represent the 1σ equivalent spread of the data (data from Casanova et al., 1995; Feigelson et al., 1993; Flaccomio et al., 2003a; Micela et al., 1999b; Randich et al., 1996b; Schmitt, 1997; Stern et al., 1995b). For comparison the data corresponding to the Sun (circles) during the solar minimum and maximum and during a bright flare are reported (Peres et al., 2000). Dashed lines represent the saturation level for dG stars (see text).

from Lachaume et al. (1999) between the $R'_{\rm HK}$ index and age (using the $R'_{\rm HK}$ Hyades data of Duncan et al., 1984), Hyades stars would appear to have an age spanning almost an order of magnitude, $8.26 \leq \log t \leq 9.16$ yr, decreasing to $8.26 \leq \log t \leq 8.71$ yr for stars with $B-V > 0.6$. In the X-ray regime there is a non-negligible overlap between the luminosity distributions of stars of very different age. In the case of the Pleiades and Hyades, which have an age differing by approximately one order of magnitude, this is particularly evident: the median X-ray luminosity of Pleiades stars corresponds to the 11

percentile of the Hyades distribution, and the 80 percentile of the Pleiades coincides with the median of the Hyades. This implies that a star with L_X in the range $28.8 < \log L_X < 29.5\,\mathrm{erg\,s^{-1}}$ can be attributed an age between 10^8 and 10^9 yr.

Given the tight relationship between L_X and rotation (Fig. 9), the spread in the X-ray luminosity distribution should reflect the spread in the rotational velocity distribution, at least when the rotational velocity is smaller than the saturation limit. Bouvier et al. (1997) have shown that stars arrive on the ZAMS with a very large spread in rotational velocity; later, during the main sequence lifetime, fast and slow rotators spin down on different time scales. The rotation velocity of dG stars apparently converge at the Hyades age, implying a null expected spread in L_X at this age.

In practice the dG stars of Hyades show a significant spread in X-ray luminosity, which reflects the dependence of rotation on spectral type. Fig. 22 shows how the rotational period in Hyades stars changes with color. It is evident that there is a well defined trend, with the early-dG stars rotating twice as fast than the late-dG ones. Stars of a given color have a relative spread in rotational period of only 25%. Fig. 22 shows the change of L_X with stellar color for the same stars. In this case there is a clear decrease of the X-ray luminosity with increasing color, as expected from the relationship between X-ray luminosity and rotation for non-saturated stars. The spread of L_X at a given color is no more than a factor of two, fully consistent with the long term X-ray variability observed in the Hyades (Stern et al., 1995b). The only discrepant point refers to the star VB 50 which is an X-ray-bright binary system. In the case of Hyades the spread observed in the X-ray luminosity distribution can be thus fully explained as due to the dependence of rotation on color within the considered color range and to the presence of some bright binaries.

9.2. Results from open cluster studies: low mass stars

Cluster observations suggest that age evolution of coronal activity is present for all spectral types, but with different time scales (Micela et al., 1988; Micela et al., 1990). Fig. 23 shows the age evolution of the X-ray luminosity of dM stars (analogous to Fig. 21 for dG stars). Most of the dM stars in Pleiades and α Per, and part of ones in Hyades are saturated, and the decrease of L_X with age starts at a later age with respect to the dG stars. The different evolution of dM stars with respect to the dG stars can be explained as being due to the different bolometric luminosity and it is probably related to the dependence of rotational evolution on stellar mass (Bouvier et al., 1997): as dM stars spin down more slowly they will emit at the saturation level for a longer time, even though this saturation X-ray luminosity will be lower than for higher mass stars.

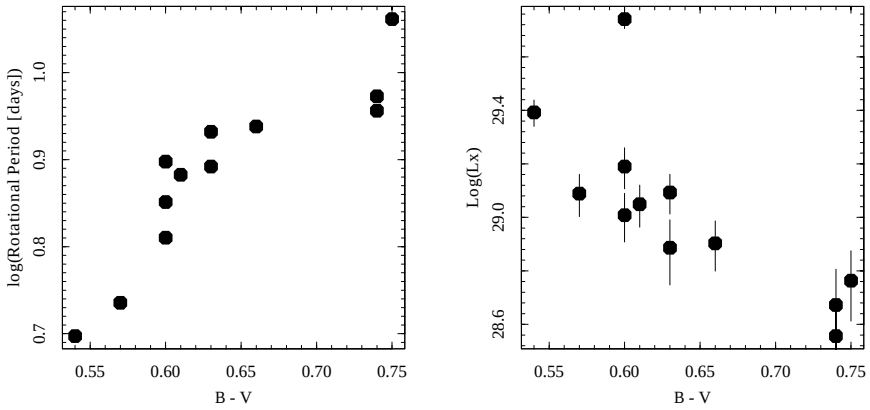

Figure 22. Left: Rotational periods vs. stellar color for the dG stars in the Hyades. The stars in the sample are all the stars from Stern et al. (1995b) for which photometric rotational periods from Radick et al. (1995) are available. Typical errors for rotational periods are smaller than the size of the dot used in the plot. Right: X-ray luminosity vs. stellar color of the dG stars in the Hyades. According to the Pallavicini et al. (1981) law X-ray luminosity decreases with increasing rotational period, and as a consequence (in the case of Hyades) with the increasing color. The observed spread at a given color (and hence for a given rotational period) is within a factor of two, fully consistent with the variability observed in the Hyades. The only outlier is the peculiar binary system VB 50.

Another issue is the evolution of X-ray emission of brown dwarfs. Indeed most of the brown dwarfs detected in X-rays belong to star-forming regions (see Sect. 4.3.1), i.e. they are very young. Only recently with a moderately deep XMM-*Newton* exposure it has been possible to detect a brown dwarf in the Pleiades, with an emission level close to the saturation limit (Briggs, private communication). The weakness of the X-ray source makes it impossible to determine if the detected X-rays are due to flaring or quiescent emission.

9.3. CORONAL SPECTRAL EVOLUTION

The coronal spectral characteristics also change, together with the luminosity level, during the stellar life. Assuming a solar analogy, in which the more active regions host hotter plasma and the cooler plasma is associated with less X-ray bright regions, the evolution of the coronal spectrum implies that the relative contribution of different coronal structures changes in time. Already the first *Einstein* observations (Schmitt et al., 1990a) showed that L_X and average coronal temperature are well related, and since L_X decreases with increasing age, one expects that at the same time a decrease of the average coronal temperature with age.

Even today, with the *Chandra* and XMM-*Newton* grating spectrographs, it is possible to obtain high resolution X-ray spectra only for the X-ray brightest

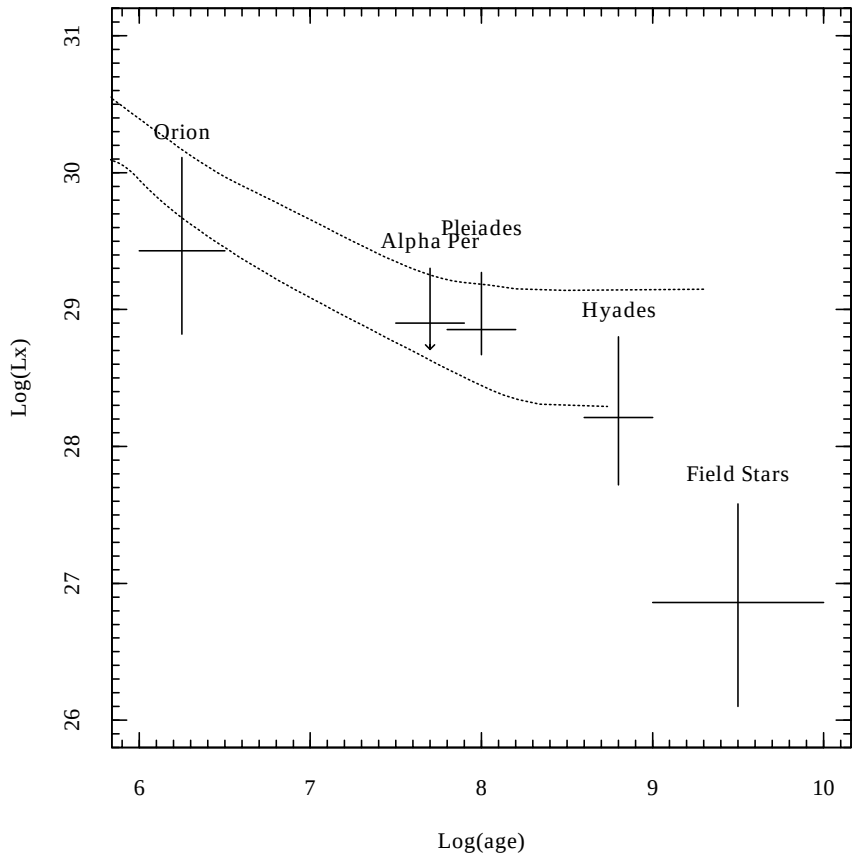

Figure 23. The median and the spread of the L_X distribution of dM stars in open clusters plotted versus the cluster's age. Vertical segments represent the 1σ equivalent spread of the data (data from Flaccomio et al., 2003a; Micela et al., 1999b; Randich et al., 1996b; Schmitt, 1997; Stern et al., 1995b). The dotted lines represent the saturation level (assumed at $L_X/L_{bol} = 10^{-3}$) for dM stars of mass 0.3 and $0.5 M_\odot$.

stars, so that (apart from a few exceptions), cluster stars can be observed only with the low resolution (CCD) spectrometers. Fig. 24 shows the result of the analysis of the ROSAT PSPC observations of the Hyades (Stern et al., 1994) and Pleiades (Gagné et al., 1995b). All the low-resolution X-ray spectra have been fit with a simple two-temperature thermal model; the resulting best-fit temperatures are plotted against each other in Fig. 24. On average, Hyades stars have coronal temperatures lower than Pleiades stars (as expected given their lower X-ray luminosities). Results of the fits to the composite spectra of Pleiades stars grouped by spectral type and rotational velocity are also

shown in the figure (data from Gagné et al., 1995b). The properties of X-ray spectra depend on spectral type and rotation level, with the fast dG rotators having hotter coronae than the other groups and the dF stars having cooler coronae than all the other types. Both the high and low best-fit temperature components of young stars' coronal emission are hotter than those of older stars.

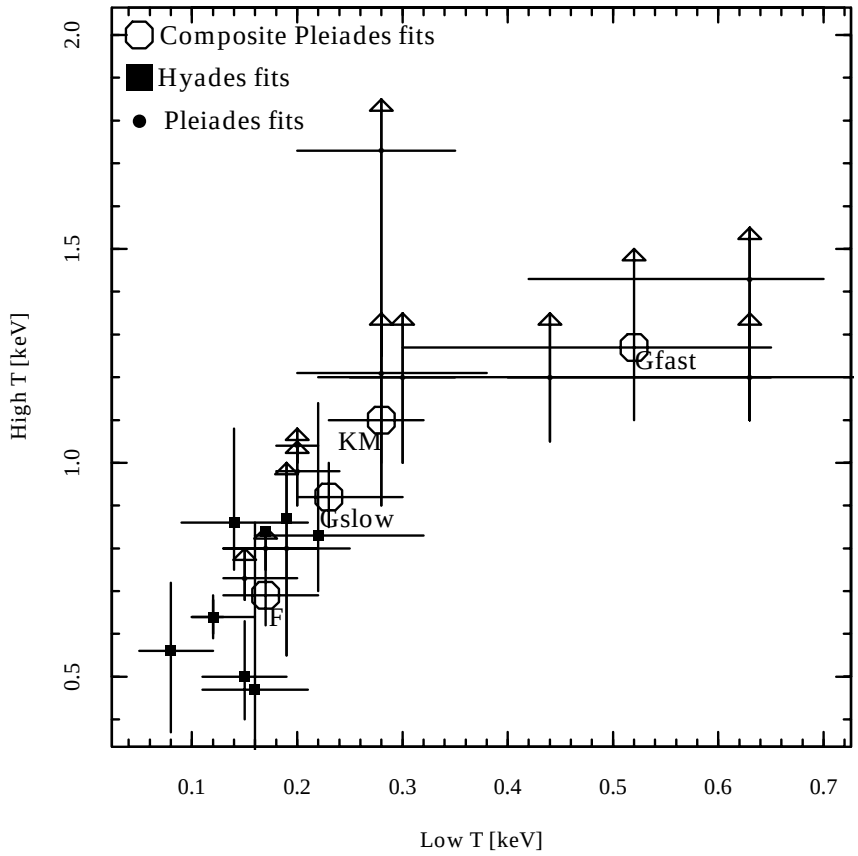

Figure 24. Temperatures derived from 2-*T* fits to the low-resolution X-ray spectra of Hyades (data from Stern et al., 1994) and Pleiades (data from Gagnè et al., 1995b) stars. Large symbols represent the fits to the composite spectra obtained by summing the spectra of stars in the Pleiades grouped by spectral type and rotational velocity.

In order to explore how the "effective" coronal temperatures of dG stars evolve with age we collected the results of two-temperature fits to the low-resolution X-ray spectra of Pleiades stars, Hyades stars, the field stars studied by Güdel et al. (1997), and the Sun (Peres et al., 2000). The resulting plot

is shown in Fig. 25. Both best-fit coronal temperature components decrease with age, with a spread of about half an order of magnitude for coeval stars. In Fig. 25 also the best-fit coronal temperatures derived for the Sun during the minimum and the maximum of the solar cycle, as well as during a bright flare, are reported. The temperatures derived for the Sun during the flare are very similar to those derived for very active and young Pleiades stars.

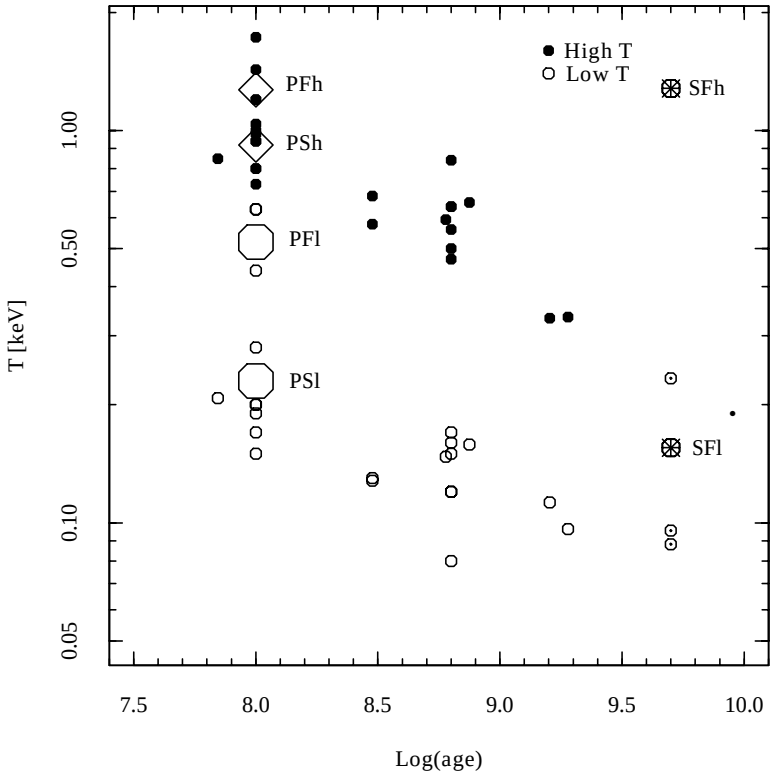

Figure 25. Temperatures derived from two-temperature spectral fitting of ROSAT PSPC data versus age for dG stars, in clusters as well as in the field. Filled symbols represent the high-temperature component, and empty symbols the low-temperature one. Large symbols represent the temperatures derived from the composite spectra of fast ("PF") and slow ("PS") rotating dG Pleiades stars. Points at $\log t = 9.7$ yr mark the temperatures derived for the Sun during different phases of solar activity as well as during a large solar flare ("SF").

The emission measure evolves together with the temperature, with the *EM* of the hot temperature component decreasing more quickly than the one of the cool temperature component, implying that probably the structures typically

associated with the hot temperature plasma (flares, active regions), evolve more rapidly than the quiet regions.

9.4. IS THE AGE EVOLUTION OF ACTIVITY UNIQUE?

The study of a relatively large number of clusters has stimulated the question whether all the clusters with a given age are also equivalent in every aspect of their coronal emission. The question is important for the understanding of many fundamental aspects of stars, as evidenced by the Hipparcos measurements which indicate that samples of coeval stars of the same chemical composition can differ significantly in stellar properties as fundamental as their position in the H-R diagram (Mermilliod et al., 1997). This problem came up also in the coronal studies, as soon as clusters other the the classical Hyades and Pleiades were observed. In particular the Praesepe ROSAT observations (Randich and Schmitt, 1995) have shown that the dG stars of this cluster are significantly X-ray fainter than their Hyades analogs. The distribution of X-ray luminosity of dG stars in Praesepe appears to be bimodal, with the brightest stars similar to the Hyades ones, but also with a population of X-ray quiet dG stars, undetected by the ROSAT observations, and which do not have a match in the Hyades.

In order to explain the difference observed in the coronal characteristics of the otherwise twin Hyades and Praesepe clusters a number of investigations have been conducted. Among the more likely hypotheses which have been advanced, the possibility of a significant contamination of the Praesepe sample with (older and less active) field stars has been excluded (Barrado y Navascués et al., 1998), and Mermilliod (1997) has shown the rotation velocity distribution of Praesepe stars to be similar to that of the Hyades. The reason for the observed difference is still a puzzle, and further observations, such as the determination of the fraction of binary systems in Praesepe, are needed.

A number of other open clusters appear anomalous with respect to the canonical Pleiades and Hyades. For example solar-type stars in NGC 2547 (Jeffries and Tolley, 1998; Jeffries et al., 2000) show a saturation level lower by a factor two with respect to the saturation level commonly observed in fast rotating stars. Jeffries et al. (2000) confirm that the rotational distribution in NGC 2547 is similar to that of coeval clusters such as IC 2391 and IC 2602, and exclude a lack of fast rotators in NGC 2547. Other clusters could show peculiar behavior (NGC 3532, Franciosini et al., 2000 and Stock 2, Sciortino et al., 2000) but in these case biases due to wrong age determination or to sample selection effects can be important given the lack of e.g. reliable and extensive membership determinations.

9.5. CHEMICAL ABUNDANCE EFFECTS ON CORONAL EMISSION

Chemical abundances play an important role in determining stellar characteristics and structure. It is hence plausible to expect some effects on coronal properties. One way to explore this issue is through the comparison of the coronal properties of clusters with similar age and different metallicity with the expectations based on e.g. stellar structure models. With this approach problems related to the peculiarity of individual stars are minimized, but of course one assumes that the only difference between the clusters under study is the chemical abundance.

In principle the influence of metal abundance on coronae can be complex. First of all there is an obvious direct effect on the coronal emission level, mainly due to the fact that most of the coronal emission is due to radiative losses from heavy ions. A change in the balance between radiative losses (which are abundance-dependent), thermal conduction (which is largely independent on metal abundance) and heating will result in a different emission measure distribution. Furthermore there is a subtler effect on the entire process since the metals are the main contributors to the opacity inside the star and, hence, determine the properties (in particular the depth) of the convection zone. As a consequence metal abundance is expected to affect the dynamo efficiency, responsible for the coronal magnetic field production. As discussed by Jeffries et al. (1997) a change in coronal emission is expected to have an effect on angular momentum loss and therefore on the rotational evolution, which in turn affects coronal evolution. One can thus expect stars with different metal abundance to have different rotational and coronal evolution.

Pizzolato et al. (2001) have computed the depth of the convection zone of dG and dK stars as a function of metallicity, using both the mixing length theory treatment of convection and the full spectrum of turbulence theory (Ventura et al., 1998a). The results indicate that the general behavior does not depend on the assumed model for convection, and that the effects are more relevant for late dF and early dG stars than for later types. In particular, if the dependence of the color-mass transformations on metallicity is taken into account, in the color range $0.5 \leq B-V \leq 0.6$ metal poor stars have convection zones deeper than metal rich ones. This apparent contradiction with respect to the naive expectations is entirely due to the color-mass relation, which makes metal-rich stars of a given mass bluer than metal-poor stars. The effect is negligible for stars redder than $B-V \simeq 0.6$. Pizzolato et al. (2001) have also estimated the combined effect expected considering also the changes in radiative losses. At the X-ray energies relevant for typical coronal temperatures, the radiative loss level changes almost linearly with the metal abundance. Assuming stars with the same rotational velocity, and an inverse quadratic relationship between L_X and the Rossby number (R_0), defined as

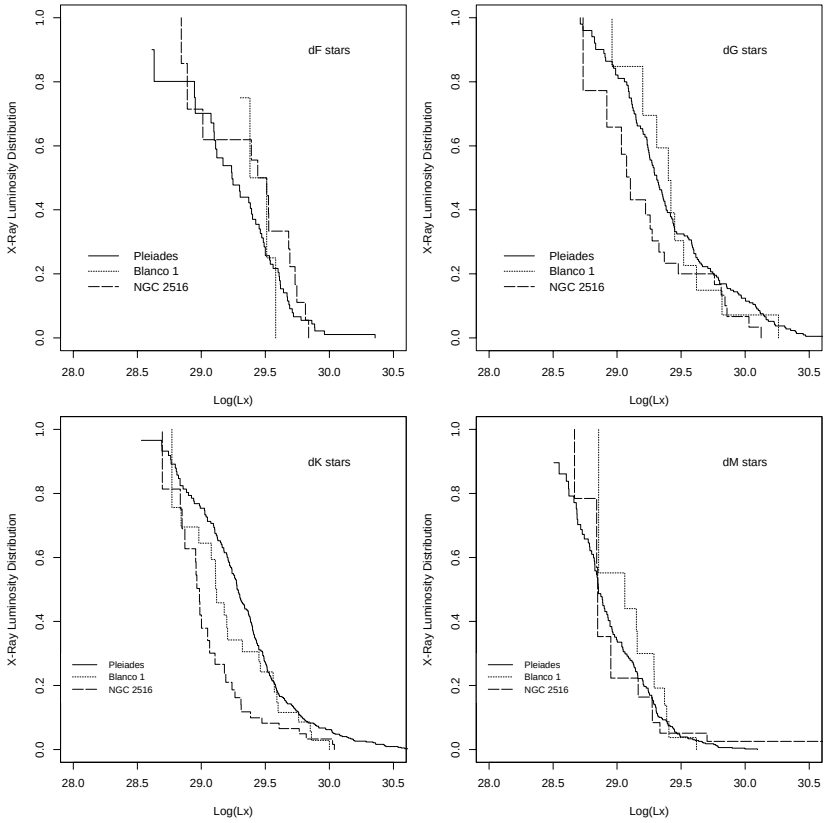

Figure 26. X-ray luminosity distributions for dF stars (top left panel), dG stars (top right panel), dK stars (bottom left panel) and dM stars (bottom right panel) for NGC 2516 (long-dashed line), Blanco 1 (dotted line) and Pleiades (solid line). See text for details. Adapted from Pillitteri et al. (2002).

the ratio between the rotational period and the convective turnover time (see Sect. 4.5), the dependence of L_X on metal abundance can be predicted.

Observational constraints on the actual metallicity dependence of coronal emission can be derived from the observation of coeval clusters with different metal abundance. NGC 2516, the Pleiades and Blanco 1 have the same age ($t \simeq 100$ Myr) and metallicity values of $Z \simeq 0.5, 1, 2\ Z_\odot$ respectively[5], and hence are well suited to explore the metallicity effects on coronal emission of young stars.

NGC 2516 has been observed in X-rays with several detectors and in this context we will use the recent *Chandra* observations (Harnden et al., 2001), for the Pleiades we will use the ROSAT observations (Stauffer et al.,

[5] The metallicity determination for NGC 2516 is based on photometric measurements only, and thus to be taken with some caution.

1994; Micela et al., 1999b), and for Blanco 1 we will use the ROSAT HRI observations of Micela et al. (1999a) with the X-ray luminosity distributions recomputed using a new astrometric membership (Pillitteri et al., 2002). Fig. 26 shows the X-ray luminosity distributions for the dF, dG, dK, and dM stars for the three clusters. The data suggest that the X-ray luminosity distributions of dF stars in the three clusters are indistinguishable, while metal-poor dG and dK stars appear to be less active than their more metal-rich counterparts. For dM stars no significant difference is visible between the samples, indicating that the role played by metal abundance in determining their coronal emission is minor.

9.6. Evidence for the existence of old active field stars

The observations available today allow to explore with a reasonable detail clusters with ages younger than 10^9 yr, while observations of older clusters are still prohibitive with present instrumentation, due to the relatively low X-ray emission level of old stars and the large distance from the Sun of available old clusters. In order to explore the range and the properties of "old" stars with ages comprised between Hyades and the Sun we have to rely on observations of field stars.

Nearby stars (within 13 pc from the Sun) have been studied in detail by Schmitt (1997) – see Sect. 4.1. Their L_X spans more than one and half orders of magnitude, with a distribution well described by a log-normal curve. The Schmitt (1997) sample contains stars with different ages, reflecting the population mixture of the solar neighborhood, and an accurate determination of their age is presently unavailable.

In order to explore the age-L_X relation in the field stars we have analyzed a sample derived from the work of Ng and Bertelli (1998) who, comparing the accurate position of stars in the H-R diagram with their own stellar evolutionary tracks, have dated the individual stars with a reasonable accuracy. The original sample was derived from the work of Edvardsson et al. (1993) on the study of chemical evolution of the galactic disk, in which detailed chemical abundances for each star were determined. Using the abundances of Edvardsson et al. (1993) and the Hipparcos distances Ng and Bertelli (1998) have been able to derive reliable ages. For the 0.8–1.0 $M_\odot$ stars the X-ray count rates measured during the RASS (and reported in the RASS bright and faint source catalogs) have been collected (Micela, 2002). For the stars undetected in the RASS, upper limits to the X-ray flux have been computed from the original RASS images.

The derived L_X values are plotted as a function of age in Fig. 27, together with data for Pleiades, Hyades, and the Sun. The sample of Ng and Bertelli (1998) is not complete, (and may therefore be affected by unknown biases), and cannot be used to compute X-ray luminosity distributions, but it can still

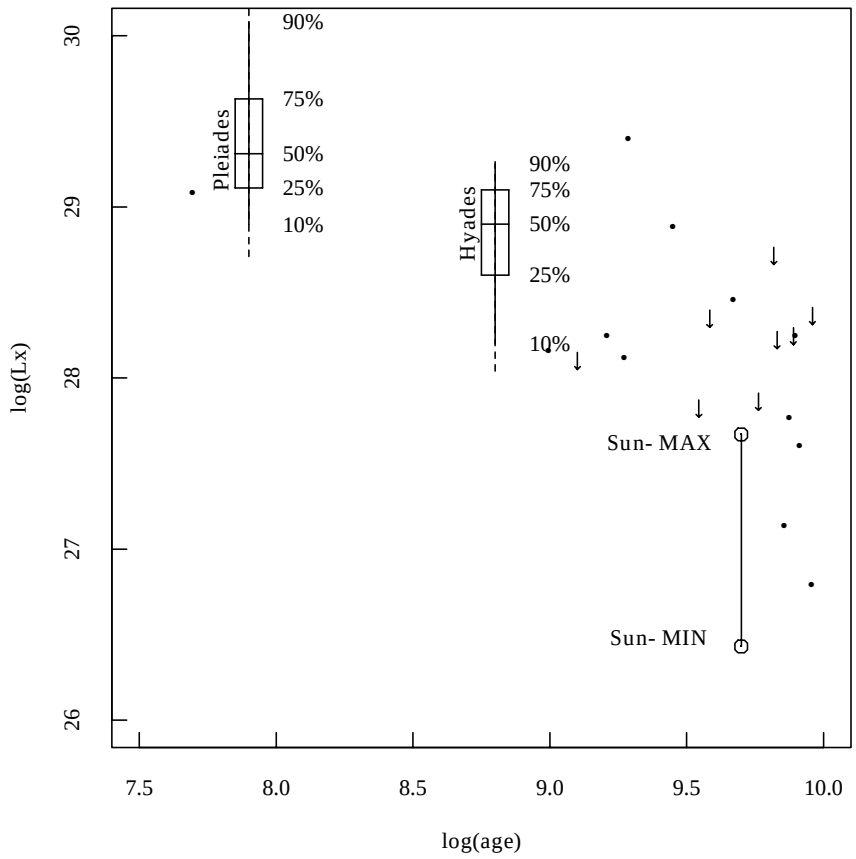

Figure 27. X-ray luminosity of stars in the sample of Ng and Bertelli (1998), compared with the Pleiades and Hyades distributions for dG stars (boxes). The line at age 5×10^9 yr connect the minimum and maximum X-ray emission levels of the Sun. Arrows mark the upper limits to the X-ray luminosity for stars that have not been detected in X-rays.

be used to show that old main sequence stars, with age greater than 10^9 yr can have a high X-ray luminosity level, comparable with that of the Hyades. Present data do not allow to determine which fraction of the stars maintain this high L_X for a long time, nor whether this apparent slow evolution of X-ray activity is related to a slow evolution of rotation (rotation measurements for these stars are lacking), or to other stellar properties, but the existence of these long-lived active stars cannot be neglected for a full understanding of stellar coronal evolution.

10. Coronal abundances

10.1. THE SOLAR CASE

Differences in the chemical composition of the solar wind with respect to the composition of the photosphere were noticed already in the early observations (e.g. Pottasch, 1963b). Meyer (1985) reviewed extensively the literature existing at the time, conclusively showing that the heavy element composition of the solar corona, of the solar wind, and of the solar energetic particles show the same abundance pattern, with a relative under-abundance of heavy elements with first ionization potential (FIP) $\gtrsim 10$ eV relative to elements with lower FIP, by typical factors of $\simeq 4$ to 6 (this latter ratio being referred to as the "FIP bias"). While it initially appeared that the high-FIP elements were depleted with respect to their photospheric values, it soon became apparent (and it remains the general agreement to date) that on the contrary the FIP bias observed in solar active regions results in an enhancement of the abundance of the low-FIP elements (including Fe) with respect to their photospheric value (Feldman, 1992), so that the solar corona is more metal rich than the photosphere.

The level of FIP bias in the solar corona is variable with location and with time. A given active region will show a FIP bias increasing roughly linearly with time: newly formed active regions show essentially photospheric composition, but start to develop a FIP bias as soon as they appear (Sheeley, 1996; Widing and Feldman, 2001). Typical average coronal values for the FIP bias are reached in two to three days, with values as high as 8 typically reached in four to five days. Individual active regions with FIP biases as high as 15 have been observed. The typical large-scale average value of 4–5 for the solar coronal FIP bias is then likely to represent an average over time and over a number of active regions.

No agreed theoretical explanation for the FIP effect observed in the solar corona exists yet; a recent review of the theoretical explanations proposed is provided by Hénoux (1998).

10.2. INITIAL STELLAR EVIDENCE

10.2.1. *Data analysis approaches*

Two basic classes of approaches are currently in use in the X-ray astronomical community for the determination, from an X-ray stellar spectrum, of the chemical abundance of the emitting plasma. The first approach is based on a global fit to the spectrum, i.e. a search for the model spectrum which minimizes the differences (in a χ^2 optimal sense) between the observations and the model. This normally implies an a priori choice regarding the thermal structure of the corona, i.e. on the number of isothermal "components" present in the spectrum; experience shows that in most cases, when CCD spectra are

fit, a limited number of components is needed (2 or 3), giving rise to the so-called 2–*T* or 3–*T* models (although larger numbers of isothermal components have occasionally been used, approaching a "continuous differential emission measure"). This approach has also been applied to high resolution spectra, both from EUVE and, more recently, from the XMM-*Newton* and *Chandra* spectrographs. Some recent applications of this approach include e.g. Audard et al. (2001), using the XMM-*Newton* RGS spectrum shown in Fig. 35.

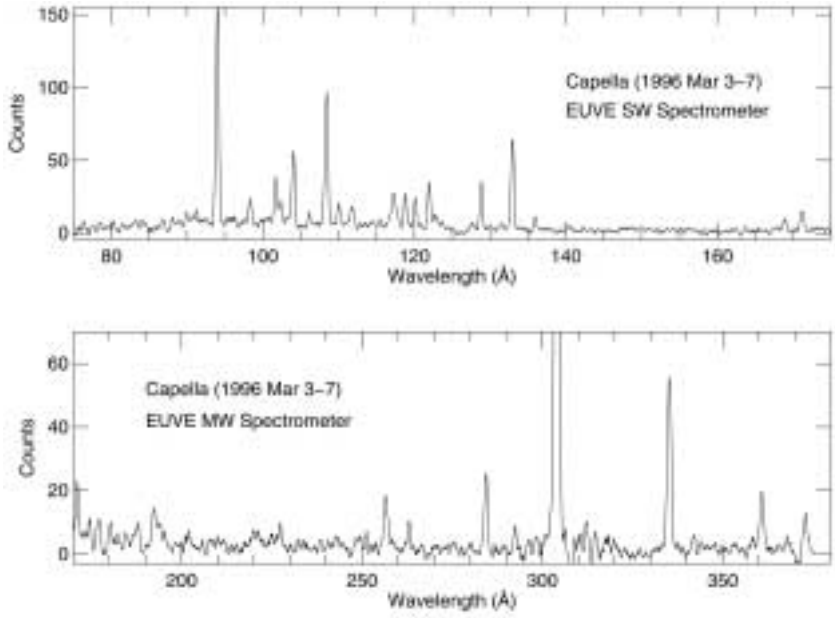

Figure 28. The EUVE spectrum of Capella from Brickhouse et al. (2000).

The other commonly used approach for the analysis of high resolution spectra is the determination of individual line fluxes, and the construction of a differential emission measure which can successfully predict these line fluxes. An example of this is the analysis of the Capella EUVE spectrum – similar to the one shown in Fig. 28 – by Brickhouse et al. (1995). The key difference between the two approaches is whether one uses the information of the whole spectrum or whether only the information relative to the lines of interest is used. The global fitting approach in principle makes use of the information present in the whole spectrum, but it has the disadvantage of including, in this way, spectral regions which suffer from e.g. calibration problems or for which the emission models are not reliable. For example, weak lines which are present in the actual data but missing from the models may result in a wrong estimate of the continuum and thus of the abundance derived from the relevant lines. In addition, the a priori choice of the tem-

perature structure may have an influence on the results. Unfortunately, up to now no comparative systematic analysis of the same data set with the two approaches is available, and it is thus difficult to assess whether the two are bound to produce compatible results.

10.2.2. *Early results*

In the *Einstein* and ROSAT eras coronal abundances were not a strong issue, even though the initial analysis of intermediate resolution spectra of active binaries obtained with the *Einstein* SSS detector (Swank and White, 1980) – Fig. 29 – included a discussion of the coronal metal abundances for a number of elements. The limited spectral resolution of the IPC and PSPC detectors was such that Collisional Ionization Equilibrium (CIE) plasma models computed assuming solar photospheric metal abundances were in most cases sufficient to describe the source spectra (but see e.g. the abundance variations seen in the Algol PSPC flare, Sect. 10.4.1). However, when the ASCA/SIS spectra of stellar sources became available, it was immediately evident that in many cases spectral models with solar photospheric abundances did not produce satisfactory fits to the spectra. This issue was already raised with the first ASCA/SIS stellar spectrum, the early observation of the active binary AR Lac (White et al., 1994) which was shown to be incompatible with *solar photospheric* abundances.

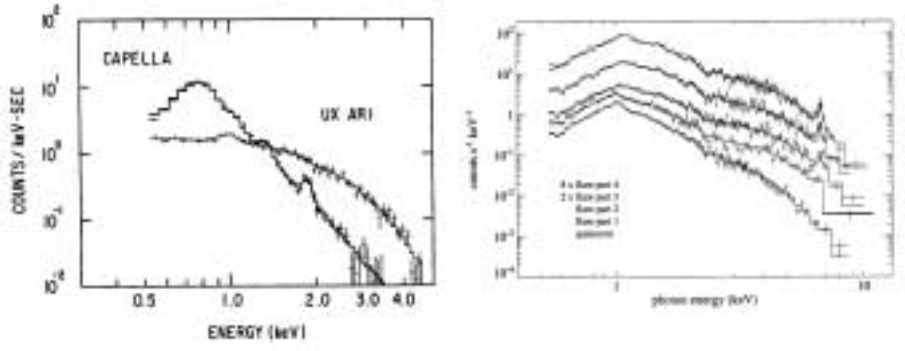

Figure 29. The left panel shows the early *Einstein* SSS spectra of Capella and UX Ari, from Swank et al. (1981), on which the first discussion of stellar coronal abundance was based. The right panel shows the ASCA SIS spectra of UX Ari in quiescence and during the rise of a flare, from Güdel et al. (1999).

The assumption of solar photospheric abundance for the coronal plasma of stars other than the Sun was essentially one based on the lack of better knowledge, both because the solar *coronal* abundances were already known to differ from the photospheric ones (see Sect. 10.1) and because the solar photospheric abundance mix is far from being universal. Indeed, nearby stars display a wide range of photospheric metal abundances (see e.g. Edvardsson et al., 1993), with a very weak correlation with age, and the Sun itself appears

to lie in the "high-abundance" tail of a broad distribution (so that assuming the solar photospheric abundance as universal would likely result in a bias). It would thus have indeed been surprising to find that all coronae had solar photospheric metal abundances.

Also, while the assumption of the same composition for the photosphere and the corona (which has a much smaller mass and is continuously "fed" by the photosphere) may appear "natural", in practice this is equivalent to claiming (see Jordan et al., 1998) that the amount of mixing between the two is sufficient to counteract natural processes (e.g. thermal diffusion, gravitational settling, Coulomb drag in the mass flow into the solar wind, etc.) which will tend to chemically fractionate the corona.

The early results (see e.g. Drake, 1996b) indicated that the "best-fit" abundances for many coronal sources were quite low. The Fe abundance, which – thanks to the large number of Fe lines in the spectra – is in general the best determined one, and the one which dominates global fits, was found to often be as low as 0.3 times the solar photospheric value.

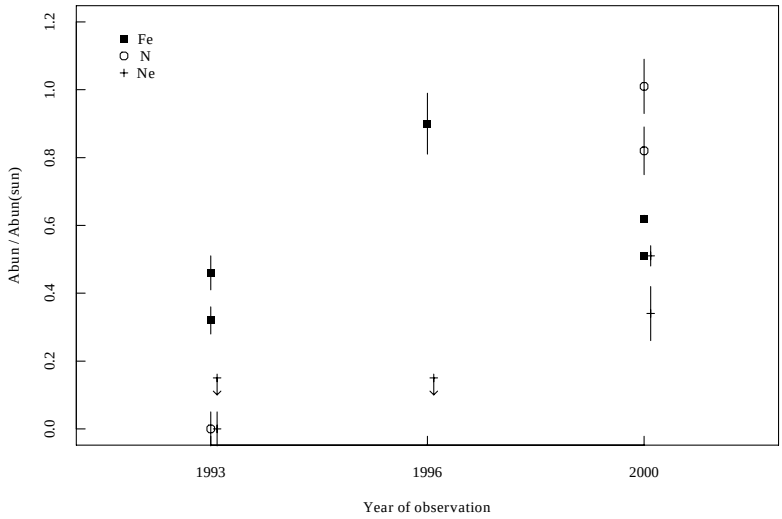

Figure 30. Different determinations of the abundance of Fe, N and Ne for Capella plotted as a function of time. The points for 1993 are the analyses of the ASCA/SIS PV data by Drake (1996b) and by Brickhouse et al. (2000), the 1996 points are the analysis of the ASCA/SIS 1996 data also by Brickhouse et al. (2000), while the 2000 points are the analyses of the XMM-*Newton* RGS high-resolution spectra by Audard et al. (2001). See the main text for details.

The difficulty in assessing the quality of the "best-fit" values obtained from X-ray spectra is perhaps best shown by looking at the "history" of the coronal abundance of Capella (see Fig. 30). Capella, being one of the

strongest X-ray sources in the sky, has been regularly observed at high S/N, and thus provides a good set of measurements which can be compared with each other. Few stars (if any) have a comparable database of observations with different detectors.

The first determination of Capella's coronal abundance was published by Drake (1996b), who analyzed a 1993 ASCA/SIS observation using a 2–T model, and reported Fe $= 0.46$, N $= 0.0$ and Ne $= 0.0$ (all values relative to the solar photospheric values, and in the present paper we will consistently use fractional, rather than logarithm abundances), with quite small formal uncertainties (≤ 0.05). It is worth noting that the fit was far from satisfactory, with a reduced $\chi^2 \gg 1$. The same data were later re-analyzed by Brickhouse et al. (2000), who did add a number of "missing lines" to the models, improving the fits significantly. In addition to a more sophisticated joint ASCA/EUVE analysis they repeated the 2–T analysis. The ASCA/SIS 1993 Capella data, with a similar 2–T model gave (with a much improved χ^2) abundances Fe $= 0.32 \pm 0.04$, Ne ≤ 0.15. The same analysis conducted on the ASCA 1996 observation of Capella (still using the SIS0 detector) yielded Fe $= 0.90 \pm 0.09$, Ne ≤ 0.15. Barring large changes in the intrinsic coronal abundance, these significant difference in the abundance obtained from two spectra of the same object obtained using the same detector and analyzed with the same model and approach point to the large sensitivity of the best-fit metal abundances obtained from CCD spectra to e.g. calibration issues. In the case of Capella, however, intrinsic abundance changes could in principle be present in the spectrum if indeed, as discussed by Johnson et al. (2002), either of the two components of the binary system can dominate the emission at different times.

More recently, the Capella coronal abundance has been determined by Audard et al. (2001) using the high-resolution XMM-*Newton* RGS spectrum shown in Fig. 35. The approach used has also been a "global best-fit" one (see Sect. 10.2.1), with a 3–T model. The abundances derived from the 2 (independent) RGS spectrographs are, for the RGS1, Fe $= 0.62 \pm 0.01$, Ne $= 0.51 \pm 0.03$, N $= 0.82 \pm 0.07$, while for the RGS2, Fe $= 0.51 \pm 0.01$, Ne $= 0.34 \pm 0.02$ and N $= 1.01 \pm 0.08$. Also here the difference e.g. for Ne between the values determined for the two detectors is much larger than the formal uncertainty reported (although, as stated in Audard et al., 2001, "the uncertainties do not include systematic uncertainties that may be introduced by calibration uncertainties"), again perhaps pointing to the sensitivity of the best-fit values to e.g. calibration issues. The very low Ne and N abundances (compatible with 0) produced from the early CCD data are incompatible with the high values (specially for N) resulting from the high-resolution analysis.

More in general, global fitting methods do not include, to date, an analysis of the uncertainties introduced e.g. by errors in the calibration and atomic physics. Therefore the resulting (often very small) quoted confidence inter-

vals are in general incorrect, and likely to be a significant underestimate of the true uncertainties in the abundance values, making it difficult to compare results by different studies.

Similarly, for the active binary UX Ari, Güdel et al. (1999) determined a set of coronal abundances from the ASCA SIS spectra shown in Fig. 29. The values determined during the quiescent phase (the initial phase of a flare is also present in the ASCA observation) can be compared with the abundances derived from the XMM-*Newton* RGS spectrum by Audard et al. (2002). As the latter work only gives abundances relative to O (rather than absolute abundances) we have also reduced the ASCA abundances to the same scale. Some ASCA-derived values are: $\mathrm{N/O} = 0$ (with a large uncertainty), $\mathrm{Ne/O} = 3.6$, $\mathrm{Fe/O} = 0.71$, $\mathrm{Ni/O} = 6.6$. The same abundance ratios as derived from the XMM-*Newton* RGS spectrum are $\mathrm{N/O} \simeq 3.5$, $\mathrm{Ne/O} \simeq 2.5$, $\mathrm{Fe/O} \simeq 0.4$, $\mathrm{Ni/O} \simeq 0.5$. Once more, the values are different by factors which can be rather large (e.g. for Ni). Comparable discrepancies are present for the other elements (e.g. Mg, Si, S).

An additional problem in comparing abundance values determined by different authors is that often a value relative to the "solar photospheric value" is reported, without specifying what the latter is (although most often this implies the values reported by Anders and Grevesse, 1989, which is taken as standard by many spectral analysis codes). Given that agreed "best" Fe solar photospheric abundance has changed by as much as 0.17 dex in recent years (and changes have been even larger for some other elements: Allende Prieto et al., 2001 have recently revised the O abundance for the Sun by 0.24 dex downward with respect to the "canonic" value of Anders and Grevesse, 1989), this may introduce an additional systematic difference in some of the literature values with respect to newer determinations.

As shown e.g. by the above review of the data for Capella and UX Ari, the formal confidence ranges quoted for abundances (specially for elements other than Fe) in works relying on global fits to the spectra are likely to be significantly under-estimated. In practice, hindsight based on the use of more recent, high resolution spectra, shows that some results claimed on the basis of the analysis of ASCA CCD spectra were correct (e.g. the often low, in comparison with the solar photosphere, abundance of Fe, and the high Ne abundances often found, specially in active binaries, e.g. AR Lac White et al., 1994). At the same time (as discussed in more detail e.g. by Drake, 2002), other results (like the very low abundances derived for e.g. N and O) were clearly incorrect. A discussion of effects which depend on abundance ratios (e.g. the presence of FIP-like, or inverse FIP effects), based, or making use of, these early (mostly ASCA) data is thus not possible on a solid basis. For these reasons in the following we will only discuss recent results obtained from high resolution spectra, even though even these are not always consistent, see e.g. Table V. A thorough reanalysis of the large legacy of ASCA

spectra of stellar coronae, performed using a consistent approach, and supported and verified through the new (where available) high-resolution spectra, would likely supply significant additional insight in the chemical composition of stellar coronae. A recent review of the current status of abundance determination in stellar coronae is given by Drake (2002).

The increase in collecting area and spatial resolution provided by *Chandra* and XMM-*Newton* is producing CCD-resolution spectra (two examples are shown in Fig. 31) for an unprecendented number of coronal sources. This will allow to explore coronal abundances in an unprecedented large number and variety of coronal sources, most of which are still too faint for the grating spectrographs onboard both satellites.

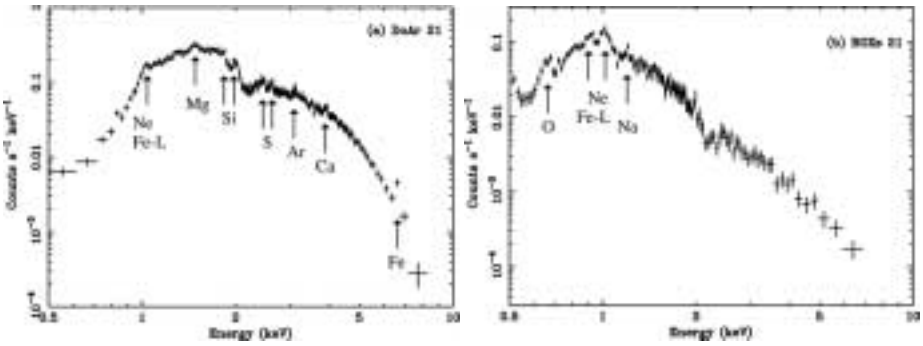

Figure 31. The *Chandra* ACIS spectra of two pre-main sequence stars in the ρ Oph association, from Imanishi et al. (2001). DoAr 21 has a hotter, more absorbed spectrum, while ROXs 21 has a softer and less absorbed spectrum. The location of the main line complexes due to the various elements are shown. The XMM-*Newton* EPIC detectors have comparable spectral resolution and energy coverage.

10.3. PHOTOSPHERIC ABUNDANCES

One additional element of uncertainty in the discussion about coronal abundances, and the presence (or lack thereof) of selective enhancement and depletion of elements (FIP-like, etc.) is introduced by the scarce knowledge of the photospheric abundances of active stars. To evaluate whether a FIP-like effect is present in a stellar corona, the comparison once more should be made with the actual photospheric abundance of the star under study, rather than with the solar photospheric mix. The photospheric composition of individual different stars can indeed differ significantly from the solar mix, as reviewed e.g. by McWilliam (1997).

Unfortunately, accurate studies of the photospheric abundance of active stars are still few. Many typical targets of coronal abundance studies have at most a single determination of the photospheric Fe abundance available, and for most no determinations of the abundance of some of the key elements in

the X-ray spectra (such as O, Si, S and Mg) are available. This applies even to well known sources such as Capella, HR 1099, AR Lac, etc. In part the difficulty is intrinsic, i.e. determining the photospheric parameters of cool, fast rotating stars is fraught with difficulties, even more when they are in binary systems in which both spectra are visible (SB2 systems). At the same time, however, part of the lack of this type of data, even on stars which are technically less challenging, is likely to reflect a lack of interaction between the X-ray coronal community and the high-resolution optical spectroscopy community.

Some photospheric abundance analyses of active stars have appeared in the last few years in the literature. Determination of the abundance of a small number of active binaries was performed by Fekel and Balachandran (1993); later Randich et al. (1993) and Randich et al. (1994) determined the Fe abundance on a sample of some tens of active binaries (and other active stars), using a small number of Fe lines and photometrically determined effective temperatures. In many cases they find puzzling results, with some systems displaying severe under-abundances, and some SB2 systems displaying different abundances for the two components. Ottmann et al. (1998) and Gehren et al. (1999) have concentrated on a more detailed analysis of a smaller number of systems, using a self-consistent approach (which does not make use of the photometric temperatures), and determining abundances also for elements other than Fe. In some cases Ottmann et al. (1998) find results which are in significant disagreement (again based on the quoted formal uncertainties) with Randich et al. (1993) and Randich et al. (1994), as well as with Fekel and Balachandran (1993). For example, for the well observed RS CVn system λ And, Fekel and Balachandran (1993) find a Fe abundance of 0.63 solar, while Randich et al. (1993) find a value of 0.25 solar, with Ottmann et al. (1998) finding an intermediate value of 0.4 solar. For another well known system, II Peg, Randich et al. (1993) find a photospheric Fe abundance of 0.31 solar, while Ottmann et al. (1998) find a value of 0.63. These discrepancies show that the photospheric abundances are often not known – when they are known at all – to better than a factor of two or more, pointing to the need for more work in this area, a critical one for the proper understanding of the chemistry pattern observed in stellar coronae.

10.4. PRESENT-DAY EVIDENCE

Given the problems in comparing coronal abundances derived from different detectors (specially CCD spectrometers – see Sect. 10.2.2) we will concentrate in the present section on recent results obtained mainly with the XMM-*Newton* and *Chandra* grating spectrographs. Audard et al. (2002) have produced an initial study of the coronal abundances in active binaries observed with the XMM-*Newton* RGS spectrographs. The abundance values

in their study are determined through global simultaneous fits to the RGS and EPIC spectra with 10 discrete temperature components. They compare the abundance patterns for several elements in four active binaries, i.e. (in order of activity) HR 1099, UX Ari, λ And and Capella, finding evidence for an "inverse FIP" effect (i.e. low-FIP elements appear depleted with respect to high-FIP elements) in the more active systems (HR 1099 and UX Ari), while no selective depletion or enhancement is present in the two less active systems (λ And and Capella). The caveat about the Audard et al. (2002) study is that the assessment of the chemical pattern is made by comparison with the solar photospheric abundances, rather than with the (unknown) photospheric abundances of the target stars.

Huenemoerder et al. (2001) have studied the *Chandra* HETGS spectrum of the active binary II Peg (a segment of which is shown in Fig. 32), for which the photospheric abundance has been determined both by Ottmann et al. (1998) who found $\mathrm{Fe/H} = 0.6$, $\mathrm{Mg/H} = \mathrm{Si/H} = 0.7$ (with a quoted uncertainty of $\simeq 20\%$) and by Berdyugina et al. (1998) who found $\mathrm{Fe/H} = 0.3$–0.5, more in line with the Randich et al. (1993) value. The *Chandra* spectrum yields for the coronal abundances (through a full DEM analysis) $\mathrm{Fe/H} = 0.1$, $\mathrm{Mg/H} \simeq \mathrm{Si/H} \simeq 0.4$, thus significantly depleted with respect to the photospheric values[6]. Some evidence of "inverse FIP" effect is also present here, with much higher abundances for O ($\mathrm{O/H} = 1.1$) and for the noble gases (see below) than for Fe.

Another often studied high-activity object is AB Dor, for which a photospheric Fe abundance similar to the solar value has been reported (Vilhu et al., 1987). Its coronal abundances have been recently determined (with a global fit approach), using high-resolution XMM-*Newton* RGS spectra, by Güdel et al. (2001a), who find low Fe (as well as Mg, Si and other elements) abundance (with $\mathrm{Fe/H} = 0.22$, $\mathrm{Mg/H} = 0.27$, $\mathrm{Si/H} = 0.14$), and higher O and Ne abundances ($\mathrm{O/H} = 0.40$, $\mathrm{Ne/H} = 0.99$). The same authors also fit the XMM-*Newton* EPIC pn data of the same star, finding abundances values which are in many cases compatible with the high-resolution ones, although there are some discrepancies (e.g. $\mathrm{S/H} = 0.04$ in the RGS data but $\mathrm{S/H} = 0.38$ in the EPIC pn data). Comparison of the AB Dor XMM-*Newton* results with the earlier joint ASCA/EUVE abundance determinations by Mewe et al. (1996) shows that, once more, while for some elements the derived values are fully compatible, for other elements (notably Mg and S) differences of factors of two and larger are present.

For lower activity, "near-normal" solar-type stars (with reasonably well determined photospheric abundances) recent results have been presented by

[6] The coronal Fe abundance obtained for II Peg by Mewe et al. (1997) from an analysis of the ASCA spectrum is in very good agreement with the one derived on the basis of the *Chandra* HETGS data, while the abundance of the other elements is consistently too low by a factor of 2–5 with respect to the values derived from the *Chandra* spectra.

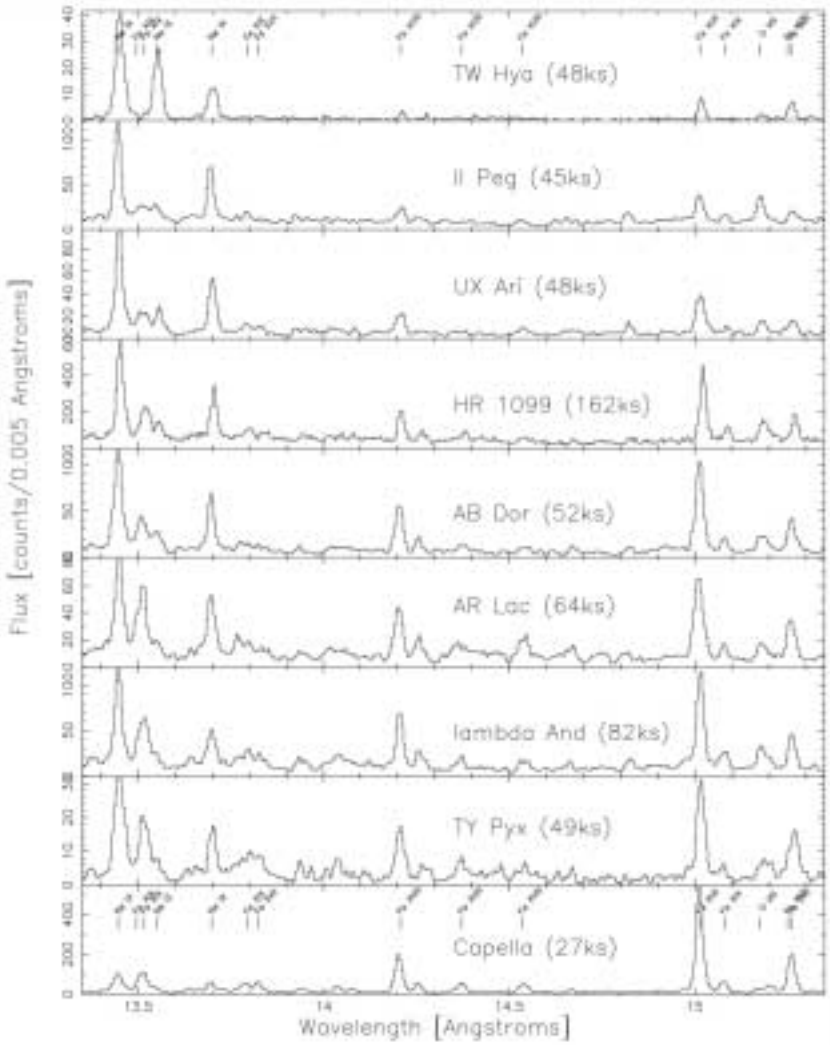

Figure 32. The *Chandra* HETGS spectra of a variety of active stars, from Kastner et al. (2002). Only a limited spectral interval, obtained with the MEG grating, is shown for clarity. The top spectrum is from TW Hya, a CTTS, while all the others (with the exception of the young single star AB Dor) are from active binaries.

Güdel et al. (2002c). They have analyzed the RGS spectra of – among others – AB Dor, EK Dra, π^1 UMa and χ^1 Ori. While in the more active AB Dor a similar depletion pattern as in the high-activity active binaries is visible, in the lower activity objects π^1 UMa and χ^1 Ori, Fe – as well as Mg and Si – is highly *enhanced* with respect to the photospheric value, while e.g. O and N have similar abundances in the corona as in the photosphere, thus closely following the pattern of the FIP effect visible in the solar corona.

The presence of a solar-like FIP effect in these stars is in agreement with earlier results obtained with EUVE, e.g. Drake and Kashyap (2001) derived the coronal abundances – from EUVE spectra – of the intermediate activity G8V star ξ Boo A (another star with reasonably well determined photospheric abundances), finding that Fe is enhanced in the corona by a factor of 2 or 3. Similar results had already been obtained – also using EUVE spectra – for α Cen (Drake et al., 1997) and for ε Eri (Laming et al., 1996), with similar enrichment factors for the low-FIP elements. Although the limited S/N of the EUVE spectra did not allow to draw strong conclusions, the presence of a FIP-like effect in moderate-activity solar analogs and the dependence of the depletion pattern on the level of stellar activity – now being claimed in e.g. the XMM-*Newton* data – was already discussed by Drake et al. (1996a).

A specific interesting peculiarity has been recently discussed by Drake et al. (2001) using the *Chandra* HETGS spectra of HR 1099: there, the abundance of the noble gases Ne and Ar are found to be much enhanced relative to e.g. Fe, with $\mathrm{Ne/Fe} = 9.8 \pm 1.3$ and $\mathrm{Ar/Fe} = 25 \pm 3.5$ (again, relative to the solar photospheric value). The strength of the Ne IX line at $\lambda \simeq 13.45$ Å in the X-ray spectrum of many active binaries is well evident in the *Chandra* HETGS spectra in Fig. 32. Some evidence (with all the caveat discussed in Sect. 10.2.2) for high Ne abundances was present in the low resolution (CCD) spectra of several active binaries, e.g. for AR Lac White et al. (1994) had already reported $\mathrm{Ne/Fe} = 5.1$. Several additional references on past evidence for Ne overabundance in CCD spectra are provided by Drake et al. (2001). In the abundances reported for active binaries by Audard et al. (2002), Ne is the only element which is systematically overabundant with respect to O, with $\mathrm{Ne/O} = 1.8$–3.5 (the Drake et al., 2001 value for HR 1099 is $\mathrm{Ne/O} = 3.2$). For II Peg Huenemoerder et al. (2001) report a very high noble gas abundance, with $\mathrm{Ne/Fe} = 22$ and $\mathrm{Ar/Fe} = 22$, so that the evidence for a systematic Ne overabundance is strong. The Ne X-ray line in high-resolution spectra is reasonably free from e.g. significant blending, so that the determination of its abundance should be reliable. The situation is less clear for Ar, which in the Audard et al. (2002) sample spans the range $\mathrm{Ar/O} \simeq 1.0$–2.0, significantly lower than the value found by Drake et al. (2001) for HR 1099, $\mathrm{Ar/O} = 8.1$. Note that for HR 1099 itself Audard et al. (2002) find $\mathrm{Ne/O} \simeq 2.5$ and $\mathrm{Ar/O} \simeq 1.0$; while the Ne value is reasonably compatible with the Drake et al. (2001) one, the Ar abundance is different by a large factor.

One important issue is whether compatible coronal abundances are derived for the same object using different high-resolution spectrographs and different data analysis techniques. In Table V the coronal abundances derived from the published analyses of high resolution data are listed for HR 1099 and AB Dor. For both of these stars results have been published from *Chandra* and XMM-*Newton* data, and for HR 1099 the XMM-*Newton* RGS data have been analyzed using a global fitting approach (Audard et al., 2001) and a

Table V. A comparison of the coronal abundances for HR 1099 and AB Dor derived from *Chandra* and XMM-*Newton* high-resolution spectra. Key: (1) Drake et al. (2001), (2) Brinkman et al. (2001), (3) Audard et al. (2001), (4) Linsky and Gagnè (2001), (5) Güdel et al. (2001a).

Element	FIP	HR 1099 HETGS (1)	HR 1099 RGS (B) (2)	HR 1099 RGS (G) (3)	AB Dor HETGS (4)	AB Dor RGS (5)
Ni/H	7.63		0.33	0.06		0.47
Mg/H	7.64	0.78	0.95	0.10	0.50	0.27
Fe/H	7.87	0.31	0.25	0.15	0.25	0.22
Si/H	8.15	0.59		0.18	0.65	0.14
S/H	10.36	0.46	0.45	0.07	0.55	0.04
O/H	13.61	0.93	1.0	0.35	0.75	0.40
N/H	14.53		1.4	0.60		0.53
Ar/H	15.78	7.6		1.23		0.86
Ne/H	21.56	3.0	3.8	0.93	1.3	0.99

detailed derivation of the DEM (Brinkman et al., 2001). Some abundances (notably Fe) are reasonably consistent across different analyses and different instruments, while for some other large differences (e.g. for Mg and S factors of 5 or more) are present. There is a systematic trend for the abundances derived with the global fitting approach to be lower than the ones derived with the full DEM derivation, even when comparing analyses done on the same data set (the XMM-*Newton* RGS HR 1099 spectrum), so that the difference would appear to be related more to the analysis technique than to the instrument used. The large discrepancies apparent in Table V indicate that the systematic uncertainties on the derived abundancies are still significantly larger than the (often small) quoted statistical error bars. Raassen et al. (2002) derived abundances for Procyon using a global fitting approach on both XMM-*Newton* and *Chandra* grating spectra, obtaining, for the two instruments, similar results[7].

Thus, on the basis of the first harvest of high-resolution spectroscopic data, some patterns are starting to be apparent, even though the still rather large uncertainties present in the determined abundance values impose caution on the quantitive aspects. In a number of high-activity stars the coronal abundance of Fe appears depleted by factors of a few, in strong contrast with the solar case, for which the most recent data (White et al., 2000) show that the abundance

[7] For Procyon Raassen et al. (2002) find coronal metal abundances compatible with the solar photospheric ones, and no evidence for FIP-dependent fractionation, confirming the previous EUV results (Drake et al., 1995).

of Fe is *enhanced* by a factor of about 4. Also – again in high-activity stars – a number of other elements appear depleted. The depleted elements are in general low-FIP ones, while noble gases have high abundances, leading to postulate the existence of an "inverse FIP" effect in the coronae of active stars. Such an effect is apparently not universal, with some stars (such as Capella and λ And, which however, as evident from the DEM distribution, are lower-activity objects when compared to e.g. HR 1099) showing similar abundance in corona as in the photosphere, and some less active stars showing a solar-like pattern, with enhanced coronal abundance of Fe and other low-FIP elements. Some claims have been made (e.g. Güdel et al., 2002c) of a correlation between e.g. the mean coronal temperature and the amount of inverse-FIP depletion; it will have to be seen whether this will be confirmed when larger samples will be available.

The only dMe star for which an abundance determination based on an high-resolution X-ray spectrum is available is AD Leo (Maggio et al., 2002), which shows evidence for a Fe abundance compatible with its photospheric value and a mild relative overabundance of several other elements including Ne. Sanz-Forcada and Micela (2002) have analyzed the EUVE spectrum of AD Leo, finding a significantly higher Ne overabundance than found by Maggio et al. (2002).

AD Leo also is one of the few dM stars for which a photospheric metal abundance determination is available; Jones et al. (1996) report $\mathrm{Fe/H} \simeq 0.2$, making AD Leo a relatively metal poor star. The absolute coronal Fe abundance of AD Leo reported by Maggio et al. (2002) is in agreement with the photospheric abundance, while the mild overabundance reported for the other metals (e.g. Si, S) with respect to Fe (by a factor of $\simeq 2$ or so) is in line with the expectations for the photosphere of a relatively metal-poor star, (the "α enhancement", McWilliam, 1997). Therefore AD Leo shows no evidence for either FIP-like (or inverse-FIP) effects or for significant Fe depletion.

Two long-standing issues about the reliability of coronal abundance determinations are whether the atomic data (on which all abundance derivations rest) are reliable (i.e. whether the atomic rates are known with sufficient accuracy) and whether a large number of lines is missing in the spectral databases; these lines could indeed mimic a pseudo-continuum and result in artificially low abundances. That many weak lines are indeed missing in most codes, and that they have an effect on the resulting spectral parameters, has been shown e.g. by Brickhouse et al. (2000), who showed that addition of a number of Fe L-shell lines to the spectral synthesis strongly improves the fit to the Capella spectrum (filling a flux deficit around 1.2 keV).

The current status of atomic data for X-ray stellar spectroscopy has recently been reviewed by Laming (2002), who concludes that atomic rates are rarely known to better than $\simeq 20\%$, but that in general the current generation of atomic data are to be trusted, although still with some caveat and qualifica-

Table VI. Coronal abundance analyses obtained to date using high-resolution XMM-*Newton* and *Chandra* spectra. "GF" indicates analyses based on global fitting to the spectra, "EM" analyses based on derivations of the DEM from individually determined line fluxes.

Reference	**Star**	**Instr.**	**GF**	**EM**
Drake et al. (2001)	HR 1099	*Chandra*	-	X
Brinkman et al. (2001)	HR 1099	XMM/RGS	-	X
Audard et al. (2002)	HR 1099	XMM/RGS	X	-
Audard et al. (2002)	UX Ari	XMM/RGS	X	-
Huenemoerder et al. (2001)	II Peg	*Chandra*/HETGS	-	X
Audard et al. (2002)	λ And	XMM/RGS	X	-
Audard et al. (2002)	Capella	XMM/RGS	X	-
Güdel et al. (2001a)	AB Dor	XMM/RGS	X	-
Linsky and Gagnè (2001)	AB Dor	*Chandra*/HETGS	-	X
Güdel et al. (2002c)	EK Dra	XMM/RGS	X	-
Raassen et al. (2002)	Procyon	RGS, LETGS	X	-
Güdel et al. (2002c)	π^1 UMa	XMM/RGS	X	-
Güdel et al. (2002c)	χ^1 Ori	XMM/RGS	X	-
Maggio et al. (2002)	AD Leo	*Chandra*/LETGS	-	X

tions. In particular, there still are some pathologic cases, including important species such as Fe XVII, which has many strong lines in both *Chandra* and XMM-*Newton* grating spectra.

The fractionation mechanisms responsible for the observed coronal abundance patterns (and for their "variety") are not yet identified; one interesting proposal however has been made by Drake (1998), who draw the attention to the possible role of He in causing the observed strong coronal under-abundances observed in some active stars (e.g. AB Dor): an increase in the He abundance in the coronal plasma would manifest itself in the form of a larger number of available He nuclei, raising the level of the continuum and decreasing the line to continuum ratio, causing an apparent under-abundance.

10.4.1. *Coronal abundance variarions during flares*

Significant evidence has accumulated, in the past few years, showing that the coronal abundances in active stars are variable, at least during intense flaring episodes. Such variations are of particular interest, because they represent conclusive evidence for the presence of fractionation mechanisms at work in the stellar coronae, independently from the relationship between the coronal abundance and the (often poorly known) photospheric one. Furthermore,

knowledge of the time scale at which the fractionation mechanism operates represents a strong physical constraint on its nature.

Changes in the equivalent width of the Fe K line during a flare (with respect to the value expected for a solar photospheric abundance plasma) were first reported by Tsuru et al. (1989) for a flare observed with GINGA on the active binary UX Ari. Stern et al. (1992b) later also reported evidence for similar changes in the equivalent width of the Fe K complex during a large flare also seen with GINGA on Algol. Several possible explanations were discussed, with variation of the metal abundance mentioned as a possibility. Later, additional evidence was obtained by Ottmann and Schmitt (1996) by studying a large flare seen, also on Algol, with the ROSAT PSPC; they reported that the coronal abundance increased from $Z = 0.2\ Z_\odot$ in the quiescent phase to $Z = 0.8\ Z_\odot$ during the flare, decaying after the flare. Given the limited instrumental passband and spectral resolution of the ROSAT PSPC detector, the evidence for abundance changes was considered tentative. Also, the temporal coverage of the flare was limited and thus did not allow to study the event in detail. Variations in abundance during the rising phase of a flare seen by ASCA (for which the decay was not observed) were also reported for UX Ari by Güdel et al. (1999), again showing an increase during at the beginning of the event by a factor of $\simeq 3$ to $\simeq 4$ with respect to the quiescent phase.

Later events, which had better statistics and temporal coverage, in addition to being studied with detectors with higher spectral resolution, allowed to study the phenomenon in more detail. In particular the large and long-lasting Algol event observed by SAX (Favata and Schmitt, 1999) has allowed to study the temporal evolution of the metal abundance and compare it with the evolution of the other flare spectral parameters.

During the Algol SAX flare, the Fe abundance is observed to rise quickly (with a faster time scale than the emission measure *EM*) at the beginning of the flare, by a factor of $\simeq 3$ with respect to the quiescent value (going from $Z \simeq 0.3\ Z_\odot$ to $Z \simeq Z_\odot$), and to subsequently decay back to the quiescent value on a time scale faster than either the temperature or the emission measure (see Fig. 33). The decay follows rather accurately an exponential law.

Similar changes in the coronal abundance of the flaring plasma have also been clearly observed in a flare on the pre-main sequence binary V773 Tau (Tsuboi et al., 1998), in one on the active binary σ^2 CrB (Osten et al., 2000) and in one on the flare star EV Lac (Favata et al., 2000c). In all these cases the behavior appears similar to the Algol one, with an initial rise from a characteristic quiescent value of $Z \simeq 0.3 Z_\odot$ (value around which the coronal abundance of many active coronae appears to cluster) to $Z \simeq Z_\odot$, and a subsequent decay to the pre-flare value.

All the determinations of abundance variations discussed above are the result of global fits to low-resolution (PSPC, GSPC or CCD-based) spectra. The

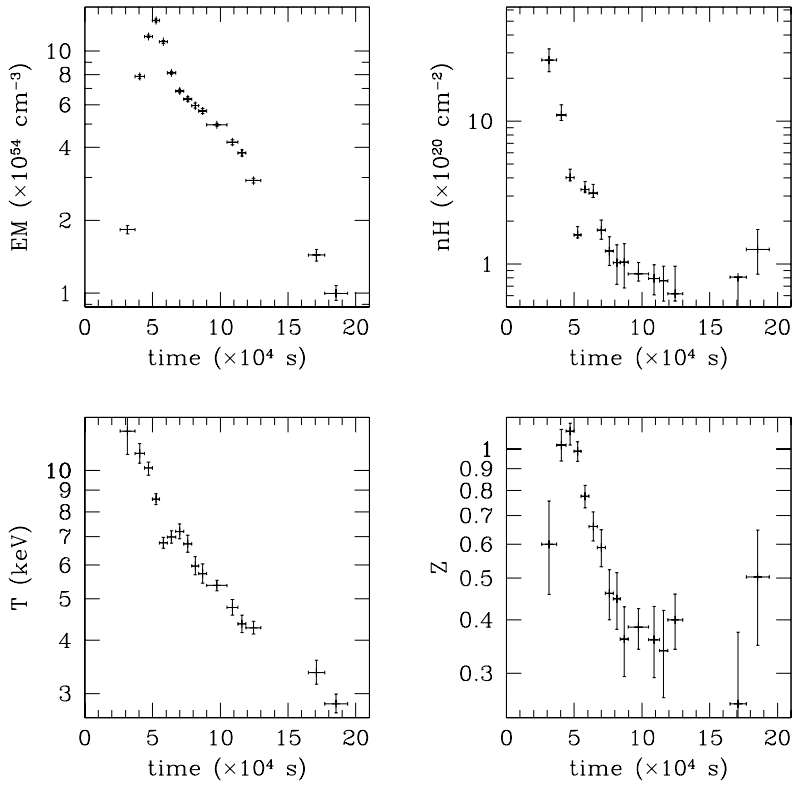

Figure 33. The time evolution of Algol's coronal parameters during the SAX flare (from Favata and Schmitt, 1999). From the top left clockwise the emission measure *EM*, the absorbing column density $n_{\rm H}$, the global metal abundance Z and the plasma temperature T are shown. The time axis is relative to the beginning of the observation.

caveat about the reliability of the abundance values determined from global fits (see Sect. 10.2.1) therefore applies here, so that the derived abundances in the case of a flaring spectrum (for which the single-temperature fit is by necessity an approximation) might have to be treated with care. However, for the hot temperatures involved in large flares the spectrum is significantly simplified by the fact that the only line emission visible is from the Fe K complex, so that the abundance determined from the spectrum is essentially driven by the line-continuum ratio for the Fe K line, which has very little "cross-talk" with the other spectral parameters, and should therefore provide a reliable estimate of the Fe abundance.

Variation of the Fe abundance during flares does not however appear to be an universal feature. In some other well studied flaring events the variation in

Fe abundance is (if at all present) much smaller than the factors of three observed e.g. in Algol. For example for the flares observed by SAX on AB Dor (Maggio et al., 2000) and UX Ari (Franciosini et al., 2001) the variation in abundance during the flare is at the level of $< 50\%$, although some hint of a small variation is indeed present in the data. AB Dor itself however showed significant variations in the coronal abundance during two flares observed with ASCA (Ortolani et al., 1998), in which the abundance rose from a low quiescent value $Z \simeq 0.1\,Z_\odot$ to $Z \simeq 0.6\,Z_\odot$ at the flare peak. Similar variations were seen in the AB Dor flare recently observed with XMM-*Newton* (Güdel et al., 2001a), which shows a decrease of the abundance during the decay of the flare by a factor of $\simeq 2.5$, from $Z = 0.5 \times Z_\odot$ to $Z = 0.2 \times Z_\odot$ Therefore, the presence (or lack) of abundance variations during a flare would appear to be something which can change from event to event on the same star.

A small flare on II Peg has been observed at high spectral resolution with the *Chandra* HETGS by Huenemoerder et al. (2001); the statistics are sufficient to study the abundance of a number of elements, both in the quiescent and in the flaring state. The evidence for abundance variations from these high-resolution spectra is marginal (with Fe/H changing from 0.1 in quiescence to 0.15 during the flare, a 2σ effect), although the flaring spectrum covers the rise phase as well as $\simeq 10$ ks of the decay phase, so that if the abundance decay is rapid (as e.g. in Algol) this may "dilute" the abundance changes in the flaring spectrum. The other elements in the II Peg flaring spectrum show a similar marginal increase, with the exception of Si which decreases from $\mathrm{Si/H} = 0.80$ to $\mathrm{Si/H} = 0.45$.

Temporal variations in the chemical abundance have not yet been reported in solar flares. Sylwester et al. (1998) have analyzed the X-ray spectra of a large number of solar flares, determining the abundance of Ca, and found no evidence for changes during the flare decay phase. At the same time, analyses of a number of different flaring events show that the average value for the abundance of different elements can vary by a factor of $\simeq 5$ from event to event (e.g. Fludra and Schmelz, 1999; Antonucci and Martin, 1995).

The simple interpretation for the type of abundance variations observed during flares is that at the beginning of the event fresh chromospheric (and likely photospheric) material is evaporated in the flaring loop(s), thus enhancing its abundance; once the material is brought in the flaring coronal structure the fractionation mechanism which is responsible for the lower abundances observed in the coronal plasma would start operating, bringing the coronal abundance back to its quiescent value.

11. Other results from high-resolution spectroscopy

11.1. DENSITY

Once spectral lines are resolved, several direct diagnostics of the plasma density become available. They include both the forbidden to intercombination ratio of the triplet of He-like ions as well as line ratios of different ionization states of the same species. The details of the techniques of density determination have been extensively reviewed by several authors (e.g. Mewe, 1999), and will not be discussed here in detail. Briefly, each triplet is composed, as shown in Fig. 34, of three lines, the resonance line (r), the intercombination line (i) and the forbidden line (f). The line flux ratio f/i is sensitive to density, over the range where collisions redistribute excitation from the long-lived metastable upper level of the forbidden line to the upper level of the intercombination line. This range of densities differs from triplet to triplet. The ratio $(i+f)/r$ is sensitive to the plasma temperature. Each triplet also has a typical range of plasma temperatures in which it is excited (as with any other spectral line), so that the densities measured from the different triplets refer to different temperature regimes in the corona, and need not, a priori, to yield the same values.

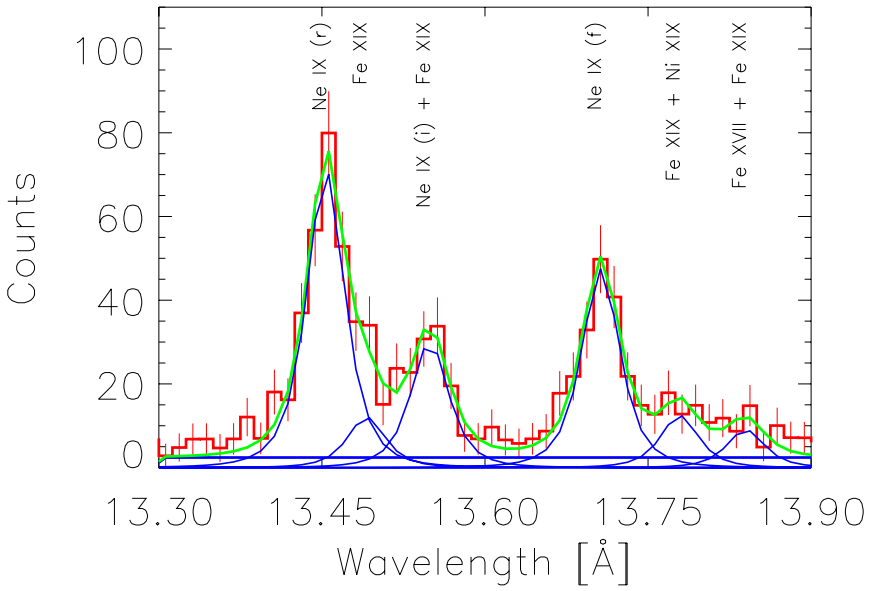

Figure 34. The Ne IX density-sensitive triplet, as observed in the *Chandra* LEGTS spectrum of AD Leo, from Maggio et al. (2002). Note the presence of line blends, which can influence the resulting density, if not properly accounted for.

The first instrument to give access to density diagnostics for a significant number of coronal sources has been EUVE (which however did not make

use of He-like triplets, but rather of ratios of Fe lines originating from the same ionization state). EUVE results have recently been extensively reviewed by Bowyer et al. (2000), in which the original references are available. In general, density diagnostics for the $T \simeq 1$ MK plasma are visible in the EUVE spectra of low-activity stars (e.g. Procyon, α Cen) and yield densities $n_e \simeq 5 \times 10^{10}$ cm^{-3}. For comparison, typical plasma densities in solar active regions are $n_e \simeq 3 \times 10^9$ cm^{-3}, while during solar flares the density rises to $n_e > 1 \times 10^{10}$ cm^{-3}. In the few stars in which the spectral S/N is sufficient to observe the presence of both low-temperature ($T \simeq 1$ MK) and high-temperature ($T \simeq 10$ MK) material in the EUVE spectrum, the low-temperature material has similar low densities, while the high-temperature material has significantly higher densities: for Capella the high-T material has density $n_e \simeq 1 \times 10^{12}$ cm^{-3}, while the low-T material has $n_e \simeq 1 \times 10^9$ cm^{-3}. For the stars whose emission is dominated by the high-T plasma (and therefore no low-T density diagnostics are visible) the densities are consistently high ($n_e \simeq 1 \times 10^{12}$ cm^{-3} and higher). As pointed out e.g. by Bowyer et al. (2000) such high densities imply – under the perhaps questionable assumption that the plasma is confined in quasi-static coronal loops following the scaling laws of Rosner et al. (1978), see Sect. 6.1 – that the emitting structures are quite small (with loop lengths of only $\simeq 10^8$ cm), with small filling factors sufficient to explain the observed emission measure. The confining (equipartition) magnetic fields are $B \simeq 1$ kG. The large difference between the density of the low- and high-T material observed in the same star (Capella) implies that the emitting material cannot be confined in the same (quasi-static) coronal structures, as in quasi-static loops (which are in hydrostatic equilibrium) the opposite effect would be expected (higher density for the cooler material). The EUVE results do not allow (for lack of diagnostics covering a wide enough range of temperatures) to assess whether a dichotomy between the low- and high-T material is present (and thus two physically distinct classes of coronal structures are present in the corona), or whether there is a continuum in the relationship between T and n_e.

Recent density determinations from high-resolution spectra include, for XMM-*Newton*, Capella (Audard et al., 2001) AB Dor (Güdel et al., 2001a), HR 1099 (Audard et al., 2001) and YY Gem (Güdel et al., 2001b; Stelzer et al., 2002), and for *Chandra*, Capella (Mewe et al., 2001; Ness et al., 2001; Canizares et al., 2000), AB Dor (Linsky and Gagné, 2001), II Peg (Huenemoerder et al., 2001), HR 1099 (Ayres et al., 2001) and Algol (Ness et al., 2002b). Raassen et al. (2002) determined the coronal density in Procyon using both XMM-*Newton* and *Chandra* data. As shown later, these results appear to confirm the trend observed with EUVE of hotter plasma being associated with higher densities, with some evidence for a smooth relationship rather than a dichotomy (see Fig. 36).

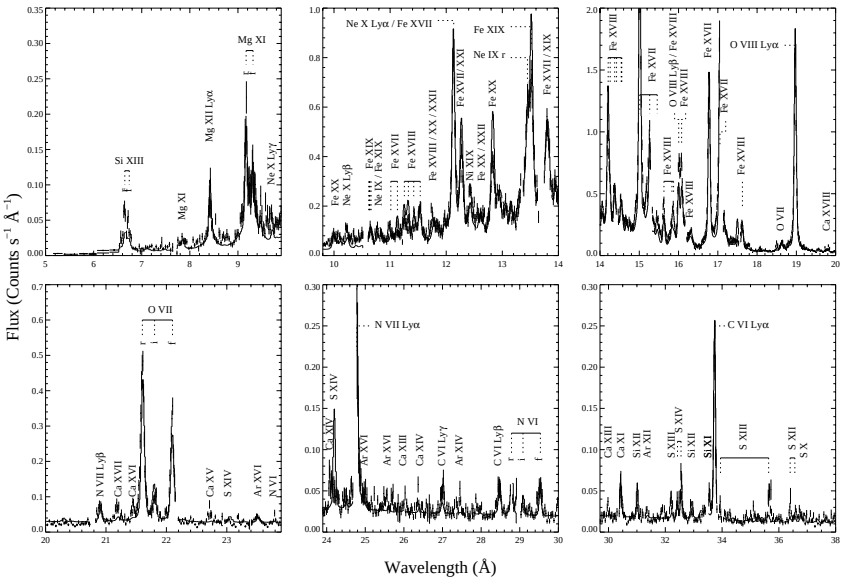

Figure 35. The XMM-*Newton* RGS spectrum of Capella, adapted from Audard et al. (2001). The data from the RGS1 spectrograph are plotted together with the best-fit model derived from a continuous DEM distribution. Major lines are identified; in particular the forbidden, intercombination and resonance lines of the density-sensitive triplets of O VII at $\simeq$ 22 Å and N VI at $\simeq$ 29 Å are clearly visible.

For AB Dor the density from the XMM-*Newton* RGS observation of the O VII triplet is 3×10^{10} cm^{-3} (Güdel et al., 2001a). A flare is present in the second part of the observation, but no increase in the density of the 2 MK plasma is visible in the flaring spectra. Audard et al. (2001) report a similar analysis for HR 1099, for which they find a rather low density ($n_e < 1 \times 10^{10}$ cm^{-3}) for the 2 MK plasma. Again, a flare is present in the data, but no increase in the density of the 2 MK plasma is visible. The same O VII diagnostic yields $n_e = 1.6 \times 10^{10}$ cm^{-3} for YY Gem and $n_e \lesssim 1.6 \times 10^{10}$ cm^{-3} for Castor.

Coronal densities for AB Dor have been derived from a *Chandra* HETGS observation (see Fig. 32) by Linsky and Gagné (2001), who find $n_e = 5 \times 10^{10}$ cm^{-3} for the 2 MK plasma (from O VII), while the higher temperature triplets all yield only upper limits compatible with the lower temperature density.

Ayres et al. (2001) have analyzed the data from a joint *Chandra* and EUVE observation of HR 1099. Their data cover a number of density-sensitive triplets, spanning a decade in temperature, from O VII at $T = 2$ MK to Ar XVII at $T = 20$ MK. The density measured at 2 MK is $n_e = 2 \times 10^{10}$ cm^{-3}, while the higher temperature-sensitive triplets are consistent with their low-density limit of $n_e \lesssim 1 \times 10^{12}$ cm^{-3}. The densities derived from the EUVE simultaneous Fe XXI data yield $n_e \lesssim 1 \times 10^{12}$ cm^{-3}.

Higher densities have been derived using the *Chandra* HETGS observation of II Peg by Huenemoerder et al. (2001), who derive 68% confidence ranges of $n_e = 4 \times 10^{10}$ cm^{-3} – 4×10^{11} cm^{-3} for O VII, $n_e = 1 \times 10^{11}$ cm^{-3}–1×10^{12} cm^{-3} for Ne IX and $n_e = 6 \times 10^{12}$ cm^{-3}–6×10^{13} cm^{-3} for Mg XI (for which the temperature of formation is $T \simeq 6$ MK). Huenemoerder et al. (2001) discuss in detail the systematic effects (blends, etc.) which could result in apparently incompatible densities derived from the different diagnostics (even though there's no reason to assume a priori that plasma at different temperature should be at the same density).

The density of Capella has been studied, from EUVE spectra, by Dupree et al. (1993), who found (using Fe XXI lines), for the plasma at $T \simeq 10$ MK, high densities comprised between $n_e = 4 \times 10^{11}$ cm^{-3}–1×10^{13} cm^{-3}. From *Chandra* LETGS spectra Mewe et al. (2001) derive the density from a number of He-like transitions, finding, for the low temperature plasma ($T \lesssim 2$ MK, using C V, N VI and O VII transitions) densities comprised in a range $n_e = 3 \times 10^9$ cm^{-3} and $n_e = 6 \times 10^9$ cm^{-3}, while for the hotter plasma ($T \simeq 6$ MK) the densities are much higher, at $n_e = 3 \times 10^{12}$ cm^{-3} for Mg XI and $n_e = 4 \times 10^{13}$ cm^{-3} for Si XIII (a very high value which Mewe et al., 2001 caution might be affected by low spectral resolution and thus blending). The high densities at the higher temperatures are consistent with the densities derived from the ratio of density-sensitive Fe ions, which give $n_e \simeq 1 \times 10^{12}$ cm^{-3}. Again, a clear trend is present for the higher-temperature plasma being at higher densities. Ness et al. (2001) have analyzed the same Capella *Chandra* LETGS spectra, concentrating on the low-temperature plasma only, finding densities comparable to the Mewe et al. (2001) values.

Ness et al. (2001) have also analyzed the *Chandra* LETGS spectrum of Procyon again finding similar densities (between $n_e = 2 \times 10^9$ cm^{-3} and $n_e = 9 \times 10^9$ cm^{-3}) for the low-temperature plasma. Procyon is a moderate-activity ($L_X \simeq 10^{28}$ erg s^{-1}) nearby F5V star, with sufficient X-ray flux to allow detailed study of its spectrum, making it a good prototype of solar-like activity in other stars. The moderate values for the pressure in the corona of Procyon has already been established with EUVE data (Schmitt et al., 1996a), who showed that the corona is indeed dominated by material at $T \simeq 2$ MK, with a characteristic density $n_e = 3 \times 10^9$ cm^{-3}. Such density is typical of the value encountered in solar active regions, but it is lower than the values found in solar flares ($n_e > 1 \times 10^{10}$ cm^{-3}). From the emission measure and density, and under the assumption of magnetically confined static loops, Schmitt et al. (1996a) derive an average height for the coronal loops in Procyon of $H \simeq 2 \times 10^9$ cm, or $H \simeq 0.02 R_*$, and a moderate filling factor $f \simeq 0.2$. Therefore, the density measurements result in a rather "solar-like" picture for Procyon's corona.

The only density determinations from high-resolution X-ray spectroscopy for dMe stars available to date are the work of Maggio et al. (2002) on

AD Leo using *Chandra* spectra and of Stelzer et al. (2002) on YY Gem using XMM-*Newton* spectra. For AD Leo, among the available diagnostics, only the O VII triplet is considered to yield a reliable density determination, $n_e = 2 \times 10^{10}$ cm^{-3} (a value similar to values obtained for other types of active stars), while all other triplets are considered to yield only upper limits. Similar considerations are reached for YY Gem, where an upper limit of $n_e \leq 2 \times 10^{10}$ cm^{-3} is derived.

The density determination obtained by analysis of the He-like triplets can be affected by radiative pumping (Ness et al., 2002a) due to the (photospheric and chromospheric) UV fields. Neglecting the influence of the UV field can result in spurious high densities, in some cases by an order of magnitude. The effect is more marked for the low-Z ions, and thus for the lower plasma temperatures. This is also relevant for stars such as e.g. Algol, where the UV field comes from the nearby hot companion (Ness et al., 2002b).

Some of the high densities obtained from the *Chandra* and EUVE spectra have been questioned (e.g. by Drake, 1996a; Bowyer et al., 2000; Drake, 2001), as small amounts of systematic errors in the spectra, such as the presence of small amounts of blending, or errors in the line ratio calculations would bring them back to the low-density limit, where they would not be sensitive and therefore only provide an upper limit to the density.

In Fig. 36 all He-like triplet-based density determinations available at the time this review has been written are plotted against the formation temperature of the relevant ion, for Procyon, Capella, HR 1099, II Peg and AB Dor. Both XMM-*Newton* and *Chandra* grating results are included, and, when more analyses or data sets are available for a given star, all are shown. A clear trend for high-T material being apparently associated with higher densities is visible. Also, data from different stars fall on the same locus. In part this is a clear "selection effect" because higher-T triplets are sensitive to a higher density range. Such a broad distribution in density in the same star (if indeed real) is incompatible with the plasma being confined in quasi-static loop structures, where the cooler material would be at higher density. Whether stellar coronae are therefore not constituted by an ensemble of quasi-static loop structures, or whether the problem lies with the density measurements themselves, is not clear. Many of the measurements tend to lie very close to the low-density limit (i.e. the density at which collisional excitation begins to dominate over radiative decay for the forbidden level), so that even limited amounts of blending from weak lines, calibration problems, etc. could result in a spurious determination of a density when indeed only an upper limit should be derived.

Spectroscopic density measurements from stellar coronae are (because of the long time necessary to collect enough photon statistics) averages over relatively long time scales. Observations of the solar corona, where spectra can be collected at high temporal resolution, shows that densities in a flare can

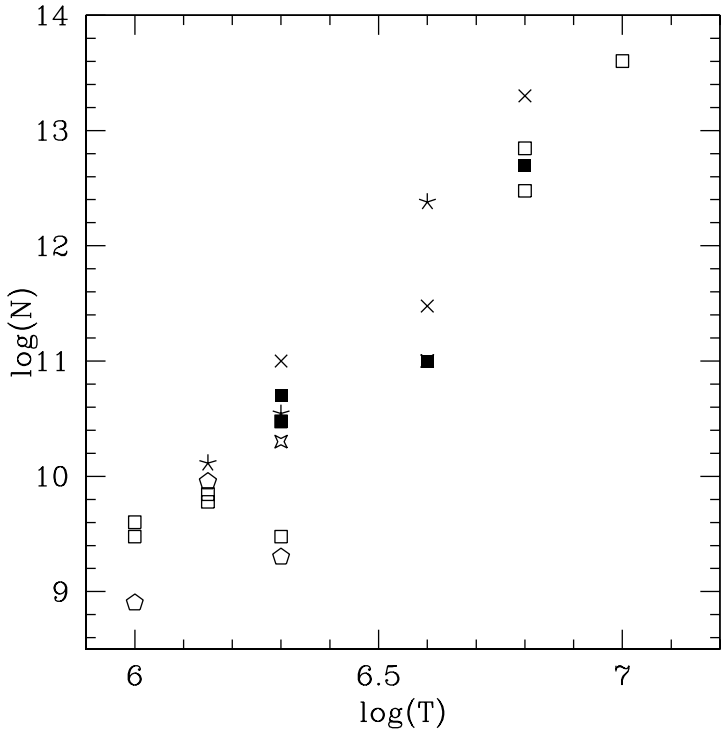

Figure 36. Density derived from the analysis of He-like triplets for a number of stars from *Chandra* and XMM-*Newton* grating spectra. Temperatures are in *K*, densities in cm^{-3}. Note the strong correlation between temperature of formation for the triplet and the inferred density. Different symbols represent different stars (open squares: Capella; filled squares: AB Dor; pluses: II Peg; crosses: HR 1099; pentagons: Procyon; stars: Algol.

vary rapidly and attain very high values. Phillips et al. (1996) have analyzed the data from SMM observations of intense solar flares, finding densities as high as $n_e = 1 \times 10^{13}$ cm^{-3} 1 minute after the flare peak, rapidly decaying to $n_e = 2 \times 10^{12}$ cm^{-3} a few minutes later. If indeed such large temporal variation in density is also present in active stars (as it's likely in the context of the microflaring hypothesis discussed in Sect. 7.1.2) this is an additional reason to interpret the long-term averages implied by the stellar observations with caution. These very high densities observed in solar flares (for which the volume is known because the observations are spatially resolved) also imply very small filling factors (Judge, 2002), with Phillips et al. (1996) deriving a value of $f \leq 10^{-3}$ for the above densities.

More in general, the relationship between the disk-integrated density determination from a stellar high-resolution spectrum, which is a time- and space-average over a very complex structure and the actual structuring and

physics of the underlying corona (and thus the diagnostic power of density measurements) is not very clear (Judge, 2002).

11.2. THERMAL STRUCTURING

Even with the limited spectral resolution of the *Einstein* IPC detector it became soon evident that – given sufficient S/N – the coronal plasma is not isothermal, and that two discrete temperature components offered a better fit to the observed spectrum (Schmitt et al., 1990a). With the advent of the ROSAT PSPC detector (with somewhat better but still quite limited spectral resolution) the 2-T spectral model became the standard tool with which most coronal spectra would be fitted. Even with the higher resolution offered by the ASCA SIS spectrometer, most coronal spectra would still be reasonably fitted with 2 (or sometimes 3) temperatures. Of course, a continuum of temperatures is present in the solar corona (or even in a single hydrostatic loop) so that the physical basis for such fits was unclear. A lively debate went on for some time about whether indeed two discrete temperatures were dominating in stellar coronae or whether this would be a simple parameterization of a more complicated underlying temperature structure (see e.g. Singh et al., 1996b).

An insight in the physical meaning of the discrete temperature fits (whether 1-, 2- or 3-T) can be derived by studying the Sun as if it were an unresolved stellar X-ray source. Orlando et al. (2000) have developed a technique that makes use of Yohkoh data, taking advantage of the spatial resolution of the detector and of its two filters, to determine the effective temperature of each image pixel from which they derive the emission measure distribution of the Sun. They then synthesize the emitted spectra and fold them through the response of e.g. the ROSAT PSPC detector, analyzing the resulting spectrum as a stellar observation. In this way one can study the Sun as would appear when observed as a star during different stages of the cycle, what is the effect of rotational modulation, what are the properties of individual coronal components as the active regions, flares, etc. Applications of this technique have been presented by Peres et al. (2000), Reale et al. (2001), Orlando et al. (2001) and Peres et al. (2001).

In Fig. 37 the emission measure distribution of the Sun is reported, derived during the minimum and the maximum of the solar cycle (Peres et al., 2000). We see that during the minimum the emission measure distribution peaks at $\simeq 10^6$ K, while during the maximum the peak is broader and a significant quantity of material at hot temperatures is present. In addition, large quantities of cooler material (10^4–10^5 K) are present in the transition region, emitting mainly in the ultraviolet bandpass. Since Yohkoh is sensitive to X-ray emission only, this material is not present in the derived distributions. The symbols in Fig. 37 mark the temperatures and the corresponding emission measures

obtained when the emitted spectra, derived from the two emission measure distributions, are folded through the spectral response of the ROSAT PSPC, the detector that has performed the largest number of stellar observations to date, and analyzed with a one- or two-temperature fitting procedure. In the case of the Sun observed during the minimum to explain the spectrum the PSPC only one temperature is needed, very close to the peak of the original distribution, while during the maximum two temperatures around the broad peak are needed.

The same analysis performed when the Sun undergoes a large flare shows that a very pronounced broad peak appears in the DEM distribution at $T \gtrsim 10\,\mathrm{MK}$; the spectral fitting procedure identifies the presence of hot plasma, finding one component above 10 MK, again as shown in Fig. 37. In both cases (quiescent and flaring) the resulting discrete temperature fits result in a satisfactory (from the χ^2 point of view) description of the data for statistics similar to the ones typically obtained for relatively bright stellar sources. Thus the stellar discrete temperature fits are likely to "hide" a continuous temperature distribution, and the resulting discrete temperatures should be taken as parameterizations of a more complex emission measure distribution, pointing to the location of the bulk of the emission measure.

At the same time, the comparison of multiple temperature fits from different detectors should be performed with caution, as different instrumental features can influence the resulting temperature distribution. For example, the location and depth of the absorption edges (e.g. the carbon edge in the windows of proportional counters such as the *Einstein* IPC and the ROSAT PSPC) and the way that detected photons are redistributed due to the relatively poor spectral resolution of these detectors may bias the fitted temperatures distributions in a way which, coupled with the relevant calibration uncertainties, may not be entirely predictable.

The actual detailed determination of the emission measure distribution in a significant number of active stars became possible with the availability of the high-resolution EUVE spectra (as in the case of the determination of stellar coronal densities). The high spectral resolution of EUVE allowed the flux in individual spectral lines to be reliably determined, and thus for the emission measure distribution to be derived. At the typical densities of stellar coronae (which are assumed in this context to be optically thin), the flux emitted in a given line is given by

$$I \propto \int G(T) N_e^2(T) \frac{dV(T)}{d\log T} d\log T \tag{4}$$

where the atomic physics is contained in the contribution function $G(T)$ and

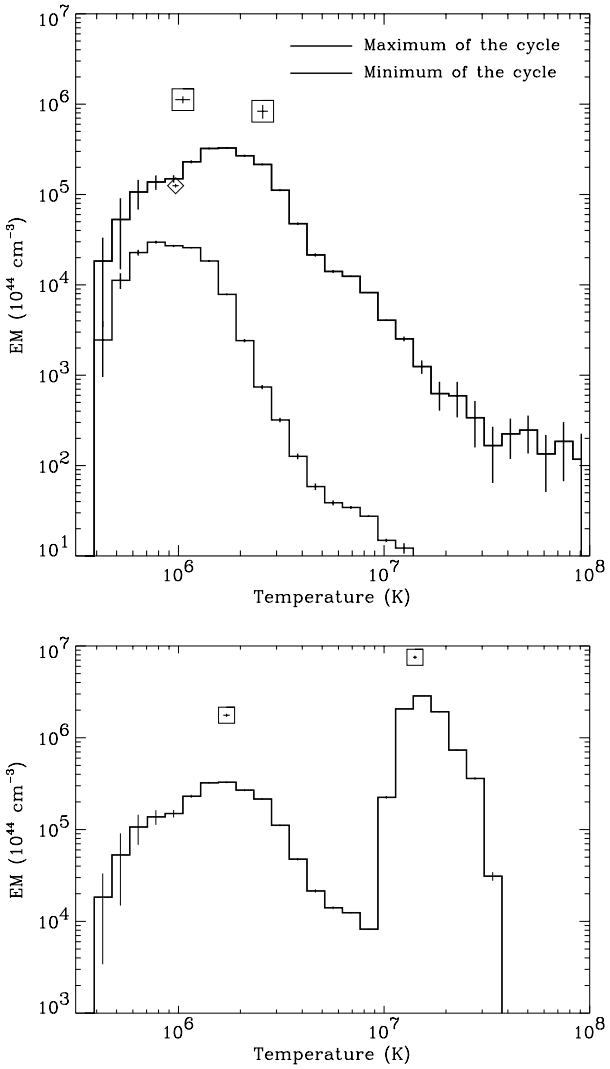

Figure 37. Top panel: Emission measure distributions of the solar corona, derived during the minimum and the maximum of the solar cycle. Symbols mark the temperatures and the emission measures obtained by the 1 or 2-T fit when the spectra, derived from the emission measure distributions, are folded through the ROSAT PSPC response. The solar maximum spectrum is fit with two temperatures, the solar minimum one with one temperature. Bottom panel: the same during a large flare. Adapted from Peres et al. (2000).

$$EM(T) = N_e^2(T)\frac{dV(T)}{d\log T} \tag{5}$$

is called the *differential emission measure* (DEM in brief[8]). In principle, inversion of Eq. 4, using the measurement of fluxes in a range of spectral lines as inputs, should yield the DEM (i.e. the distribution of emitting material as a function of the plasma temperature). In practice, the problem is mathematically ill-posed and thus the result is potentially ambiguous, and somewhat dependent on the analysis technique used. A technique for producing the DEM given the set of line fluxes was already pioneered by Pottasch (1963a) in the case of the solar corona UV emission, and was later widely applied by many authors on the chromospheres of cool stars using the wealth of observations produced by the IUE satellite (e.g. Jordan et al., 1987).

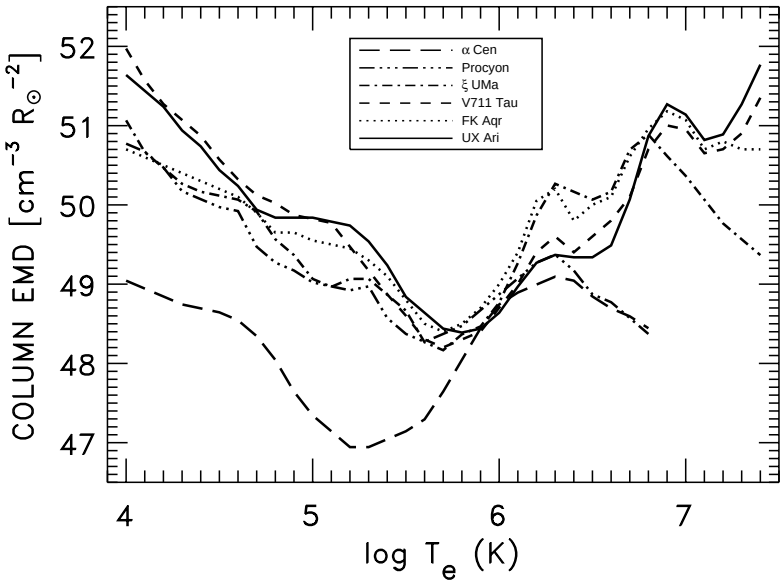

Figure 38. The DEM distributions obtained from EUVE data for a number of stars with varying levels of activity (the part below $10^{5.5}$ K is obtained with non-simultaneous IUE data). The DEM values are normalized to the stellar surface area. Adapted from Sanz-Forcada et al. (2002b).

The same type of technique was applied to the EUVE spectra of cool stars, e.g. by Dupree et al. (1993) on the spectrum of Capella, producing DEM distributions spanning the whole range of coronal temperatures, all the way up to $\simeq 2 \times 10^7$ K (although for the higher temperatures only few lines are present in EUVE spectra). The existing body of EUVE results regarding the DEM of cool stars coronae is reviewed by Bowyer et al. (2000), to which the reader is referred for the original references. More recently, Sanz-Forcada

[8] note that different authors use at times slightly different definition of the DEM.

et al. (2002a) and Sanz-Forcada et al. (2002b) have performed a systematic survey of the DEM for a sample of active stars for which EUVE observations are available, which they complemented with non-simultaneous IUE observations to constrain the shape of the DEM at $T \lesssim 10^6$ K.

The analysis of these EUVE spectra show that the DEM in active stars is continuous, spanning a wide range of temperatures – as expected from the fact that lines spanning a wide range of formation temperatures are detected in the spectra. As visible in Fig. 38 active stars show evidence for significant amounts of very hot material (up to tens of MK), with a peak in the DEM at around 10 MK (the so-called "bump"). The similarity of the DEM for active stars of different types (independently from their being single, binary, main sequence or evolved), is remarkable, in particular the persistence of the "bump". Less active stars (e.g. α Cen and Procyon) do not show the material at high temperature which is present in more active stars. It has been suggested that the hot material responsible for the bump is, also given the high densities derived from the same spectra, concentrated in a spatially compact structure, likely located near the pole of the active star (Brickhouse and Dupree, 1998; Brickhouse et al., 2001), a suggestion consistent with the frequent polar location of flaring structures discussed in Sect. 6.2.2.

Studies of the DEM derived from *Chandra* and XMM-*Newton* high resolution spectra with the same approach are still in their early phases (e.g. Maggio et al., 2002). Some studies have been published using a "global fitting" approach to the DEM derivation, which however suffer from similar problems as the abundance derivations using the same approach and will not be further discussed here.

While the above approach to the DEM determination has a clear physical basis, its disadvantage is the difficulty in estimating, in a quantitative way, the uncertainties on the derived DEM distributions, and thus the reality of individual features such as the bump visible in Fig. 38. This applies both to the systematics (in the calibration, or in the atomic rates) and to the effects of the statistical errors on the measured line fluxes onto the final shape of the DEM distribution. Stern et al. (1995a) discuss, in the case of the EUVE observations of Algol, the relationship between uncertainties in the spectra and uncertainties in the DEM distribution (as well as in the chemical abundance of the emitting plasma, which is determined simultaneously). A new technique for DEM reconstruction has been developed by Kashyap and Drake (1998), based on a Monte Carlo method. The technique has the advantage of relaxing the (non-physical) smoothness constraints imposed on the DEM by many other methods and of allowing upper limits to be properly used. At the same time it allows a more rigorous estimation of the errors on the resulting DEM. An application of this approach to stellar data is presented by Drake et al. (2001) on the spectrum of HR 1099.

Similarly to the integrated density measurements discussed in Sect. 11.1, the derived DEMs are an average over time and space obtained from a complex and dynamic underlying plasma. Again, their diagnostic power and their capability to constrain the underlying physics and structuring of the corona, are not straightforward (Judge, 2002).

11.2.1. *Loop modeling of stellar coronal spectra*

Already with the *Einstein* IPC data, which had limited spectral resolution, attempts were made to fit more physical models to the IPC data, based on the expected X-ray differential emission measure distribution of the quasi-static loop structures described in Sect. 6.1. For example, Schmitt et al. (1985) studied the spectrum of Procyon, and Stern et al. (1986) studied the X-ray spectra of the brightest Hyades emitters. Both works came to the conclusion that high-pressure, compact loops would be the most likely scenario.

Later, Ventura et al. (1998c) – and previous papers in the series – fit ROSAT PSPC spectra of active stars with the DEM derived under the assumption that two distinct populations of loops are present in the corona. The physical insight gained from these efforts has however been limited, as the assumption that one class (or a small number of classes) of similar coronal structures are dominating the emission is perhaps too simplistic. In fact, the slope of the EUVE-derived DEM (Fig. 38) is steeper than the distribution which can be generated from quasi-static loops, once more questioning whether the simple quasi-static loop is an appropriate building block for active stellar coronae, also given that, as discussed in Sect. 6.1, even the comparatively "simple" solar corona shows evidence for the presence of very dynamic loops.

12. X-ray surveys as a tool for the study of Galactic structure

Since the coronal X-ray luminosity decreases by some 3 to 4 orders of magnitude during the stellar lifetime (see Sect. 9), X-ray surveys are a very powerful method to find and study young stars. In particular since most of the decrease in the X-ray emission level takes place during the main-sequence lifetime, X-ray observations are very useful to select young main sequence stars which are indistinguishable from older (and coronally quieter) stars in optical surveys. Due to their higher X-ray luminosity young stars can be seen in X-ray surveys at much larger distances than old stars, so that young stars will be oversampled in X-ray observations and will dominate the detected population of coronal sources. This can be, and has been extensively used to derive global properties of young stellar populations from X-ray surveys.

To understand the composition of the coronal source population detected in X-ray unbiased surveys one needs to fold together several ingredients, such

as the spatial distribution of stars of different ages, the spatial distribution of interstellar gas (to take into account the interstellar absorption of soft X-ray photons), and the stellar X-ray luminosity distributions. An early example of this type of work is the estimate by Rosner et al. (1981) of the contribution of M dwarfs to the soft X-ray background. The first systematic effort in this direction was the X-COUNT model (Favata et al., 1992), which only included the Galactic disk component, based on the Bahcall & Soneira model (Bahcall and Soneira, 1980, modified to take into account the dependence of scale height and X-ray luminosity on age, Micela et al., 1993). To represent the age dependence of L_X, stars are divided in three age ranges corresponding to the Pleiades, Hyades, and nearby field stars. Another model with similar aims has been built by Guillout et al. (1996), based on the Besançon model of the Galaxy, in which (unlikely the Bahcall & Soneira model on which the X-COUNT model is based) the different spatial distribution of stellar populations with different ages is explicitly taken into account (also resulting in a smaller scale height of all the stellar populations).

The major contribution to X-ray source counts comes from the high luminosity tails of the X-ray luminosity distributions, since the more luminous stars will be seen through a much larger volume. These tails are typically determined through the observation of few stars, hence the relative uncertainty is a major source of uncertainty in predictions.

The comparison between the model predictions and the X-ray coronal source counts in unbiased, flux-limited X-ray surveys allows to deduce some properties of the X-ray active populations and more in general on the distribution of stars in different age ranges in the Galaxy.

One early result (Favata et al., 1988) has been the identification of a large population of yellow stars observed in the *Einstein* Extended Medium Sensitivity Survey (*EMSS*, Gioia et al., 1990), well in excess of what would have been expected on the basis of the X-ray emitting populations known at the time. Follow-up spectroscopic observations have shown that this population is dominated – on the basis of their very high average photospheric Li abundance – by young (i.e. with ages of at most some 10^8 yr) main sequence (or near main sequence) stars (Favata et al., 1993; Favata et al., 1995). The youth of the detected source population has been confirmed also on the basis of their position on evolutionary tracks determined using the Hipparcos parallaxes of a subsample of these stars (Micela et al., 1997a; Favata et al., 1998).

Similar results have also been obtained for the sample of coronal sources serendipitously detected in EXOSAT observations (Tagliaferri et al., 1994) and for the sample of coronal sources serendipitously detected in the EUV survey performed with the ROSAT WFC (Jeffries, 1995).

The study of the stellar population visible in the ROSAT All Sky Survey also shows that young stars with ages close to the Zero Age Main Sequence form the dominant population (Sterzik and Schmitt, 1997; Guillout et al.,

1998b; Guillout et al., 1998a; Guillout et al., 1999) and that the Gould belt, a "ring", or "disk" of recent star formation which had been identified already since a long time through the massive young OB stars, is also replete with young low-mass stars which are well visible in X-rays (see Sect. 12.2). However, no fully identified sample of ROSAT X-ray sources (like the *EMSS*) is available to date, so that it has not been possible to perform the same type of statistically unbiased analysis as it was possible with the *EMSS*. Efforts to supply fully identified samples of X-ray sources detected in *Chandra* and XMM-*Newton* observations are under way. Given the much higher sensitivity these surveys will supply information on the distribution of older, less active coronal sources, which are almost absent in either *Einstein* or ROSAT surveys.

12.1. CONSTRAINTS ON STELLAR BIRTHRATE

Comparisons of observed and model-predicted number density of X-ray selected stars as a function of the limiting X-ray flux (their $\log N$–$\log S$ distribution) can constrain the stellar birthrate in the solar neighborhood in the last billion year (Micela et al., 1993; Guillout et al., 1996), i.e. in the age interval which will dominate – because of the high coronal X-ray luminosity – X-ray flux-limited surveys. Such information is difficult to obtain otherwise, as stars in this age range are not easy to identify from their optical properties.

In Fig. 39 the expected total $\log N$–$\log S$ for stellar coronal sources at high galactic latitude obtained with the X-COUNT model assuming a constant stellar birthrate is plotted, together with the predicted contribution to the $\log N$–$\log S$ of stars in different age ranges. At high fluxes the youngest stars dominate (this is the domain best sampled by *Einstein* and ROSAT surveys), at intermediate fluxes essentially all the young stars have been detected (i.e. the limiting distance of the survey for the X-ray luminous young stars reaches outside the Galactic disk), and the intermediate-age stars dominate; at faint fluxes also all intermediate-age stars have been observed, and only old, X-ray faint stars will add to the source counts. This is the domain which is starting to be sampled with *Chandra* and XMM-*Newton* observations. At any given flux the relative contribution of the various populations depends on the number of stars in each age range and thus on the stellar birthrate. Fig. 40 shows the $\log N$–$\log S$ expected assuming four different scenarios for the time evolution of the birthrate, the highest line corresponding to an increase of the stellar birthrate, the second to a constant birthrate and the remaining to a slow and rapid decrease of the birthrate, respectively. The data points are derived from the *Einstein Extended Medium Sensitivity Survey* (EMSS, Gioia et al., 1990), and they appear to rule out a decreasing stellar birthrate in recent times. Points at high fluxes are below any predictions since the EMSS is biased against high X-ray flux sources.

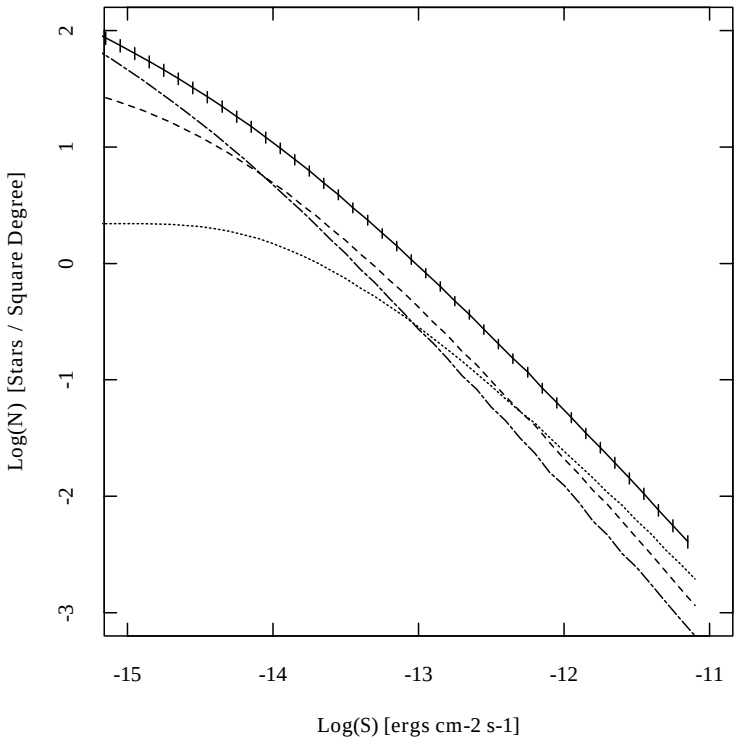

Figure 39. Expected $\log N$–$\log S$ at high galactic latitude (solid line) obtained with the X-COUNT model, assuming a constant stellar birthrate. Vertical segments are the error bars due to the uncertainties on the X-ray luminosity distributions. The contributions of young stars (dotted line), intermediate age stars (dashed line), and old stars (dotted-dashed line) are shown separately. Adapted from Micela et al. (1993).

12.2. IDENTIFICATION OF A LARGE SCALE STRUCTURE: THE GOULD BELT

The cross-correlation (Guillout et al., 1998a) between the sources detected in the RASS and the Tycho optical catalog (Høg et al., 2000) has shown that the distribution of coronal sources presents, besides the expected vertical density gradient due to the shape of the galactic disk, an asymmetry with respect to the galactic equator with a concentration of young stars at longitudes 180–360°, with an apparent inclination of $\simeq 20^\circ$ to the Galactic plane. This density enhancement is in good agreement with the position of the so-called Gould Belt (see Fig. 41), the large-scale ring structure of recent star formation traced by the spatial distributions of OB associations. This has been the first detec-

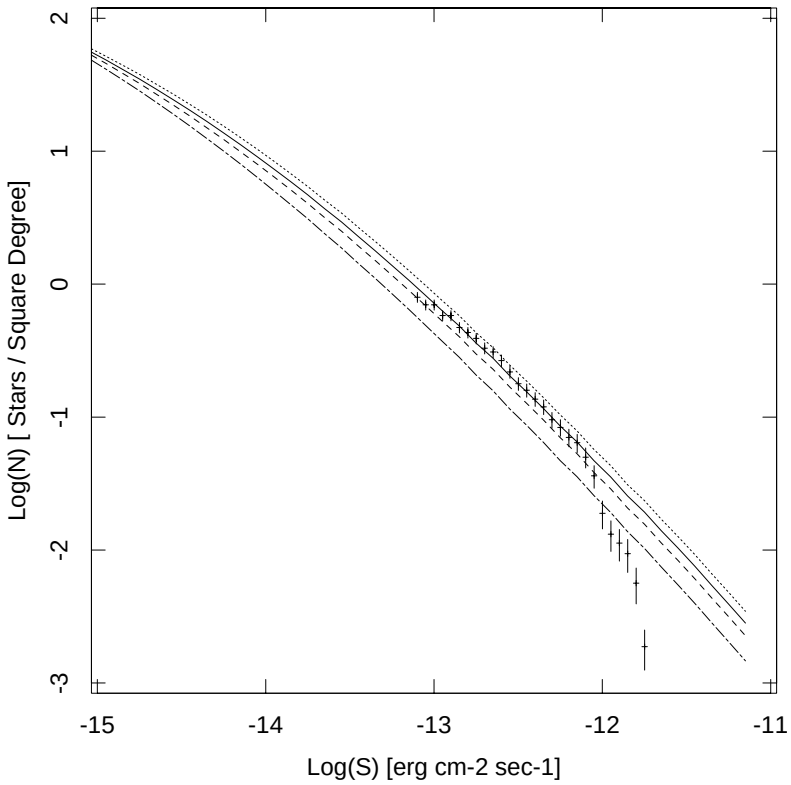

Figure 40. X-ray $\log N$–$\log S$ for coronal sources in the 0.16–4.0 keV band predicted in the direction $l = 90°$ assuming a constant birthrate (solid line), a slowly decreasing birthrate (dashed line), a slowly increasing (dotted line) and rapidly decreasing birthrate (short-dashed line). Vertical segments are the experimental points (with error bars) obtained from the *Einstein EMSS*. From Micela et al. (1993).

tion of the late-type members of the Gould Belt population. These stars are thought to have formed through a common sequence of events, and have an age $t < 10^8$ yr. The analysis of the surface density, together with the distances obtained for the subsample observed with Hipparcos suggests that the Gould Belt is not a ring but more likely a disk-like structure (Guillout et al., 1998a; de Zeeuw et al., 1999)

The physical reality of a structure like the Gould Belt is still controversial, since it could be the result of a chance alignment of several OB associations. Hipparcos observations have allowed to explore the early type stars of the Gould Belt (de Zeeuw et al., 1999), but with very scarce data on the fainter, late-type stars. A detailed analysis of the Tycho-RASS sample has shown

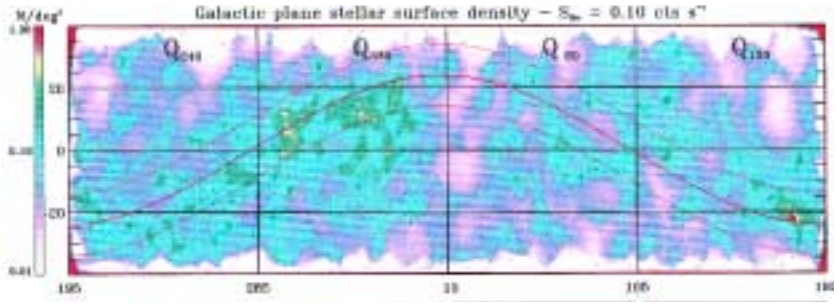

Figure 41. The spatial distribution (in galactic coordinates) of the active stars detected in the RASS and present in the Tycho catalog, plotted as surface density, from Guillout et al. (1998b). The Gould belt is plotted as a wide strip.

that in the gaps between known star-forming regions which are considered to belong to the Gould Belt, the density of X-ray selected active stars is still very high, comparable with that in the star-forming regions, supporting the reality of the Gould Belt structure as a physical association.

13. Conclusions

We have tried in this review to chart the state of the field at the beginning of a new era, marked by the availability of the *Chandra* and XMM-*Newton* data. These offer unprecedented sensitivity, allowing to study fainter sources than previously possible, excellent spatial resolution, allowing for the study of crowded fields and for detailed morphological studies, and much enhanced spectral resolution, allowing for the first time to resolve individual spectral lines in the X-ray domain in a significant number of coronal sources.

The work being performed through *Chandra* and XMM-*Newton* observations builds on a previous era of *Einstein* observations first, followed by (among other) ROSAT, ASCA, EUVE and SAX, and on the massive amount of work invested in understanding the large body of observations.

In the future new observations should allow to study new phenomena and to extend the domain in which observations are possible. Examples include the study of star-forming regions, for which X-ray emission represents an excellent (perhaps one of the best) ways of identifying very young stars, and in which *Chandra*'s high spatial resolution finds an excellent application. The large ongoing effort relative to the analysis of the *Chandra* and XMM-*Newton* data has only briefly been referred to in the present review, as trying to summarize it would be premature. Notable new results however include the systematic detection of young brown dwarfs (see Sect. 4.3.1) in star-forming regions and the recent detection of X-ray emission from Herbig-Haro objects

(Pravdo et al., 2001; Favata et al., 2002), both of which show the importance of X-rays in all stages of the star forming process.

Significant progress is also being booked through the study of high resolution spectra; notably, the availability of high-resolution spectra of early type stars (which have not been covered in the present review) is challenging our understanding of the relevant emission mechanisms at a rather fundamental level (e.g. Cassinelli et al., 2001).

Acknowledgements

F. Favata would like to thank his former Division Head B. G. Taylor for granting him the sabbatical time needed to complete the present work, as well as the warm hospitality of the Osservatorio Astronomico G. S. Vaiana in Palermo, Italy, where much of this review has been written. G. Micela acknowledges partial support from ASI and MIUR. We would like to thank E. Flaccomio, D. Huenemoerder, J. Linsky, S. Orlando, I. Pillitteri, N. Pizzolato, F. Reale, J. Sanz-Forcada for sharing with us results in advance of their publication. We thanks M. Audard, M. Guedel, R. Osten, P. Testa for kindly providing us with adapted figures from their papers. We would also like to thank A. Maggio for the for the careful reading of an early draft of the manuscript and the resulting many useful discussions, and the two referees (R. Stern and J. Drake) for the extensive and careful reading of the manuscript and for the many very useful suggestions.

References

Alcalá, J. M., J. Krautter, E. Covino, R. Neuhäuser, J. H. M. M. Schmitt, and R. Wichmann: 1997, 'A study of the Chamaleon star forming region from the ROSAT all-sky survey. II. The pre-main sequence population'. *A&A* **319**, 184.

Allende Prieto, C., D. L. Lambert, and M. Asplund: 2001, 'The forbidden abundance of oxygen in the Sun'. *ApJ* **556**, L63.

Ambruster, C. W., S. Sciortino, and L. Golub: 1987, 'Rapid, low-level X-ray variability in active late-type dwarfs'. *ApJS* **65**, 273.

Anders, E. and N. Grevesse: 1989, 'Abundances of the elements – Meteoritic and solar'. *Geochimica and Cosmochimica Acta* **53**, 157.

Antonucci, E. and R. Martin: 1995, 'Differential emission measure and iron-to-calcium abundance in solar flare plasmas'. *ApJ* **451**, 402.

Aschwanden, M. J.: 2001, 'An evaluation of coronal heating models for active regions based on Yohkoh, SOHO, and TRACE observations'. *ApJ* **560**, 1035.

Aschwanden, M. J., R. W. Nightingale, and D. Alexander: 2000, 'Evidence for nonuniform heating of coronal loops inferred from multithread modeling of TRACE Data'. *ApJ* **541**, 1059.

Audard, M., M. Güdel, and E. F. Guinan: 1999, 'Implications from extreme-ultraviolet observations for coronal heating of active stars'. *ApJ* **513**, L53.

Audard, M., E. Behar, M. Güdel, A. J. J. Raassen, D. Porquet, R. Mewe, C. R. Foley, and G. E. Bromage: 2001, 'The XMM-Newton view of stellar coronae: High-resolution X-ray spectroscopy of Capella'. *A&A* **365**, L329.

Audard, M., M. Güdel, and R. Mewe: 2001, 'The XMM-Newton view of stellar coronae: flare heating in the coronae of HR 1099'. *A&A* **365**, L318.

Audard, M., M. Güdel, A. Sres, R. Mewe, A. J. J. Raassen, E. Behar, C. R. Foley, and R. J. L. van der Meer: 2002, 'A study of the coronal plasma in RS CVn binary systems: HR 1099 and co.'. In: F. Favata and J. J. Drake (eds.): *ASP Conf. Ser. 277: Stellar coronae in the Chandra and XMM era*. p. 65, ASP, San Francisco.

Ayres, T. R., A. Brown, R. A. Osten, D. P. Huenemoerder, J. J. Drake, N. S. Brickhouse, and J. L. Linsky: 2001, 'Chandra, EUVE, HST, and VLA multiwavelength campaign on HR 1099: instrumental capabilities, data reduction, and initial results'. *ApJ* **549**, 554.

Bahcall, J. N. and R. M. Soneira: 1980, 'The universe at faint magnitudes. I – Models for the galaxy and the predicted star counts'. *ApJS* **44**, 73.

Baliunas, S. L., R. A. Donahue, W. H. Soon, J. H. Horne, J. Frazer, and et al.: 1995, 'Chromospheric variations in main-sequence stars. II'. *ApJ* **438**, 269.

Barbera, M., G. Micela, S. Sciortino, F. R. Harnden, and R. Rosner: 1993, 'X-ray emission at the low mass end: results from an extensive Einstein observatory survey'. *ApJ* **414**, 846.

Barbera, M., G. Micela, A. Collura, S. S. Murray, and M. V. Zombeck: 2000, 'In-flight calibration of the ROSAT HRI ultraviolet sensitivity'. *ApJ* **545**, 449.

Barbera, M., F. Bocchino, F. Damiani, G. Micela, S. Sciortino, F. Favata, and F. R. Harnden: 2002, 'ROSAT PSPC/HRI observations of the open cluster NGC 2422'. *A&A* **387**, 463.

Barrado y Navascués, D., J. R. Stauffer, and S. Randich: 1998, 'Stellar activity in coeval open clusters: Praesepe and the Hyades'. *ApJ* **506**, 347.

Belloni, T. and F. Verbunt: 1996, 'Soft X-rays from the intermediate-age open cluster NGC 752'. *A&A* **305**, 806.

Berdyugina, S. V., S. Jankov, I. Ilyin, I. Tuominen, and F. C. Fekel: 1998, 'The active RS Canum Venaticorum binary II Pegasi. I. Stellar and orbital parameters'. *A&A* **334**, 863.

Bookbinder, J. A.: 1985, 'Observations of non-thermal radiation from late-type stars'. Ph.D. thesis, Harvard University.

Bouvier, J.: 1990, 'Rotation in T Tauri stars. II – Clues for magnetic activity'. *AJ* **99**, 946.

Bouvier, J., M. Forestini, and S. Allain: 1997, 'The angular momentum evolution of low-mass stars'. *A&A* **326**, 1023.

Bowyer, S., J. J. Drake, and S. Vennes: 2000, 'Extreme ultraviolet astronomy'. *ARA&A* **38**, 231.

Brandenburg, A., D. Moss, and I. Tuominen: 1992, 'Turbulent pumping in the solar dynamo'. In: K. L. Harvey (ed.): *The solar cycle*, Vol. 27 of *ASP Conference Series*. p. 536, ASP, San Francisco.

Brickhouse, N. S., J. C. Raymond, and B. W. Smith: 1995, 'New model of iron spectra in the extreme ultraviolet and application to SERTS and EUVE observations: a solar active region and Capella'. *ApJS* **97**, 551.

Brickhouse, N. S. and A. K. Dupree: 1998, 'EUVE observations of the W UMa contact binary 44i Boo: coronal structure and variability'. *ApJ* **502**, 918.

Brickhouse, N. S., A. K. Dupree, R. J. Edgar, D. A. Liedahl, S. A. Drake, N. E. White, and K. P. Singh: 2000, 'Coronal structure and abundances of Capella from simultaneous EUVE and ASCA spectroscopy'. *ApJ* **530**, 387.

Brickhouse, N. S., A. K. Dupree, and P. R. Young: 2001, 'X-Ray Doppler Imaging of 44i Bootis with Chandra'. *ApJ* **562**, L75.

Briggs, K. R., J. P. Pye, R. D. Jeffries, and E. J. Totten: 2000, 'X-ray source populations in the region of the open clusters NGC 6633 and IC 4756'. *MNRAS* **319**, 826.

Brinkman, A. C., E. Behar, M. Güdel, M. Audard, A. J. F. den Boggende, G. Branduardi-Raymont, J. Cottam, C. Erd, J. W. den Herder, F. Jansen, J. S. Kaastra, S. M. Kahn, R. Mewe, F. B. S. Paerels, J. R. Peterson, A. P. Rasmussen, I. Sakelliou, and C. de Vries: 2001, 'First light measurements with the XMM-Newton reflection grating spectrometers: evidence for an inverse first ionization potential effect and anomalous Ne abundance in the coronae of HR 1099'. *A&A* **365**, L324.

Caillault, J. P. and D. J. Helfand: 1985, 'The Einstein soft X-ray survey of the Pleiades'. *ApJ* **289**, 279.

Canizares, C. R., D. P. Huenemoerder, D. S. Davis, D. Dewey, K. A. Flanagan, J. Houck, T. H. Markert, H. L. Marshall, M. L. Schattenburg, N. S. Schulz, M. Wise, J. J. Drake, and N. S. Brickhouse: 2000, 'High-resolution X-ray spectra of Capella: initial results from the Chandra high-energy transmission grating spectrometer'. *ApJ* **539**, L41.

Casanova, S., T. Montmerle, E. D. Feigelson, and P. Andre: 1995, 'ROSAT X-ray sources embedded in the ρ Ophiuchi cloud core'. *ApJ* **439**, 752.

Cassinelli, J. P., N. A. Miller, W. L. Waldron, J. J. MacFarlane, and D. H. Cohen: 2001, 'Chandra detection of Doppler-shifted X-ray line profiles from the wind of ζ Puppis (O4 F)'. *ApJ* **554**, L55.

Catura, R. C., L. W. Acton, and H. M. Johnson: 1975, 'Evidence for X-ray emission from Capella'. *ApJ* **196**, L47.

Charbonneau, P. and K. B. MacGregor: 1992, 'Angular momentum transport in magnetized stellar radiative zones. I – Numerical solutions to the core spin-up model problem'. *ApJ* **387**, 639.

Choi, C. S. and T. Dotani: 1998, 'ASCA observation of a long-duration X-ray flare from the W UMa-type binary VW Cephei'. *ApJ* **492**, 761.

Christensen-Dalsgaard, J.: 2002, 'Helioseismology'. *Rev. Mod. Phys.* **74**, 1073.

Ciaravella, A., G. Peres, A. Maggio, and S. Serio: 1996, 'Loop modeling of coronal X-ray spectra. I. General properties'. *A&A* **306**, 553.

Copeland, H., J. O. Jensen, and H. E. Jorgensen: 1970, 'Homogeneous models for Population I and Population II compositions'. *A&A* **5**, 12.

Covino, S., M. R. Panzera, G. Tagliaferri, and R. Pallavicini: 2001, 'Quiescent and flare analysis for the chromospherically active star Gl 355 (LQ Hya)'. *A&A* **371**, 973.

Cox, A. N., G. Shaviv, and S. W. Hodson: 1981, 'On the ratio of mixing length to scale height in red dwarfs'. *ApJ* **245**, L37.

Craig, I. J. D., A. N. McClymont, and J. H. Underwood: 1978, 'The temperature and density structure of active region coronal loops'. *A&A* **70**, 1.

Crosby, N. B., M. J. Aschwanden, and B. R. Dennis: 1993, 'Frequency distributions and correlations of solar X-ray flare parameters'. *Solar Physics* **143**, 275.

Cully, S. L., O. H. W. Siegmund, P. W. Vedder, and J. V. Vallerga: 1993, 'Extreme Ultraviolet Explorer deep survey observations of a large flare on AU Microscopii'. *ApJ* **414**, L49.

Cully, S. L., G. H. Fisher, S. L. Hawley, and T. Simon: 1997, 'Extreme Ultraviolet Explorer spectra of the 1993 March flares on AD Leonis: the differential emission measure and implications for coronal structure'. *ApJ* **491**, 910.

Dachs, J. and W. Hummel: 1996, 'ROSAT survey of stellar X-ray sources in the young open cluster NGC 2516'. *A&A* **312**, 818.

Dahn, C. C., J. Liebert, and R. S. Harrington: 1986, 'LHS 292 and the luminosity function of the nearby M dwarfs'. *AJ* **91**, 621.

Damiani, F., G. Micela, S. Sciortino, and F. R. Harnden: 1994, 'Einstein X-ray observations of Herbig Ae/Be stars'. *ApJ* **436**, 807.

D'Antona, F. and I. Mazzitelli: 1997, 'Evolution of low mass stars'. *Mem. Soc. Astron. Ital.* **68**, 807.

de Zeeuw, P. T., R. Hoogerwerf, J. H. J. de Bruijne, A. G. A. Brown, and A. Blaauw: 1999, 'A Hipparcos census of the nearby OB associations'. *AJ* **117**, 354.

Deliyannis, C. P. and R. A. Malaney: 1995, 'Flare production of ^{6}Li in population II stars'. *ApJ* **453**, 810.

DeLuca, E. E. and P. A. Gilman: 1991, 'The solar dynamo'. In: A. Cox, W. C. Livingston, and M. S. Matthews (eds.): *Solar interior and atmosphere*. Tucson, p. 275, Univ. of Arizona Press.

Dempsey, R. C., J. L. Linsky, T. A. Fleming, and J. H. M. M. Schmitt: 1993a, 'The ROSAT all-sky survey of active binary coronae. I. Quiescent fluxes from the RS Canum Venaticorum systems'. *ApJS* **86**, 599.

Dempsey, R. C., J. L. Linsky, T. A. Fleming, and J. H. M. M. Schmitt: 1993b, 'The ROSAT all-sky survey of active binary coronae. II. Coronal temperatures of the RS Canum Venaticorum systems'. *ApJ* **413**, 333.

Dempsey, R. C., J. L. Linsky, T. A. Fleming, and J. H. M. M. Schmitt: 1997, 'The ROSAT all-sky survey of active binary coronae. III. Quiescent coronal properties for the BY Draconis-type binaries'. *ApJ* **478**, 358.

Drake, J. J.: 1996a, 'Stellar spectroscopy with the Extreme Ultraviolet Explorer'. In: R. Pallavicini and A. K. Dupree (eds.): *ASP Conf. Ser. 109: Cool Stars, Stellar Systems, and the Sun*. p. 203, ASP, San Francisco.

Drake, J. J.: 1998, 'Excess helium as an explanation for metal deficiency in coronal plasma?'. *ApJ* **496**, L33.

Drake, J. J.: 2001, 'Stellar coronae: the first 25 years'. In: R. Giacconi, L. Stella, and S. Serio (eds.): *ASP Conf. Ser. 234: X-ray Astronomy 2000*. p. 53, ASP, San Francisco.

Drake, J. J.: 2002, 'The chemical composition of stellar coronae'. In: F. Favata and J. J. Drake (eds.): *Stellar coronae in the Chandra and XMM-Newton era*, Vol. 277 of *ASP Conference Series*. San Francisco, p. 75, ASP.

Drake, J. J., J. M. Laming, and K. G. Widing: 1995, 'Stellar coronal abundances. 2: The first ionization potential effect and its absence in the corona of procyon'. *ApJ* **443**, 393.

Drake, J. J., J. M. Laming, and K. G. Widing: 1996a, 'The FIP effect and abundance anomalies in late-type stellar coronae'. In: S. Bowyer and R. F. Malina (eds.): *IAU Colloq. 152: Astrophysics in the Extreme Ultraviolet*. p. 97.

Drake, J. J., R. A. Stern, G. S. Stringfellow, M. Mathioudakis, J. M. Laming, and D. L. Lambert: 1996b, 'Detection of quiescent extreme-ultraviolet emission from the very low mass dwarf van Biesbrowk 8: evidence for turbulent field dynamo'. *ApJ* **469**, 828.

Drake, J. J., J. M. Laming, and K. G. Widing: 1997, 'Stellar coronal abundances V: evidence for the FIP effect in α Centauri'. *ApJ* **478**, 403.

Drake, J. J., G. Peres, S. Orlando, J. M. Laming, and A. Maggio: 2000, 'On stellar coronae and solar active regions'. *ApJ* **545**, 1074.

Drake, J. J., N. S. Brickhouse, V. Kashyap, J. M. Laming, D. P. Huenemoerder, R. Smith, and B. J. Wargelin: 2001, 'Enhanced noble gases in the coronae of active stars'. *ApJ* **548**, L81.

Drake, J. J. and V. Kashyap: 2001, 'The coronal metallicity of the intermediate activity dwarf ξ Boo A'. *ApJ* **547**, 428.

Drake, S. A.: 1996b, 'X-ray measurements of coronal abundances'. In: S. S. Holt and G. Sonneborn (eds.): *ASP Conf. Ser. 99: Cosmic Abundances*. p. 215, ASP, San Francisco.

Duncan, D. K., S. Baliunas, R. Noyes, and A. Vaughan: 1984, 'Chromospheric emission and rotation of the Hyades lower main sequence'. *PASP* **96**, 707.

Dupree, A. K., N. S. Brickhouse, G. A. Doschek, J. C. Green, and J. C. Raymond: 1993, 'The extreme ultraviolet spectrum of α Aurigae (Capella)'. *ApJ* **418**, L41.

Durney, B. R., D. S. de Young, and I. W. Roxburgh: 1993, 'On the generation of the large-scale and turbulent magnetic fields in solar-type stars'. *Solar Phys.* **145**, 207.

Edlén, B.: 1945, 'The identification of the coronal lines (George Darwin Lecture)'. *MNRAS* **105**, 323.

Edvardsson, B., J. Andersen, B. Gustafsson, et al.: 1993, 'The chemical evolution of the galactic disk'. *A&A* **275**, 101.

Endl, M., K. G. Strassmeier, and M. Kurster: 1997, 'A large X-ray flare on HU Virginis'. *A&A* **328**, 565.

Favata, F.: 2001, 'The coronal structure of active stars'. In: R. Giacconi, L. Stella, and S. Serio (eds.): *ASP Conf. Ser. 234: X-ray Astronomy 2000*. p. 234, ASP, San Francisco.

Favata, F., R. Rosner, S. Sciortino, and G. S. Vaiana: 1988, 'The stellar composition of X-ray surveys from the Einstein Observatory'. *ApJ* **324**, 1010.

Favata, F., G. Micela, S. Sciortino, and G. S. Vaiana: 1992, 'The stellar coronal component of the Galaxy. I. The X-COUNT numerical model'. *A&A* **256**, 86.

Favata, F., M. Barbera, G. Micela, and S. Sciortino: 1993, 'A search for yellow young disk population stars among EMSS stellar X-ray sources by means of lithium abundance determination'. *A&A* **277**, 428.

Favata, F., M. Barbera, G. Micela, and S. Sciortino: 1995, 'Lithium, X-ray activity and rotation in an X-ray selected sample of solar-type stars'. *A&A* **295**, 147.

Favata, F., G. Micela, S. Sciortino, and F. D'Antona: 1998, 'The evolutionary status of activity-selected solar-type stars and of T-Tauri stars as derived from Hipparcos parallaxes: evidence for a long-lived T-Tauri disk'. *A&A* **335**, 218.

Favata, F. and J. H. M. M. Schmitt: 1999, 'Spectroscopic analysis of a super-hot giant flare observed on Algol by BeppoSAX on 30 August 1997'. *A&A* **350**, 900.

Favata, F., G. Micela, and F. Reale: 2000a, 'The corona of AD Leo'. *A&A* **354**, 1021.

Favata, F., G. Micela, F. Reale, S. Sciortino, and J. H. M. M. Schmitt: 2000b, 'The structure of the Algol corona from an analysis of all known X-ray flares: a consistent scenario for the X-ray and radio emission'. *A&A* **362**, 628.

Favata, F., F. Reale, G. Micela, S. Sciortino, A. Maggio, and H. Matsumoto: 2000c, 'An extreme X-ray flare observed on EV Lac by the ASCA observatory in July 1998'. *A&A* **353**, 987.

Favata, F., G. Micela, and F. Reale: 2001, 'Coronal structure geometries on pre-main sequence stars'. *A&A* **375**, 485.

Favata, F., C. V. M. Fridlund, G. Micela, S. Sciortino, and A. A. Kaas: 2002, 'Discovery of X-ray emission from the protostellar jet L1551 IRS5 (HH 154)'. *A&A* **386**, 204.

Feigelson, E., S. Casanova, T. Montmerle, and J. Guibert: 1993, 'ROSAT X-ray study of the Chamaleon dark cloud. I. The stellar population'. *ApJ* **416**, 623.

Feigelson, E. D. and T. Montmerle: 1999, 'High-energy processes in young stellar objects'. *ARA&A* **37**, 363.

Feigelson, E. D., P. Broos, J. A. Gaffney, et al.: 2002a, 'X-ray emitting young stars in the Orion nebula'. *ApJ* **574**, 258.

Feigelson, E. D., G. P. Garmire, and S. H. Pravdo: 2002b, 'Magnetic flaring in the pre-main-sequence Sun and implications for the early solar system'. *ApJ* **572**, 335.

Fekel, F. and S. Balachandran: 1993, 'Lithium and rapid rotation in chromospherically active single giants'. *ApJ* **403**, 708.

Feldman, U.: 1992, 'Elemental abundances in the upper solar atmosphere'. *Physica Scripta Volume T* **46**, 202.

Flaccomio, E., G. Micela, S. Sciortino, F. Damiani, F. Favata, F. R. Harnden, and J. Schachter: 2000, 'HRI observations of PMS stars in NGC 2264'. *A&A* **355**, 651.

Flaccomio, E., F. Damiani, G. Micela, S. Sciortino, F. R. Harnden, S. S. Murray, and S. J. Wolk: 2003a, 'Chandra X-ray observations of the Orion nebula cluster. II Relationship between X-ray activity indicators and stellar parameters'. *ApJ* **582**, 398.

Flaccomio, E., G. Micela, and S. Sciortino: 2003b, 'Observational clues for a role of circumstellar accretion in PMS X-ray activity'. *A&A* **397**, 611.

Fleming, T. A., J. H. M. M. Schmitt, and M. S. Giampapa: 1995, 'Correlations of coronal X-ray emission with activity, mass and age of the nearby K and M dwarfs'. *ApJ* **450**, 401.

Fleming, T. A., M. S. Giampapa, and J. H. M. M. Schmitt: 2000, 'An X-ray flare detected on the M8 dwarf VB 10'. *ApJ* **533**, 372.

Fludra, A. and J. T. Schmelz: 1999, 'The absolute coronal abundances of sulfur, calcium, and iron from Yohkoh-BCS flare spectra'. *A&A* **348**, 286.

Franciosini, E., S. Randich, and R. Pallavicini: 2000, 'A ROSAT HRI study of the open cluster NGC 3532'. *A&A* **357**, 139.

Franciosini, E., R. Pallavicini, and G. Tagliaferri: 2001, 'BeppoSAX observation of a large long-duration X-ray flare from UX Arietis'. *A&A* **375**, 196.

Gagné, M., J.-P. Caillault, and J. R. Stauffer: 1995a, 'Deep ROSAT HRI observations of the Orion nebula region'. *ApJ* **445**, 280.

Gagné, M., J.-P. Caillault, and J. R. Stauffer: 1995b, 'Spectral and temporal characteristics of X-ray-bright stars in the Pleiades'. *ApJ* **450**, 217.

Gehren, T., R. Ottmann, and J. Reetz: 1999, 'Photospheric metal abundances of AR Lacertae'. *A&A* **344**, 221.

Giampapa, M. S.: 1984, 'Lithium abundances and chromospheric activity. I. Empirical results'. *ApJ* **277**, 235.

Giampapa, M. S., R. Rosner, V. Kashyap, et al.: 1996, 'The coronae of low-mass dwarf stars'. *ApJ* **463**, 707.

Giampapa, M. S., C. F. Prosser, and T. A. Fleming: 1998, 'X-Ray activity in the open cluster IC 4665'. *ApJ* **501**, 624.

Giampapa, M. S. and T. A. Fleming: 2002, 'The coronae of low-mass stars and brown dwarfs'. In: F. Favata and J. Drake (eds.): *ASP Conf. Ser. 277: Stellar coronae in the Chandra and XMM era*. p. 247, ASP, San Francisco.

Gioia, I. M., T. Maccacaro, R. E. Schild, A. Wolter, J. T. Stocke, S. L. Morris, and J. P. Henry: 1990, 'The Einstein observatory Extended Medium Sensitivity Survey. I. X-ray data and analysis'. *ApJS* **72**, 567.

Glassgold, A. E., E. D. Feigelson, and T. Montmerle: 2000, 'Effects of energetic radiation in young stellar objects'. In: V. Mannings, A. P. Boss, and S. S. Russell (eds.): *Protostars and planets IV*. Tucson: University of Arizona Press, p. 429.

Golub, L.: 1983, 'Quiescent coronae of active chromosphere stars'. In: *ASSL Vol. 102: IAU Colloq. 71: Activity in Red-Dwarf Stars*. p. 83.

Graffagnino, V. G., D. Wonnacott, and S. Schaeidt: 1995, 'HR 5110 superflare: an interbinary flare identified?'. *MNRAS* **275**, 129.

Güdel, M., A. O. Benz, J. H. M. M. Schmitt, and S. L. Skinner: 1996, 'The Neupert effect in active stellar coronae: chromospheric evaporation and coronal heating in the dMe flare star binary UV Ceti'. *ApJ* **471**, 1002.

Güdel, M., E. F. Guinan, R. Mewe, J. S. Kaastra, and S. L. Skinner: 1997, 'A determination of the coronal emission measure distribution in the young solar analog EK Draconis from ASCA/EUVE spectra'. *ApJ* **479**, 416.

Güdel, M., J. L. Linsky, A. Brown, and F. Nagase: 1999, 'Flaring and quiescent coronae of UX Arietis: results from ASCA and EUVE campaigns'. *ApJ* **511**, 405.

Güdel, M., M. Audard, K. Briggs, F. Haberl, H. Magee, A. Maggio, R. Mewe, R. Pallavicini, and J. Pye: 2001a, 'The XMM-Newton view of stellar coronae: X-ray spectroscopy of the corona of AB Doradus'. *A&A* **365**, L336.

Güdel, M., M. Audard, K. Briggs, F. Haberl, H. Magee, A. Maggio, R. Mewe, R. Pallavicini, and J. Pye: 2001b, 'The XMM-Newton view of stellar coronae: coronal structure in the Castor X-ray triplet'. *A&A* **365**, L344.

Güdel, M., M. Audard, K. W. Smith, E. Behar, A. J. Beasley, and R. Mewe: 2002a, 'Detection of the Neupert effect in the corona of an RS Canum Venaticorum binary system by XMM-Newton and the Very Large Array'. *ApJ* **577**, 371.

Güdel, M., M. Audard, K. W. Smith, et al.: 2002b, 'A systematic spectroscopic X-ray study of stellar coronae with XMM-Newton: early results'. In: *Cool stars, stellar systems and the Sun 12* in press.

Güdel, M., M. Audard, A. Sres, R. Wehrli, E. Behar, R. Mewe., A. J. J. Raassen, and H. Magee: 2002c, 'XMM-Newton probes the solar past: coronal abundances of solar analogs at different ages'. In: F. Favata and J. J. Drake (eds.): *ASP Conf. Ser. 277: Stellar coronae in the Chandra and XMM era*. p. 497, ASP, San Francisco.

Güdel, M., M. Audard, V. L. Kashyap, J. J. Drake, and E. F. Guinan: 2003a, 'Are coronae of magnetically active stars heated by flares? II. EUV and X-Ray flare statistics and the Differential Emission Measure distribution'. *ApJ* **582**, 423.

Güdel, M., K. Arzner, M. Audard, and R. Mewe: 2003b, 'Tomography of a stellar corona: α Coronae Borealis'. *A&A* in press.

Guillout, P., M. Haywood, C. Motch, and A. C. Robin: 1996, 'The stellar content of soft X-ray surveys. I. An age-dependent numerical model'. *A&A* **316**, 89.

Guillout, P., M. F. Sterzik, J. H. M. M. Schmitt, C. Motch, D. Egret, W. Voges and R. Neuhäuser: 1998a, 'The large-scale distribution of X-ray active stars'. *A&A* **334**, 540.

Guillout, P., M. F. Sterzik, J. H. M. M. Schmitt, C. Motch, and R. Neuhäuser: 1998b, 'Discovery of a late-type stellar population associated with the Gould belt'. *A&A* **337**, 113.

Guillout, P., J. H. M. M. Schmitt, D. Egret, W. Voges, C. Motch, and M. F. Sterzik: 1999, 'The stellar content of soft X-ray surveys. II. Cross-correlation of the ROSAT All-Sky Survey with the Tycho and Hipparcos catalogs'. *A&A* **351**, 1003.

Gunn, A. G., V. Migenes, J. G. Doyle, R. E. Spencer, and M. Mathioudakis: 1997, 'Radio and extreme-ultraviolet observations of CF Tucanae'. *MNRAS* **287**, 199.

Hénoux, J.: 1998, 'FIP fractionation: theory'. *Space Science Reviews* **85**, 215.

Hamaguchi, K., H. Terada, A. Bamba, and K. Koyama: 2000, 'Large X-ray flare from a Herbig Be star, MWC297'. *ApJ* **532**, 1111.

Hamaguchi, K., K. Koyama, S. Yamauchi, and H. Terada: 2002, 'X-ray study of Herbig Ae/Be stars, intermediate mass young stars'. In: F. Favata and J. J. Drake (eds.): *ASP Conf. Ser. 277: Stellar coronae in the Chandra and XMM era*. p. 193, ASP, San Francisco.

Harmer, S., R. D. Jeffries, E. J. Totten, and J. P. Pye: 2001, 'X-rays from the open cluster NGC 6633'. *MNRAS* **324**, 473.

Harnden, F. R., N. R. Adams, F. Damiani, J. J. Drake, N. R. Evans, F. Favata, P. Flaccomio, E. andFreeman, R. D. Jeffries, V. Kashyap, G. Micela, B. M. Patten, N. Pizzolato, J. F. Schachter, S. Sciortino, J. Stauffer, S. J. Wolk, and M. V. Zombeck: 2001, 'Chandra observations of the open cluster NGC 2516'. *ApJ* **547**, L141.

Harra, L. K.: 2002, 'The solar corona as seen by Yohkoh'. In: F. Favata and J. J. Drake (eds.): *ASP Conf. Ser. 277: Stellar coronae in the Chandra and XMM era*. p. 277, ASP, San Francisco.

Hawley, S. L., G. H. Fisher, T. Simon, S. L. Cully, S. E. Deustua, M. Jablonski, C. M. Johns-Krull, B. R. Pettersen, V. Smith, W. J. Spiesman, and J. Valenti: 1995, 'Simultaneous Extreme-Ultraviolet Explorer and optical observations of AD Leonis: evidence for large coronal loops and the Neupert effect in stellar flares'. *ApJ* **453**, 464.

Hempelmann, A., J. H. M. M. Schmitt, M. Schultz, G. Rüdiger, and K. Stèpieǹ: 1995, 'Coronal X-ray emission and rotation of cool main sequence stars'. *A&A* **294**, 515.

Hempelmann, A., J. H. M. M. Schmitt, and K. Stèpieǹ: 1996, 'Coronal X-ray emission of cool stars in relation to chromospheric activity and magnetic cycles'. *A&A* **305**, 284.

Hodgkin, S. T., R. F. Jameson, and I. A. Steele: 1995, 'Chromospheric and coronal activity of low-mass stars in the Pleiades'. *MNRAS* **274**, 869.

Høg, E., C. Fabricius, V. V. Makarov, S. Urban, T. Corbin, G. Wycoff, U. Bastian, P. Schwekendiek, and A. Wicenec: 2000, 'The Tycho-2 catalogue of the 2.5 million brightest stars'. *A&A* **355**, L27.

Hudson, H. S.: 1991, 'Solar flares, microflares, nanoflares, and coronal heating'. *Solar Physics* **133**, 357.

Hudson, H. S., L. W. Acton, T. Hirayama, and Y. Uchida: 1992, 'White-light flares observed by YOHKOH'. *Publ. Astr. Soc. Japan* **44**, L77.

Huenemoerder, D. P., C. R. Canizares, and N. S. Schulz: 2001, 'X-ray spectroscopy of II Pegasi: coronal temperature structure, abundances, and variability'. *ApJ* **559**, 1135.

Huenemoerder, D. P., C. R. Canizares, and K. Kibbetts: 2002, 'X-ray spectra and light curves of AR Lac: temperature structure, abundances and variability'. In: *Cool stars, stellar systems and the Sun 12* in press.

Imanishi, K., K. Koyama, and Y. Tsuboi: 2001, 'Chandra observation of the ρ Ophiuchi cloud'. *ApJ* **557**, 747.

James, D. J. and R. D. Jeffries: 1997, 'Rotation, activity and lithium in NGC 6475'. *MNRAS* **292**, 252.

Jardine, M. and Y. C. Unruh: 1999, 'Coronal emission and dynamo saturation'. *A&A* **346**, 883.

Jeffries, R. D.: 1995, 'The kinematics of lithium-rich, active late-type stars: Evidence for a low-mass Local Association'. *MNRAS* **273**, 559.

Jeffries, R. D., M. R. Thurston, and J. P. Pye: 1997, 'An X-ray survey of the young open cluster NGC 2516'. *MNRAS* **287**, 350.

Jeffries, R. D. and A. J. Tolley: 1998, 'X-ray emission and low-mass stars in the young open cluster NGC 2547'. *MNRAS* **300**, 331.

Jeffries, R. D., E. J. Totten, and D. J. James: 2000, 'Rotation and activity in the solar-type stars of NGC 2547'. *MNRAS* **316**, 950.

Johnson, H. M.: 1981, 'An X-ray sampling of nearby stars'. *ApJ* **243**, 234.

Johnson, H. M.: 1986, 'An unbiased X-ray sampling of stars within 25 parsecs of the sun'. *ApJ* **303**, 470.

Johnson, O., J. J. Drake, V. Kashyap, N. S. Brickhouse, A. K. Dupree, P. Freeman, P. R. Young, and G. A. Kriss: 2002, 'The Capella giants and coronal evolution across the Hertzsprung gap'. *ApJ* **565**, L97.

Jones, H. R. A., A. J. Longmore, F. Allard, and P. H. Hauschildt: 1996, 'Spectral analysis of M dwarfs'. *MNRAS* **280**, 77.

Jordan, C.: 1980, 'The energy balance of the solar transition region'. *A&A* **86**, 355.

Jordan, C., T. R. Ayres, A. Brown, J. L. Linsky, and T. Simon: 1987, 'The chromospheres and coronae of five G-K main-sequence stars'. *MNRAS* **225**, 903.

Jordan, C., G. A. Doshek, J. J. Drake, A. B. Galvin, and J. C. Raymond: 1998, 'Coronal abundances: what are they?'. In: R. A. Donahue and J. A. Bookbinder (eds.): *ASP Conf. Ser. 154: Cool Stars, Stellar Systems and the Sun*, p. 91, ASP, San Francisco.

Judge, P.: 2002, 'Observational and interpretational challenges'. In: F. Favata and J. J. Drake (eds.): *ASP Conf. Ser. 277: Stellar coronae in the Chandra and XMM era*. p. 45, ASP, San Francisco.

Kano, R. and S. Tsuneta: 1995, 'Scaling laws of solar coronal loops obtained with Yohkoh'. *ApJ* **454**, 934.

Kashyap, V. and J. J. Drake: 1998, 'Markov-Chain Monte Carlo reconstruction of Emission Measure Distributions: application to solar extreme-ultraviolet spectra'. *ApJ* **503**, 450.

Kashyap, V. and J. J. Drake: 1999, 'On X-ray variability in active binary stars'. *ApJ* **524**, 988.

Kashyap, V., D. J. J., M. Audard, and M. Güdel: 2002, 'Flare heating of stellar coronae'. In: F. Favata and J. Drake (eds.): *ASP Conf. Ser. 277: Stellar coronae in the Chandra and XMM era*. p. 503, ASP, San Francisco.

Kastner, J. H., D. P. Huenemoerder, N. S. Schulz, C. R. Canizares, and D. A. Weintraub: 2002, 'Evidence for accretion: high-resolution X-ray spectroscopy of the Classical T Tauri Star TW Hydrae'. *ApJ* **567**, 434.

Klimchuck, J. A.: 2002, 'Scaling laws for solar and stellar coronae'. In: F. Favata and J. J. Drake (eds.): *ASP Conf. Ser. 277: Stellar coronae in the Chandra and XMM era*. p. 321, ASP, San Francisco.

Kopp, R. A. and G. Poletto: 1984, 'Extension of the reconnection theory of two-ribbon solar flares'. *Solar Physics* **93**, 351.

Krishnamurthi, A., C. S. Reynolds, J. L. Linsky, E. Martín, and M. Gagné: 2001, 'Observations of the core of the Pleiades with the Chandra X-ray observatory'. *AJ* **121**, 337.

Kürster, M. and J. H. M. M. Schmitt: 1996, 'Forty days in the life of CF Tucanae (=HD 5305). The longest stellar X-ray flare observed with ROSAT'. *A&A* **311**, 211.

Lachaume, R., C. Dominik, T. Lanz, and H. J. Habing: 1999, 'Age determinations of main-sequence stars: combining different methods'. *A&A* **348**, 897.

Laming, J. M.: 2002, 'Should you trust the atomic data?'. In: F. Favata and J. J. Drake (eds.): *ASP Conf. Ser. 277: Stellar coronae in the Chandra and XMM era*. p. 25, ASP, San Francisco.

Laming, J. M., J. J. Drake, and K. G. Widing: 1996, 'Stellar coronal abundances. IV. Evidence of the FIP effect in the corona of ε Eridani?'. *ApJ* **462**, 948.

Lawson, W. A., E. D. Feigelson, and D. P. Huenemoerder: 1996, 'An improved HR diagram for Chamaeleon I pre-main-sequence stars'. *MNRAS* **280**, 1071.

Lean, J.: 1997, 'The Sun's variable radiation and its relevance for Earth'. *ARA&A* **35**, 33.

Lim, J. and S. M. White: 1996, 'Limits to mass outflows from late-type dwarf stars'. *ApJ* **462**, L91.

Linsky, J. L., B. E. Wood, A. Brown, and R. A. Osten: 1998, 'Dissecting Capella's corona: GHRS spectra of the Fe XXI λ 1354 and He II λ 1640 lines from each of the Capella stars'. *ApJ* **492**, 767.

Linsky, J. L. and M. Gagné: 2001, 'Analysis of Chandra X-ray spectra of the young, active star AB Dor'. In: *American Astronomical Society Meeting*, Vol. 198. p. 4405.

Maggio, A., S. Sciortino, G. S. Vaiana, P. Majer, J. Bookbinder, L. Golub, F. R. Harnden, and R. Rosner: 1987, 'Einstein observatory survey of X-ray emission from solar-type stars: the late F and G dwarf stars'. *ApJ* **315**, 687.

Maggio, A., R. Pallavicini, F. Reale, and G. Tagliaferri: 2000, 'Twin X-ray flares and the active corona of AB Dor observed with BeppoSAX'. *A&A* **356**, 627.

Maggio, A., J. J. Drake, V. Kashyap, G. Micela, S. Sciortino, G. Peres, F. R. Harnden, and S. S. Murray: 2002, 'AD Leo observed with Chandra LETGS: emission measure distribution, density and element abundances of the coronal plasma'. In: F. Favata and J. Drake (eds.): *ASP Conf. Ser. 277: Stellar coronae in the Chandra and XMM era*. p. 57, ASP, San Francisco.

Majer, P., J. H. M. M. Schmitt, L. Golub, F. R. Harnden, and R. Rosner: 1986, 'X-ray spectra and the rotation-activity connection of RS Canum Venaticorum binaries'. *ApJ* **300**, 360.

Mandrini, C. H., P. Démoulin, and J. A. Klimchuk: 2000, 'Magnetic field and plasma scaling laws: their implications for coronal heating models'. *ApJ* **530**, 999.

Marino, A., G. Micela, and G. Peres: 2000, 'A systematic analysis of X-ray variability of dM stars'. *A&A* **353**, 177.

Marino, A., G. Micela, G. Peres, and S. Sciortino: 2002, 'On X-ray variability in ROSAT-PSPC observations of F7-K2 stars'. *A&A* **383**, 210.

Martín, E. L. and H. Bouy: 2002, 'XMM-Newton observations of the nearby brown dwarf LP 944-20'. *New Astronomy* **7**, 595.
McGale, P. A., J. P. Pye, and S. T. Hodgkin: 1996, 'ROSAT PSPC X-ray spectral survey of W UMa systems'. *MNRAS* **280**, 627.
McWilliam, A.: 1997, 'Abundance ratios and Galactic chemical evolution'. *ARA&A* **35**, 503.
Mermilliod, J.-C.: 1997, 'Radial velocities and binarity in open clusters'. *Mem. Soc. Astron. Ital.* **68**, 853.
Mermilliod, J.-C., C. Turon, N. Robichon, F. Arenou, and Y. Lebreton: 1997, 'The distance of the Pleiades and nearby clusters, ESA SP-402'. In: M. A. C. Perryman and P. L. Bernacca (eds.): *Hipparcos Venice 97*. Noordwijk, p. 643, ESA.
Mewe, R.: 1999, 'Atomic physics of hot plasmas'. In: J. van Paradijs and J. A. M. Bleeker (eds.): *X-ray spectroscopy in astrophysics*, Vol. 520 of *Lecture Notes in Physics*. p. 109, Springer.
Mewe, R., J. Heise, E. H. B. M. Gronenschild, A. C. Brinkman, J. Schrijver, and A. J. F. den Boggende: 1975, 'Detection of X-ray emission from stellar coronae with ANS'. *ApJ* **202**, L67.
Mewe, R., J. S. Kaastra, S. M. White, and R. Pallavicini: 1996, 'Simultaneous EUVE &; ASCA observations of AB Doradus: temperature structure and abundances of the quiescent corona'. *A&A* **315**, 170.
Mewe, R., J. S. Kaastra, G. H. J. van den Oord, J. Vink, and Y. Tawara: 1997, 'ASCA and EUVE observations of II Pegasi: flaring and quiescent coronal emission'. *A&A* **320**, 147.
Mewe, R., A. J. J. Raassen, J. J. Drake, J. S. Kaastra, R. L. J. van der Meer, and D. Porquet: 2001, 'Chandra-LETGS X-ray observations of Capella. Temperature, density and abundance diagnostics'. *A&A* **368**, 888.
Meyer, J.-P.: 1985, 'Solar-stellar outer atmospheres and energetic particles, and galactic cosmic rays'. *ApJS* **57**, 173.
Micela, G.: 2001, 'X-ray emission from open clusters'. In: R. Giacconi, L. Stella, and S. Serio (eds.): *ASP Conf. Ser. 234: X-ray Astronomy 2000*. p. 143, ASP, San Francisco.
Micela, G.: 2002, 'Evolution of stellar coronal activity on the main sequence'. In: B. Montesinos, A. Gimenez, and E. F. Guinan (eds.): *ASP Conf. Ser. 269: The evolving Sun and its influence on planetary environments*. p. 107, ASP, San Francisco.
Micela, G., S. Sciortino, and S. Serio: 1984, 'The relationship between X-ray luminosity and Rossby number for a sample of late-type stars'. In: M. Oda and R. Giacconi (eds.): *X-Ray Astronomy '84*. p. 43.
Micela, G., S. Sciortino, S. Serio, and et al.: 1985, 'Einstein X-ray survey of the Pleiades: the dependence of X-ray emission on stellar age'. *ApJ* **292**, 172.
Micela, G., S. Sciortino, G. S. Vaiana, and et al.: 1988, 'The Einstein observatory survey of stars in the Hyades cluster region'. *ApJ* **325**, 798.
Micela, G., S. Sciortino, G. Vaiana, and et al.: 1990, 'X-ray studies of coeval star samples. II. The Pleiades cluster as observed with the Einstein observatory'. *ApJ* **348**, 557.
Micela, G., S. Sciortino, and F. Favata: 1993, 'Stellar birthrate in the Galaxy in the past billion years: constraints from X-ray flux limited surveys'. *ApJ* **412**, 618.
Micela, G., S. Sciortino, V. Kashyap, F. R. Harnden, and R. Rosner: 1996, 'ROSAT observations of the Pleiades cluster. I–X-ray characteristics of a coeval stellar population'. *ApJS* **102**, 75.
Micela, G., F. Favata, and S. Sciortino: 1997a, 'Hipparcos distances of X-ray selected stars: implications on their nature as stellar population'. *A&A* **326**, 221.
Micela, G., J. P. Pye, and S. Sciortino: 1997b, 'Coronal properties of nearby old disk and halo dM stars'. *A&A* **320**, 865.
Micela, G., S. Sciortino, F. R. Harnden, and R. Rosner: 1998, 'X-ray variability and rotation in the Pleiades cluster'. *Ap&SS* **261**, 105.

Micela, G., S. Sciortino, F. Favata, R. Pallavicini, and J. Pye: 1999a, 'X-ray observations of the young open cluster Blanco 1'. *A&A* **344**, 83.

Micela, G., S. Sciortino, F. R. Harnden, V. Kashyap, R. Rosner, C. F. Prosser, F. Damiani, J. Stauffer, and J.-P. Caillault: 1999b, 'Deep ROSAT HRI observations of the Pleiades'. *A&A* **341**, 751.

Micela, G., S. Sciortino, R. D. Jeffries, M. R. Thurston, and F. Favata: 2000, 'Rosat HRI observations of the open cluster NGC 2516'. *A&A* **357**, 909.

Montmerle, T., L. Koch-Miramond, E. Falgarone, and J. E. Grindlay: 1983, 'Einstein observations of the ρ Ophiuchi dark cloud: an X-ray Christmas tree'. *ApJ* **269**, 182.

Motch, C., P. Guillout, F. Haberl, et al.: 1997, 'The ROSAT galactic plane survey: analysis of a low latitude sample area in Cygnus'. *A&A* **318**, 111.

Mullan, D. J., J. G. Doyle, R. O. Redman, and M. Mathioudakis: 1992, 'Limits on the detectability of mass loss from cool dwarfs'. *ApJ* **397**, 225.

Mutel, R. L., L. A. Molnar, E. B. Waltman, and F. D. Ghigo: 1998, 'Radio emission from Algol. I. Coronal geometry and emission mechanisms determined from VLBA and Green Bank interferometer observations'. *ApJ* **507**, 371.

Ness, J.-U., R. Mewe, J. H. M. M. Schmitt, A. J. J. Raassen, D. Porquet, J. S. Kaastra, R. L. J. van der Meer, V. Burwitz, and P. Predehl: 2001, 'Helium-like triplet density diagnostics. Applications to Chandra-LETGS X-ray observations of Capella and Procyon'. *A&A* **367**, 282.

Ness, J.-U., R. Mewe, J. H. M. M. Schmitt, and A. J. J. Raassen: 2002a, 'Influence of radiation fields on the density diagnostics. Chandra-LEGTS observations of Algol and Procyon'. In: F. Favata and J. J. Drake (eds.): *ASP Conf. Ser. 277: Stellar coronae in the Chandra and XMM era*. p. 545, ASP, San Francisco.

Ness, J.-U., J. H. M. M. Schmitt, V. Burwitz, R. Mewe, and P. Predehl: 2002b, 'Chandra LETGS observation of the active binary Algol'. *A&A* **387**, 1032.

Neuhäuser, R., C. Briceño, F. Comerón, T. Hearty, E. L. Martín, J. H. M. M. Schmitt, B. Stelzer, R. Supper, W. Voges, and H. Zinnecker: 1999, 'Search for X-ray emission from bona-fide and candidate brown dwarfs'. *A&A* **343**, 883.

Neupert, W. M.: 1968, 'Comparison of solar X-ray line emission with microwave emission during flares'. *ApJ* **153**, L59.

Ng, Y. K. and G. Bertelli: 1998, 'Revised ages for stars in the solar neighborhood'. *A&A* **329**, 943.

Noyes, R. W., L. W. Hartmann, S. L. Baliunas, D. K. Duncan, and A. H. Vaughan: 1984, 'Rotation, convection, and magnetic activity in lower main-sequence stars'. *ApJ* **279**, 763.

Orlando, S., G. Peres, and F. Reale: 2000, 'The Sun as an X-ray star. I. Deriving the emission measure distribution versus temperature of the whole solar corona from the Yohkoh/Soft X-ray telescope data'. *ApJ* **528**, 524.

Orlando, S., G. Peres, and F. Reale: 2001, 'The Sun as an X-ray star. IV. The contribution of different regions of the corona to its X-ray spectrum'. *ApJ* **560**, 499.

Ortolani, A., R. Pallavicini, A. Maggio, F. Reale, and S. White: 1998, 'Flares on AB Dor observed with ASCA'. In: R. A. Donahue and J. A. Bookbinder (eds.): *ASP Conf. Ser. 154: Cool Stars, Stellar Systems and the Sun*, p. 1532, ASP, San Francisco.

Osten, R. A. and A. Brown: 1999, 'EUVE photometry of RS CVn systems: four flaring megasecond'. *ApJ* **515**, 746.

Osten, R. A., A. Brown, T. R. Ayres, et al.: 2000, 'Radio, X-ray and EUV coronal variability of the short-period RS CVn binary σ^2 Coronae Borealis'. *ApJ* **544**, 953.

Ottmann, R. and J. H. M. M. Schmitt: 1996, 'ROSAT observations of a giant X-ray flare on Algol: evidence for abundance variations?'. *A&A* **307**, 813.

Ottmann, R., M. J. Pfeiffer, and T. Gehren: 1998, 'Photospheric metal abundances in active stellar atmospheres'. *A&A* **338**, 661.

Pagano, I., J. L. Linsky, L. Carkner, R. D. Robinson, B. Woodgate, and G. Timothy: 2000, 'HST/STIS echelle spectra of the dM1e star AU Microscopii outside of flares'. *ApJ* **532**, 497.

Pallavicini, R., S. Serio, and G. S. Vaiana: 1977, 'A survey of soft X-ray limb flare images – The relation between their structure in the corona and other physical parameters'. *ApJ* **216**, 108.

Pallavicini, R., L. Golub, R. Rosner, G. S. Vaiana, T. Ayres, and J. L. Linsky: 1981, 'Relations among stellar X-ray emission observed from Einstein, stellar rotation and bolometric luminosity'. *ApJ* **248**, 279.

Pallavicini, R., G. Tagliaferri, and L. Stella: 1990, 'X-ray emission from solar neighborhood flare stars: a comprehensive survey of EXOSAT results'. *A&A* **228**, 403.

Pan, H. C., C. Jordan, K. Makishima, et al.: 1997, 'An exceptional X-ray flare on the dMe star EQ1839.6+8002'. *MNRAS* **285**, 735.

Panzera, M. R., G. Tagliaferri, L. Pasinetti, and E. Antonello: 1999, 'X-ray emission from A0-F6 spectral type stars'. *A&A* **348**, 161.

Parker, E. N.: 1988, 'Nanoflares and the solar X-ray corona'. *ApJ* **330**, 474.

Parnell, C. E. and P. E. Jupp: 2000, 'Statistical analysis of the energy distribution of nanoflares in the quiet sun'. *ApJ* **529**, 554.

Patten, B. M. and T. Simon: 1993, 'The evolution of stellar coronae: initial results from a ROSAT PSPC observation of IC 2391'. *ApJ* **415**, L123.

Patten, B. M. and T. Simon: 1996, 'The evolution of rotation and activity in young open clusters: IC 2391'. *ApJS* **106**, 489.

Pease, D., J. J. Drake, V. Kashyap, P. W. Ratzlaff, S. H. Saar, B. Haisch, A. Dobrzycki, N. R. Adams, and S. J. Wolk: 2002, 'A lot of observations of the coronae of AR Lac'. In: F. Favata and J. J. Drake (eds.): *ASP Conf. Ser. 277: Stellar coronae in the Chandra and XMM era*. p. 551, ASP, San Francisco.

Peres, G., S. Orlando, F. Reale, R. Rosner, and H. Hudson: 2000, 'The Sun as an X-ray star. II. Using the Yohkoh/Soft X-ray telescope-derived solar emission measure versus temperature to interpret stellar x-ray observations'. *ApJ* **528**, 537.

Peres, G., S. Orlando, F. Reale, and R. Rosner: 2001, 'The distribution of the emission measure, and of the heating budget, among the loops in the corona'. *ApJ* **563**, 1045.

Phillips, K. J. H., A. K. Bhatia, H. E. Mason, and D. M. Zarro: 1996, 'High coronal electron densities in a solar flare from Fe XXI and Fe XXII X-ray line measurements'. *ApJ* **466**, 549.

Pillitteri, I., G. Micela, S. Sciortino, and F. Favata: 2002, 'The X-ray luminosity distributions of the high-metallicity open cluster Blanco 1'. *A&A* in press.

Pizzolato, N., P. Ventura, F. D'Antona, A. Maggio, G. Micela, and S. Sciortino: 2001, 'Sub-photospheric convection and magnetic activity dependence on metallicity and age: Models and tests'. *A&A* **373**, 597.

Pizzolato, N., A. Maggio, G. Micela, S. Sciortino, and P. Ventura: 2003, 'The stellar activity-rotation relationship revisited: dependence of saturated and non-saturated X-ray emission regimes on spectral class for late-type MS stars'. *A&A* **397**, 147.

Porter, L. J. and J. A. Klimchuck: 1995, 'Soft X-ray loops and coronal heating'. *ApJ* **454**, 499.

Pottasch, S. R.: 1963a, 'The lower solar corona: interpretation of the ultraviolet spectrum'. *ApJ* **137**, 945.

Pottasch, S. R.: 1963b, 'The lower solar corona: the abundance of iron'. *MNRAS* **125**, 543.

Pravdo, S. H., E. D. Feigelson, G. Garmire, Y. Maeda, Y. Tsuboi, and J. Bally: 2001, 'Discovery of X-rays from the protostellar outflow object HH2'. *Nat* **413**, 708.

Preibisch, T., H. Zinnecker, and J. H. M. M. Schmitt: 1993, 'ROSAT-detection of a giant X-ray flare on LkHα 92'. *A&A* **279**, L33.

Preibisch, T., R. Neuhäuser, and J. M. Alcalá: 1995, 'A giant X-ray flare on the young star P1724'. *A&A* **304**, L13.

Preibisch, T. and H. Zinnecker: 2001, 'Deep Chandra X-ray observatory imaging study of the very young stellar cluster IC 348'. *AJ* **122**, 866.

Preibisch, T. and H. Zinnecker: 2002, 'X-ray properties of the young stellar and substellar objects in the IC 348 cluster: the Chandra view'. *AJ* **123**, 1613.

Prosser, C. F., S. Randich, J. R. Stauffer, J. H. M. M. Schmitt, and T. Simon: 1996, 'ROSAT pointed observations of the α Persei cluster'. *AJ* **112**, 1570.

Pye, J. P. and I. M. McHardy: 1983, 'The Ariel V sky survey of fast-transient X-ray sources'. *MNRAS* **205**, 875.

Pye, J. P., S. Hodgkin, R. Stern, and J. Stauffer: 1994, 'ROSAT X-ray luminosity functions of the Hyades dK and dM stars'. *MNRAS* **266**, 798.

Raassen, A. J. J., R. Mewe, M. Audard, M. Güdel, E. Behar, J. S. Kaastra, R. L. J. van der Meer, C. R. Foley, and J.-U. Ness: 2002, 'High-resolution X-ray spectroscopy of Procyon by Chandra and XMM-Newton'. *A&A* **389**, 228.

Radick, R. R., G. W. Lockwood, B. A. Skiff, and D. T. Thompson: 1995, 'A 12 year photometric study of lower main-sequence Hyades stars'. *ApJ* **452**, 332.

Randich, S.: 1998, 'Supersaturation in X-ray emission of cluster stars'. In: R. A. Donahue and J. A. Bookbinder (eds.): *ASP Conf. Ser. 154: Cool Stars, Stellar Systems, and the Sun*, p. 501, ASP, San Francisco.

Randich, S.: 2000, 'Coronal activity among open cluster stars'. In: R. Pallavicini, G. Micela, and S. Sciortino (eds.): *ASP Conf. Ser. 198: Stellar Clusters and Associations: Convection, Rotation, and Dynamos*. p. 401, ASP, San Francisco.

Randich, S., R. G. Gratton, and R. Pallavicini: 1993, 'Lithium in RS CVn binaries and related chromospherically active stars. II. Spectrum synthesis analysis'. *A&A* **273**, 194.

Randich, S., M. S. Giampapa, and R. Pallavicini: 1994, 'Lithium in RS CVn binaries and related chromospherically active stars. III. Northern RS CVn systems'. *A&A* **283**, 893.

Randich, S. and J. H. M. M. Schmitt: 1995, 'A ROSAT X-ray study of the Praesepe cluster'. *A&A* **298**, 115.

Randich, S., J. H. M. M. Schmitt, C. F. Prosser, and J. R. Stauffer: 1995, 'A X-ray study of the young open cluster IC 2602'. *A&A* **300**, 134.

Randich, S., J. H. M. M. Schmitt, and C. Prosser: 1996a, 'Coronal activity in the Coma Berenices open cluster'. *A&A* **313**, 815.

Randich, S., J. H. M. M. Schmitt, C. F. Prosser, and J. R. Stauffer: 1996b, 'The X-ray properties of the young open cluster around α Persei'. *A&A* **305**, 785.

Randich, S., K. P. Singh, T. Simon, S. A. Drake, and J. H. M. M. Schmitt: 1998, 'ROSAT HRI observations of the intermediate-age open cluster IC 4756'. *A&A* **337**, 372.

Reale, F.: 2002, 'Stellar flare modeling'. In: F. Favata and J. Drake (eds.): *ASP Conf. Ser. 277: Stellar coronae in the Chandra and XMM era*. p. 103, ASP, San Francisco.

Reale, F., R. Betta, G. Peres, S. Serio, and J. McTiernan: 1997, 'Determination of the length of coronal loops from the decay of X-ray flares. I. Solar flares observed with Yohkoh SXT'. *A&A* **325**, 782.

Reale, F. and G. Micela: 1998, 'Determination of the length of coronal loops from the decay of X-ray flares. II. Stellar flares observed with ROSAT/PSPC'. *A&A* **334**, 1028.

Reale, F., G. Peres, and S. Orlando: 2001, 'The Sun as an X-ray star. III. Flares'. *ApJ* **557**, 906.

Reale, F., F. Bocchino, and G. Peres: 2002, 'Modeling non-confined coronal flares: dynamics and X-ray diagnostics'. *A&A* **383**, 952.

Reid, N., S. Hawley, and M. Mateo: 1995, 'Chromospheric and coronal activity in low-mass Hyades dwarfs'. *MNRAS* **272**, 828.

Rice, J. B. and K. G. Strassmeier: 2001, 'Doppler imaging of stellar surface structure. XVII. The solar-type Pleiades star HII 314 = V1038 Tauri'. *A&A* **377**, 264.

Robinson, R. D., J. L. Linsky, B. E. Woodgate, and J. G. Timothy: 2001, 'Far-ultraviolet observations of flares on the dM0e star AU Microscopii'. *ApJ* **554**, 368.

Rosner, R., W. H. Tucker, and G. S. Vaiana: 1978, 'Dynamics of the quiescent solar corona'. *ApJ* **220**, 643.

Rosner, R., Y. Avni, J. Bookbinder, R. Giacconi, L. Golub, F. R. Harnden, C. W. Maxson, K. Topka, and G. S. Vaiana: 1981, 'The stellar contribution to the galactic soft X-ray background'. *ApJ* **249**, L5.

Rucinski, S. M.: 1998, 'Extreme Ultraviolet Explorer investigation of three short-period binary stars'. *AJ* **115**, 303.

Rutledge, R. E., G. Basri, E. L. Martín, and L. Bildsten: 2000, 'Chandra detection of an X-ray flare from the brown dwarf LP 944-20'. *ApJ* **538**, L141.

Saar, S. H.: 1991, 'Recent advances in the observation and analysis of stellar magnetic fields'. In: I. Tuominen, D. Moss, and G. Ruediger (eds.): *IAU Colloquium 130, The Sun and Cool Stars: activity, magnetism, dynamos*. Berlin: Springer, p. 389.

Sanz Forcada, J.: 2001, 'Las coronas estelares de los sistemas binarios activos'. Ph.D. thesis, Univ. Complutense de Madrid, Madrid, Spain.

Sanz-Forcada, J., N. S. Brickhouse, and A. K. Dupree: 2002a, 'Quiescent and flaring structure in RS Canum Venaticorum stars'. *ApJ* **570**, 799.

Sanz-Forcada, J., N. S. Brickhouse, and A. K. Dupree: 2002b, 'The structure of stellar coronae in active binary systems'. *ApJS* in press.

Sanz-Forcada, J. and G. Micela: 2002, 'The EUVE point of view of AD Leo'. *A&A* **394**, 653.

Schmitt, J. H. M. M.: 1994, 'ROSAT observations of stellar flares'. *ApJS* **90**, 735.

Schmitt, J. H. M. M.: 1997, 'Coronae on solar-like stars'. *A&A* **318**, 215.

Schmitt, J. H. M. M.: 1998, 'Inference of stellar coronal structure'. In: R. A. Donahue and J. A. Bookbinder (eds.): *ASP Conf. Ser. 154: Cool Stars, Stellar Systems and the Sun*, p. 463, ASP, San Francisco.

Schmitt, J. H. M. M., L. Golub, F. R. Harnden, C. Maxson, R. Rosner, and G. S. Vaiana: 1985, 'An Einstein observatory X-ray survey of main-sequence stars with shallow convection zones'. *ApJ* **290**, 307.

Schmitt, J. H. M. M., A. Collura, S. Sciortino, et al.: 1990a, 'Einstein observatory coronal temperatures of late-type stars'. *ApJ* **365**, 704.

Schmitt, J. H. M. M., G. Micela, S. Sciortino, G. S. Vaiana, F. R. Harnden, and R. Rosner: 1990b, 'X-ray studies of coeval star samples. III – X-ray emission in the Ursa Major stream'. *ApJ* **351**, 492.

Schmitt, J. H. M. M., P. Kahabka, J. Stauffer, and A. J. M. Piters: 1993, 'ROSAT All-Sky X-ray Survey of the core region of the Pleiades cluster'. *A&A* **277**, 114.

Schmitt, J. H. M. M. and M. Kurster: 1993, 'A spatially resolved x-ray image of a star like the Sun'. *Science* **262**, 215.

Schmitt, J. H. M. M., T. A. Fleming, and M. S. Giampapa: 1995, 'The X-ray view of the low mass stars in the solar neighborhood'. *ApJ* **450**, 392.

Schmitt, J. H. M. M., J. J. Drake, B. M. Haisch, and R. A. Stern: 1996a, 'A close look at the coronal density of Procyon'. *ApJ* **467**, 841.

Schmitt, J. H. M. M., R. A. Stern, J. J. Drake, and M. Kürster: 1996b, 'CF Tucanae: another case of a coronal MAD syndrome?'. *ApJ* **464**, 898.

Schmitt, J. H. M. M. and F. Favata: 1999, 'Continuous heating of a giant X-ray flare on Algol'. *Nat* **401**, 44.

Schmitt, J. H. M. M. and C. Liefke: 2002, 'X-ray emission from the ultracool dwarf LHS 2065'. *A&A* **382**, L9.

Schulz, N., C. R. Canizares, D. P. Huenemoerder, J. C. Lee, and K. Tibetts: 2002, 'X-ray plasma diagnostics of stellar winds in very young massive stars'. In: F. Favata and J. J. Drake (eds.): *ASP Conf. Ser. 277: Stellar coronae in the Chandra and XMM era*. p. 165, ASP, San Francisco.

Schwabe, H.: 1843, 'Solar observations during 1843'. *Astronomische Nachrichten* **20**.

Sciortino, S., G. Micela, F. Favata, A. Spagna, and M. G. Lattanzi: 2000, 'ROSAT HRI survey of the open cluster Stock 2'. *A&A* **357**, 460.

Sciortino, S., G. Micela, F. Damiani, et al.: 2001, 'XMM-Newton survey of the low-metallicity open cluster NGC 2516'. *A&A* **365**, L259.

Serio, S., G. Peres, G. S. Vaiana, L. Golub, and R. Rosner: 1981, 'Closed coronal structures. II – Generalized hydrostatic model'. *ApJ* **243**, 288.

Serio, S., F. Reale, J. Jakimiec, B. Sylwester, and J. Sylwester: 1991, 'Dynamics of flaring loops. I. Thermodynamic decay scaling laws'. *A&A* **241**, 197.

Sheeley, N. R.: 1996, 'Elemental abundance variations in the solar atmosphere'. *ApJ* **469**, 423.

Siarkowski, M.: 1992, 'Three-dimensional deconvolution of X-ray emission from AR Lac'. *MNRAS* **259**, 453.

Siarkowski, M., P. Pres, S. A. Drake, N. E. White, and K. P. Singh: 1996, 'Corona(e) of AR Lacertae. II. The spatial structure'. *ApJ* **473**, 470.

Siess, L., E. Dufour, and M. Forestini: 2000, 'An internet server for pre-main sequence tracks of low- and intermediate-mass stars'. *A&A* **358**, 593.

Simon, T. and W. B. Landsman: 1997, 'High chromospheres of late A stars'. *ApJ* **483**, 435.

Simon, T. and B. M. Patten: 1998, 'A deep X-ray image of IC 2391'. *PASP* **110**, 283.

Singh, K. P., S. A. Drake, and N. E. White: 1995, 'A study of the coronal X-ray emission from short-period Algol binaries'. *ApJ* **445**, 840.

Singh, K. P., S. A. Drake, and N. E. White: 1996a, 'RS CVn versus Algol-type binaries: a comparative study of their X-ray emission'. *AJ* **111**, 2415.

Singh, K. P., N. E. White, and S. A. Drake: 1996b, 'Corona(e) of AR Lac: I. The temperature and abundance distribution'. *ApJ* **456**, 766.

Skumanich, A.: 1972, 'Time scales for Ca II emission decay, rotational braking, and lithium depletion'. *ApJ* **171**, 565.

Soderblom, D. R., B. F. Jones, S. Balachandran, J. R. Stauffer, D. K. Duncan, S. B. Fedele, and J. D. Hudon: 1993, 'The evolution of the lithium abundances of solar-type stars. III. The Pleiades'. *AJ* **106**, 1059.

Solanki, S. K., S. Motamen, and R. Keppens: 1997, 'Polar spots and stellar spindown: is dynamo saturation needed?'. *A&A* **325**, 1039.

Soon, W., S. Baliunas, E. S. Posmentier, and P. Okeke: 2000, 'Variations of solar coronal hole area and terrestrial lower tropospheric air temperature from 1979 to mid-1998: astronomical forcings of change in earth's climate?'. *New Astronomy* **4**, 563.

Stauffer, J. R., J.-P. Caillault, M. Gagné, C. F. Prosser, and L. W. Hartmann: 1994, 'A deep imaging survey of the Pleiades with ROSAT'. *ApJS* **91**, 625.

Stelzer, B., R. Neuhäuser, S. Casanova, and T. Montmerle: 1999, 'Rotational modulation of X-ray flares on late-type stars: T Tauri stars and Algol'. *A&A* **344**, 154.

Stelzer, B. and R. Neuhäuser: 2001, 'X-ray emission from young stars in Taurus-Auriga-Perseus: Luminosity functions and the rotation – activity – age – relation'. *A&A* **377**, 538.

Stelzer, B., V. Burwitz, M. Audard, M. Güdel, J.-U. Ness, N. Grosso, R. Neuhäuser, J. H. M. M. Schmitt, P. Predehl, and B. Aschenbach: 2002, 'Simultaneous X-ray spectroscopy of YY Gem with Chandra and XMM-Newton'. *A&A* **392**, 585.

Stern, R. A.: 1998, 'Long-term X-ray variability in cool stars'. In: R. A. Donahue and J. A. Bookbinder (eds.): *ASP Conf. Ser. 154: Cool Stars, Stellar Systems and the Sun*, p. 223, ASP, San Francisco.

Stern, R. A., M. C. Zolcinski, S. K. Antiochos, and J. H. Underwood: 1981, 'Stellar coronae in the Hyades – A soft X-ray survey with the Einstein Observatory'. *ApJ* **249**, 647.

Stern, R. A., S. K. Antiochos, and F. R. Harnden: 1986, 'Modeling of coronal X-ray emission from active cool stars. I Hyades cluster'. *ApJ* **305**, 417.

Stern, R. A., J. H. M. M. Schmitt, C. Rosso, J. P. Pye, S. T. Hodgkin, and J. R. Stauffer: 1992a, 'First results from ROSAT all-sky survey observations of the Hyades cluster'. *ApJ* **399**, L159.

Stern, R. A., Y. Uchida, S. Tsuneta, and F. Nagase: 1992b, 'GINGA observations of X-ray flares on Algol'. *ApJ* **400**, 321.

Stern, R. A., J. H. M. M. Schmitt, J. P. Pye, S. T. Hodgkin, J. R. Stauffer, and T. Simon: 1994, 'Coronal X-ray sources in the Hyades: A 40 kilosecond ROSAT pointing'. *ApJ* **427**, 808.

Stern, R. A., J. R. Lemen, J. H. M. M. Schmitt, and J. P. Pye: 1995a, 'EUVE observations of Algol: detection of a continuum and implications for the coronal [Fe/H] abundance'. *ApJ* **444**, L45.

Stern, R. A., J. H. M. M. Schmitt, and P. T. Kahabka: 1995b, 'ROSAT All-Sky Survey Observations of the Hyades Cluster'. *ApJ* **448**, 683.

Sterzik, M. F. and J. H. M. M. Schmitt: 1997, 'Young cool stars in the solar neighborhood'. *AJ* **114**, 1673.

Strassmeier, K., D. Hall, F. Fekel, and M. Check: 1993, 'A catalog of chromospherically active binary stars (second edition)'. *A&AS* **100**, 173.

Stuik, R., J. H. M. J. Bruls, and R. J. Rutten: 1997, 'Modeling Li I and K I sensitivity to Pleiades activity'. *A&A* **322**, 911.

Swank, J. H. and N. E. White: 1980, 'X-ray spectroscopy of late-type stars'. In: A. K. Dupree (ed.): *SAO Special Report 389: Cool Stars, Stellar Systems, and the Sun*. p. 47.

Swank, J. H., N. E. White, S. S. Holt, and R. H. Becker: 1981, 'Two-component X-ray emission from RS Canum Venaticorum binaries'. *ApJ* **246**, 208.

Sylwester, B., J. Sylwester, S. Serio, et al.: 1993, 'Dynamics of flaring loops. III – Interpretation of flare evolution in the emission measure-temperature diagram'. *A&A* **267**, 586.

Sylwester, J., J. R. Lemen, R. D. Bentley, A. Fludra, and M.-C. Zolcinski: 1998, 'Detailed evidence for flare-to-flare variations of the coronal calcium abundance'. *ApJ* **501**, 397.

Tagliaferri, G., G. Cutispoto, R. Pallavicini, S. Randich, and L. Pasquini: 1994, 'Photometric and spectroscopic studies of cool stars discovered in EXOSAT X-ray images. II. Lithium abundances'. *A&A* **285**, 272.

Testa, P., G. Peres, F. Reale, and S. Orlando: 2002, 'Temperature and density structure of hot and cool loops derived from the analysis of TRACE data'. *ApJ* **580**, 1159.

Tobias, S. M., N. H. Brummell, T. L. Clune, and J. Toomre: 1998, 'Pumping of Magnetic Fields by Turbulent Penetrative Convection'. *ApJ* **502**, L177.

Topka, K., L. Golub, P. Gorenstein, F. R. Harnden, G. S. Vaiana, Y. Avni, and R. Rosner: 1982, 'A magnitude limited stellar X-ray survey and the F star X-ray luminosity function'. *ApJ* **259**, 677.

Tsuboi, Y., K. Koyama, H. Murakami, et al.: 1998, 'ASCA detection of a superhot 100 million K X-ray flare on the weak-lined T Tauri star V773 Tauri'. *ApJ* **503**, 894.

Tsuboi, Y., K. Imanishi, K. Koyama, N. Grosso, and T. Montmerle: 2000, 'Quasi-periodic X-ray flares from the protostar YLW15'. *ApJ* **532**, 1089.

Tsuru, T., K. Makishima, T. Ohashi, et al.: 1989, 'X-ray and radio observations of flares from the RS Canum Venaticorum system UX Arietis'. *PASP* **41**, 679.

Uchida, Y. and T. Sakurai: 1983, 'Interacting magnetospheres in RS CVn binaries – Coronal heating and flares'. In: *IAU Colloq. 71: Activity in Red-Dwarf Stars*. p. 629.

Ulrich, R. K.: 1975, 'Solar neutrinos and variations in the solar luminosity'. *Science* **190**, 619.

Vaiana, G. S., A. S. Krieger, and A. F. Timothy: 1973, 'Identification and analysis of structures in the corona from X-ray photography'. *Solar Physics* **32**, 81.

Vaiana, G. S. and R. Rosner: 1978, 'Recent advances in coronal physics'. *ARA&A* **16**, 393.

Vaiana, G. S., G. Fabbiano, R. Giacconi, L. Golub, P. Gorenstein, F. R. Harnden, J. P. Cassinelli, B. M. Haisch, H. M. Johnson, J. L. Linsky, C. W. Maxson, R. Mewe, R. Rosner, F. Seward, K. Topka, and C. Zwaan: 1981, 'Results from an extensive Einstein stellar survey'. *ApJ* **244**, 163.

van den Oord, G. H. J., R. Mewe, and A. C. Brinkman: 1988, 'An EXOSAT observation of an X-ray flare and quiescent emission from the RS CVn binary σ^2 CrB'. *A&A* **205**, 181.

van den Oord, G. H. J. and R. Mewe: 1989, 'The X-ray flare and the quiescent emission from Algol as detected by EXOSAT'. *A&A* **213**, 245.

van den Oord, G. H. J., C. J. Schrijver, M. Camphens, R. Mewe, and J. S. Kaastra: 1997, 'EUV spectroscopy of cool stars. III. Interpretation of EUVE spectra in terms of quasi-static loops'. *A&A* **326**, 1090.

Ventura, P., A. Zeppieri, I. Mazzitelli, and F. D'Antona: 1998a, 'Full spectrum of turbulence convective mixing: I. theoretical main sequences and turn-off for 0.6 – 15 $M_{\odot}$'. *A&A* **334**, 953.

Ventura, P., A. Zeppieri, I. Mazzitelli, and F. D'Antona: 1998b, 'Pre-main sequence Lithium burning: the quest for a new structural parameter'. *A&A* **331**, 1011.

Ventura, R., A. Maggio, and G. Peres: 1998c, 'Loop modeling of coronal X-ray spectra. V. One- and two-loop model fitting of G-type star ROSAT/PSPC spectra'. *A&A* **334**, 188–200.

Vesecky, J. F., S. K. Antiochos, and J. H. Underwood: 1979, 'Numerical modeling of quasi-static coronal loops. I – Uniform energy input'. *ApJ* **233**, 987.

Vilhu, O.: 1984, 'The nature of magnetic activity in lower main sequence stars'. *A&A* **133**, 117.

Vilhu, O. and S. M. Rucinski: 1983, 'Period-activity relations in close binaries'. *A&A* **127**, 5.

Vilhu, O., B. Gustafsson, and B. Edvardsson: 1987, 'Spectroscopy of the rapidly rotating K star HD 36705'. *ApJ* **320**, 850.

Walter, F. M., P. A. Charles, and C. S. Bowyer: 1978, 'Discovery of quiescent X-ray emission from HR1099 and RS CVn'. *Nat* **274**, 569.

Walter, F. M., W. Cash, P. A. Charles, and C. S. Bowyer: 1980, 'X-rays from RS Canum Venaticorum systems – A HEAO 1 survey and the development of a coronal model'. *ApJ* **236**, 212.

Walter, F. M. and S. Bowyer: 1981, 'On the coronae of rapidly rotating stars. I – The relation between rotation and coronal activity in RS CVn systems'. *ApJ* **245**, 671.

Walter, F. M., D. M. Gibson, and G. S. Basri: 1983, 'First observations of stellar coronal structure – The coronae of AR Lacertae'. *ApJ* **267**, 665.

Walter, F. M., A. Brown, R. D. Mathieu, and P. C. Myers: 1988, 'X-ray sources in regions of star formation. III. Naked T Tauri stars associated with the Taurus-Auriga complex'. *AJ* **96**, 297.

Walter, F. M. and W. T. Boyd: 1991, 'Star formation in Taurus-Auriga: the high mass stars'. *ApJ* **370**, 318.

Wargelin, B. J. and J. J. Drake: 2002, 'Stringent X-ray constraints on loss from proxima Centauri'. *ApJ* **578**, 503.

Weber, M. and K. G. Strassmeier: 2001, 'Doppler imaging of stellar surface structure. XV. A possible detection of differential rotation and local meridional flows on the rapidly-rotating giant HD 218153 = KU Pegasi'. *A&A* **373**, 974.

White, N. E., R. A. Shafer, K. Horne, A. N. Parmar, and J. L. Culhane: 1990, 'X-ray eclipse mapping or AR Lacertae'. *ApJ* **350**, 776.

White, N., K. Arnaud, C. Day, K. Ebisawa, E. Gotthelf, K. Mukai, Y. Soong, T. Yaqoob, and A. Antunes: 1994, 'An ASCA observation of one orbital cycle of AR Lac'. *Publ. Astr. Soc. Japan* **46**, L97.

White, S. M., J. Lim, S. M. Rucinski, C. Roberts, D. Kilkenny, S. G. Ryan, P. Prado, and M. R. Kundu: 1996, 'A search for rotational modulation in the EUV emission from AB Doradus'. In: *IAU Colloq. 152: Astrophysics in the Extreme Ultraviolet*. p. 165.

White, S. M., R. J. Thomas, J. W. Brosius, and M. R. Kundu: 2000, 'The absolute abundance of iron in the solar corona'. *ApJ* **534**, L203.

Widing, K. G. and U. Feldman: 2001, 'On the rate of abundance modifications versus time in active region plasmas'. *ApJ* **555**, 426.

Winebarger, A. R., A. G. Emslie, J. T. Mariska, and H. P. Warren: 2002, 'Energetics of explosive events observed with SUMER'. *ApJ* **565**, 1298.

Young, C. A.: 1869, 'On a new method of observing contacts at the Sun's limb and other spectroscopic observations during the recent eclipse'. *The American Journal of Science and Arts* **XLVIII**(144), 370.

Zickgraf, F. J., I. Thiering, J. Krautter, I. Appenzeller, R. Kneer, W. H. Voges, B. Ziegler, C. Chavarria, A. Serrano, R. Mujica, M. Pakull, and J. Heidt: 1997, 'Identification of a complete sample of northern ROSAT All-Sky Survey X-ray sources. II. The optical observations'. *A&A* **123**, 103.

Zinnecker, H. and T. Preibisch: 1994, 'X-ray emission from Herbig Ae/Be stars: A ROSAT survey'. *A&A* **292**, 152.

Index of individual objects